European Journal of Taxonomy 859: 1–56
https://doi.org/10.5852/ejt.2023.859.2043
ISSN 2118-9773
www.europeanjournaloftaxonomy.eu
2023 · Carvalho R.N. & Kury A.B.

Monograph

urn:lsid:zoobank.org:pub:8110A1B3-C4A4-4495-8AFD-1FED3D11D0A4

Between areolated and band-shaped spots: a revision of *Lacronia* Strand, 1942 (Opiliones, Gonyleptidae)

Rafael N. CARVALHO [1,*] & Adriano B. KURY [2]

[1,2] Departamento de Invertebrados, Museu Nacional, Universidade Federal do Rio de Janeiro, Quinta da Boa Vista s/n, São Cristóvão, Rio de Janeiro–RJ, 20.940-040, Brazil.
[1] Departamento de Zoologia, Instituto de Biologia Roberto de Alcantara Gomes, Universidade do Estado do Rio de Janeiro, Rua São Francisco Xavier 524, Maracanã, Rio de Janeiro–RJ, 20.550-900, Brazil.

[*] Corresponding author: rafaelcarvalhobio@hotmail.com
[2] Email: adrianok@gmail.com

[1] urn:lsid:zoobank.org:author:63A9A0F0-7C99-4419-8449-7506664D4766
[2] urn:lsid:zoobank.org:author:60FAE1F8-87F7-4A5F-BE78-BEB25BC4F898

Abstract. The genus *Lacronia* Strand, 1942 is herein revised, and a maximum parsimony phylogenetic analysis of morphological characters (30 taxa, 115 characters, 2962 scorings) is performed to test its monophyly. As a result, *Lacronia* is herein made monophyletic by means of the inclusion of *Discocyrtus boraceae* B. Soares, 1942, *Discocyrtus niger* Mello-Leitão, 1923 and *Discocyrtus tenuis* Roewer, 1917. *Lacronia* including those species is the sister group of *Discocyrtus* s. str. inside the DRMN-clade, and should be removed from Pachylinae Sørensen, 1884, although without a new subfamilial assignment for now. Four new junior subjective synonyms are detected for the first time (*Discocyrtus rarus* B. Soares, 1944 = *Discocyrtus fazi* Piza, 1942 = *Discocyrtus niger* Mello-Leitão, 1923; *Discocyrtus infelix* Mello-Leitão, 1940 = *Discocyrtus nigrolineatus* Mello-Leitão, 1923 = *Discocyrtus tenuis* Roewer, 1917). Accordingly, the following new combinations are proposed: *Lacronia boraceae* (B. Soares, 1942) comb. nov., *Lacronia nigra* (Mello-Leitão, 1923) comb. nov. and *Lacronia tenuis* (B. Soares, 1942) comb. nov. *Lacronia* is endemic to the Atlantic province of Brazil, with verified records from the states of Rio de Janeiro, Santa Catarina and São Paulo. As a geographic note, the record of '*D. fazi*' for Chile is here discussed and considered incorrect.

Keywords. Arthropoda, Arachnida, Pachylinae, taxonomy, cladistics.

Carvalho R.N. & Kury A.B. 2023. Between areolated and band-shaped spots: a revision of *Lacronia* Strand, 1942 (Opiliones, Gonyleptidae). *European Journal of Taxonomy* 859: 1–56.
https://doi.org/10.5852/ejt.2023.859.2043

Introduction

Gonyleptidae Sundevall, 1833 is the most diverse family inside the suborder Laniatores Thorell, 1876, presenting 787 species divided into 17 subfamilies (Kury *et al.* 2022). Its diversity is mainly known

in the Atlantic Forest biome (Kury 2003a; Pinto-da-Rocha *et al.* 2005), which represents a significant global biodiversity hotspot (Myers *et al.* 2000). Nearly half of the species of Gonyleptidae are allocated in Pachylinae Sørensen, 1884 (Kury 2003a; Kury *et al.* 2022). However, Pachylinae 1) has never been recovered as a clade in the previous literature (e.g., Pinto-da-Rocha *et al.* 2014; Carvalho & Kury 2018; Benavides *et al.* 2021), and 2) its current diagnosis (Soares & Soares 1954: 225) is composed by a few meristic characters that not differentiate apomorphic and plesiomorphic states (Carvalho & Kury 2020). Today, some informal clades are used to discuss the Pachylinae composition, such as Pachylinae s. str. (composed by *Pachylus* Koch, 1839 and immediately related genera; Pinto-da-Rocha *et al.* 2014) and DRMN-group (a stable clade formed by 'false' Pachylinae – *Discocyrtus* s. str., Roeweriinae Carvalho & Kury, 2018 and Neopachylinae Carvalho & Kury, 2020 – most closely related to Mitobatinae Simon, 1879; Carvalho & Kury 2018, 2020). However, a considerable taxonomic effort is still needed to reduce Pachylinae only to its natural core.

The high diversity in Pachylinae can be partially explained because of the existence of many poorly known genera with one (or a few) specie(s) (see Kury 2003a). *Luederwaldtia* Mello-Leitão, 1923 (which remained as a monotypic genus until the beginning of the 21st century) is no exception.

Soares & Soares (1954: 269) published the most recent valid diagnosis for *Luederwaldtia* in the last century, which is only four-lines long. However, this diagnosis overlaps with that *Discocyrtus* Holmberg, 1878, in the same paper. Likewise, the diagnosis of *Discocyrtus* at that time employed broad and ambiguous characters that potentially make *Luederwaldtia* its junior synonym. However, *Luederwaldtia*'s overall status has changed notably since Kury (2003a) realized that it was a preoccupied name and, therefore, invalid, retrieving the name *Lacronia* that has already been proposed as a replacement by Strand (1942); however, overlooked by all subsequent authors. Kury (2003b) presented a new diagnosis for *Lacronia* using modern standards (not only focused on meristic characters, e.g., tarsal counts), and added the descriptions of the new species *Lacronia camboriu* Kury, 2003 and *Lacronia ricardoi* Kury, 2003. That diagnosis was further modified by Kury & Orrico (2006) to include *Lacronia ceci* Kury & Orrico, 2006. As a direct result, the current diagnosis of *Lacronia* 1) removes the possibility of synonymy with *Discocyrtus*, once some diagnostic characters as the division on the dorsal scutum area IV and the armature on legs III (femur and tibia) and IV (coxa and trochanter) are not consistently present in *Discocyrtus*, and 2) three species currently in *Discocyrtus* – *Discocyrtus boraceae* B. Soares, 1942, *Discocyrtus niger* Mello-Leitão, 1923 and *Discocyrtus tenuis* Roewer, 1917 – match the current *Lacronia* diagnosis.

As *Lacronia* was not studied from a cladistic perspective before, the present study aims to test 1) its condition as a clade, 2) its allocation in Pachylinae s. str., and 3) its relation with *Discocyrtus* s. str., a core formed by four/five species closely related to *Discocyrtus testudineus* (Holmberg, 1876), the type species of *Discocyrtus* (Carvalho & Kury 2018, 2022).

In addition, all species considered here as *Lacronia* and described before 2003 are redescribed herein, and some synonymic and geographic notes are provided.

Material and methods

Specimen description parameters

The specimen description parameters follow Carvalho & Kury (2020). Photographs of specimens immersed in alcohol were taken with a stereo microscope Leica M205C coupled to a digital camera Leica DCF450. Scanning electron microscopy (SEM) was carried out with a JEOL JSM-6390LV at the Center for Scanning Electron Microscopy of Museu Nacional/UFRJ. All measurements are reported in millimeters (mm).

The diagnosis at genus rank given here compares *Lacronia*, using as reference Kury & Orrico (2006), and representatives of *Discocyrtus* s. str. At the species rank, we compare a given species of *Lacronia* with the remaining ones of that genus.

Biogeographic units used here follow Morrone's regionalization of the Neotropics ("provinces"; Morrone *et al.* 2022).

Abbreviations of the repositories cited

FMHN = Field Museum of Natural History, Chicago, United States of America;
IBSP = Instituto Butantan, São Paulo, Brazil
INPA = Instituto Nacional de Pesquisas da Amazônia, Manaus, Brazil;
MACN = Museo Argentino de Ciencias Naturales 'Bernardino Rivadavia', Buenos Aires, Argentina
MHNCI = Museu de História Natural Capão da Imbuia, Curitiba, Brazil
MNRJ = Museu Nacional, Universidade Federal do Rio de Janeiro, Rio de Janeiro, Brazil
MNRJ-HS = private collection of Helia Soares (included in MNRJ collection)
MZSP = Museu de Zoologia, Universidade de São Paulo, São Paulo, Brazil
SMF = Naturmuseum Senckenberg Sektion Arachnologie, Frankfurt am Main, Germany

The material lost in the MNRJ's 2018 fire (see Kury *et al.* 2018) is indicated by a ! signal in the text.

Other abbreviations used

AL = abdominal scutum length
AS = abdominal scutum
AW = abdominal scutum maximum width
CL = carapace length
Cl = claw
CW = carapace maximum width
Cx = coxa
DS = dorsal scutum
Fe = femur
MS A1–A3 = basal macrosetae of VP
MS B1 = ventro-basal macrosetae of VP
MS C1–C3 = distal macrosetae of VP
MS D1 = dorso-lateral subdistal small setae of VP
MS E1–E2 = ventro-distal macrosetae of VP
Mt = metatarsus
Pa = patella
Pp = pedipalp
Ta = tarsus
Ti = tibia
Tr = trochanter
VP = ventral plate (penis) U

Tarsal formula: numbers of tarsomeres in tarsus I to IV (Tables 4–7), when an individual count is given, are ordered from left to right side (figures in parentheses denote number of tarsomeres only in the distitarsi I–II).

Phylogenetic analysis

Choice of terminals

The analysis' primary target is to test the monophyly of *Lacronia*: hence, it includes 1) the four species that currently composes *Lacronia* (*L. camboriu*, *L. ceci*, *L. ricardoi* and *L. serripes*), and 2) three species, currently in *Discocyrtus*, but that we consider as putative members of *Lacronia* (*D. boraceae*, *D. niger* and *D. tenuis*). Because *Lacronia* presents characters that resembles DRMN-group taxa (mainly by diagnostical characters on the male genitalia, as the shape and ornamentation

of its stylus and ventral process), we include the following species as outgroups (as characterized in Carvalho & Kury 2020): 1) four representatives of *Discocyrtus* s. str. – *Discocyrtus crenulatus* Roewer, 1913, *Discocyrtus flavigranulatus* Soares, 1944, *Discocyrtus moraesianus* Mello-Leitão, 1923 and *Discocyrtus testudineus* (Holmberg, 1876) (type-species of *Discocyrtus*); 2) six representatives of Roeweriinae Carvalho & Kury, 2018 – *Amazochroma carvalhoi* (Mello-Leitão, 1941), *Amazochroma pedroi* (Carvalho & Kury, 2018), *Discocyrtanus goyazius* Roewer, 1929, *Discocyrtanus pertenuis* (Mello-Leitão, 1935), *Roeweria bittencourti* Mello-Leitão, 1923 and *Roeweria virescens* (Mello-Leitão, 1940); 3) two representatives of Mitobatinae Simon, 1879 – *Mitobates triangulus* Sundevall, 1833 and *Mitobatula castanea* Roewer, 1931; 4) six representatives of Neopachylinae Carvalho & Kury, 2020 – *Neopachylus bellicosus* Roewer, 1913, *Neopachylus imaguirei* Soares & Soares, 1947, *Pachylobos littoralis* (Mello-Leitão, 1932), *Pachylobos longicornis* (Mello-Leitão, 1922), *Senu leonardosi* (Mello-Leitão, 1935) and *Senu vestita* (Mello-Leitão, 1922). As *Lacronia* nowadays is nested in Pachylinae, we also used two representatives of Pachylinae s. str., as defined by Pinto-da-Rocha *et al.* (2014) and Benavides *et al.* (2021): *Acanthopachylus aculeatus* (Kirby, 1819) and *Pachylus chilensis* (Gray, 1833). The other members of Gonyleptidae used here as outgroups are 1) *Goniosoma varium* Perty, 1833, type species of the type genus of Goniosomatinae Mello-Leitão, 1935, sister-group of DRMN-group in Carvalho & Kury (2020, 2021b), and 2) *Gonyleptes horridus* Kirby, 1818, type species of the type genus of Gonyleptidae. As Carvalho & Kury (2018, 2020, 2021b) presented, we used *Ampycus telifer* (Butler, 1873, type species of Ampycidae Kury, 2003) to root our analysis. The specimen vouchers for the all outgroups used in the analyses are resumed in Table 1.

Maximum parsimony (MP) analysis

The character states were organized in a matrix using Mesquite ver. 3.10 (Maddison & Maddison 2017, available at: http://mesquiteproject.org). The annotated list of characters is in Table 2. The matrix of characters states and terminals (30 taxa; 115 characters; 2962 scorings; 488 missing data) is in Table 3. Trees were searched in TNT (Goloboff & Catalano 2016) using parsimony under equal weights and implied weights (Goloboff *et al.* 2008), traditional search algorithm and with tree bisection-reconnection (TBR branch-swapping). Space was allocated for 99 999 trees in memory, and 100 replicates with 10 000 trees each were carried out. To evaluate the stability of results under different concavity values, we followed Mendes (2011) protocol. We used nine different concavity values (k = 1, 2, 3, 4, 5, 6, 10, 15, 20) and the results were summarized on space plots (Navajo rugs) in Fig. 1. The branch-support was estimated using Absolute symmetric frequencies (SFq) (10 000 replicates, cut = 50, change probability = 33). The data substantiation was valued with absolute Bremer (or branch) support, aka "decay index" (Bremer 1994). Both parameters were calculated using TNT and are shown in Fig. 1. The tree which presented the shortest number of steps (and obtained most often during the analysis) was chosen for discussion in Figs 1–2. Its character distribution was accessed with WINCLADA and optimized using ACCTRAN (Nixon 2002, available at: http://www.cladistics.com) (Fig. 2). Most of the characters used here were retrieved from papers that discussed the internal relationships of DRMN (Carvalho & Kury 2020, 2021b, 2022; Carvalho *et al*. 2021) and modified when necessary to codify the character states of *Lacronia* members. When a character state is cited throughout the text to describe some relevant pattern, it is presented by the character number between square brackets and the associated character state between parentheses.

Results

Results of the phylogenetic analysis

MP analysis yielded 1) a single tree for k-values = 1, 4, 5, 6, 10, 15 and 20, and 2) two trees for k-values = 2 and 3. The summary of those results with indication of supraspecific groups is in Fig. 1, and the characters are mapped in Fig. 2. The consistency index (CI), retention index (RI) and the number of steps of these trees are summarized in Table 4. The discussion is based on the parsimonious tree (recovered by k-values = 3, 4, 5, 6, 10, 15 and 20).

Table 1. List of the outgroup species (with specimen vouchers) selected for the present cladistic analysis.

Subfamily/Group	Species	Voucher (♂)	Voucher (♀)
Ampycinae	*Ampycus telifer* (Butler, 1873)	FMHN!	FMHN!
Discocyrtus s. str.	*Discocyrtus crenulatus* (Roewer, 1913	SMF 1440	SMF 1439
Discocyrtus s. str.	*Discocyrtus flavigranulatus* Soares, 1944	MNRJ 723	MNRJ 723
Discocyrtus s. str.	*Discocyrtus moraesianus* Mello-Leitão, 1923	MNRJ 163	MNRJ 163
Discocyrtus s. str.	*Discocyrtus testudineus* (Holmberg, 1876)	MACN 41506	MACN 41506
Goniosomatinae	*Goniosoma varium* Perty, 1833	MNRJ 58930	MNRJ 58930
Gonyleptinae	*Gonyleptes horridus* Kirby, 1819	MNRJ 293	MNRJ 293
Mitobatinae	*Mitobates triangulus* Sundevall, 1833	MNRJ 59010	MNRJ 59010
Mitobatinae	*Mitobatula castanea* (Roewer, 1931)	MNRJ 332	MNRJ 332
Neopachylinae	*Neopachylus bellicosus* Roewer, 1913	MZSP 30815	MZSP 30815
Neopachylinae	*Neopachylus imaguirei* Soares & Soares, 1947	MNRJ 2531!	MNRJ 2531!
Neopachylinae	*Pachylobos littoralis* (Mello-Leitão, 1932)	IBSP 9478	MZSP 18639
Neopachylinae	*Pachylobos longicornis* (Mello-Leitão, 1922)	MZSP 17657	MZSP 17657
Neopachylinae	*Senu leonardosi* (Mello-Leitão, 1935)	MZSP 14017	MZSP 14017
Neopachylinae	*Senu vestita* (Mello-Leitão, 1922)	MZSP 14404	MZSP 459
Pachylinae	*Acanthopachylus aculeatus* (Kirby, 1819)	MNRJ-HS 76!	MNRJ-HS 76!
Pachylinae	*Pachylus chilensis* (Gray, 1833)	MNRJ 1384!	MNRJ 1384!
Roeweriinae	*Amazochroma carvalhoi* (Mello-Leitão, 1941)	INPA OP 2730	INPA OP 2730
Roeweriinae	*Amazochroma pedroi* Carvalho & Kury, 2018	MNRJ 7631!	MNRJ 9267!
Roeweriinae	*Discocyrtanus goyazius* Roewer, 1929	MHNCI 6551	MHNCI 6551
Roeweriinae	*Discocyrtanus pertenuis* (Mello-Leitão, 1935)	IBSP 12132	IBSP 12132
Roeweriinae	*Roeweria bittencourti* Mello-Leitão, 1923	IBSP 5250	IBSP 5241
Roeweriinae	*Roeweria virescens* (Mello-Leitão, 1940)	MNRJ 60552	MNRJ 60552

Table 2 (continued on next eight pages). List of character descriptions and states used herein in the cladistic analysis of *Lacronia* Strand, 1942.

1. Penis, macrosetae A, insertion on VP
- (0) lateral (Fig. 8B)
- (1) dorsal (Bragagnolo & Pinto-da-Rocha 2009: fig. 5b)

2. Penis, podium, relative position to the ventral plate
- (0) reaching distally half or more of the ventral plate height longitudinally
- (1) reaching distally third of the ventral plate height longitudinally (Fig. 8B)

3. Penis, glans, pedestal
- (0) absent (Bragagnolo & Pinto-da-Rocha 2009: fig. 5l)
- (1) present (Fig. 8B)

4. Penis, glans, pedestal, insertion angle of the stylus on the pedestal
- (0) 90°
- (1) more than 90°
- (2) 45° (Fig. 8B)

5. Penis, glans, stylus, stem, shape
- (0) medially inclined 45° to ventral portion
- (1) with subapical curvature, ventrally oriented
- (2) dorsoventrally flattened
- (3) sigmoid and longitudinally elongated
- (4) sigmoid (Kury & Carvalho 2016: fig. 9f)
- (5) straight (Fig. 20B)
- (6) with subapical curvature, dorsally oriented (Carvalho & Kury 2020: fig. 10d)
- (7) ventrally convex (Bragagnolo & Pinto-da-Rocha 2009: fig. 5f)

6. Penis, glans, stylus, stem, distal or medial spines
- (0) absent (Bragagnolo & Pinto-da-Rocha 2009: fig. 5f)
- (1) present (Fig. 11D)

7. Penis, glans, stylus, stem, distal or medial spines, occurrence
- (0) ventral portion (Fig. 11D)
- (1) dorsal portion

8. Penis, glans, stylus, apical portion, shape
- (0) laterally flattened
- (1) transversely flattened (Carvalho & Kury 2018: figs 6f–g)
- (2) without an undifferentiated apex (Fig. 20A)
- (3) plateau with dorsal curvature (Carvalho & Kury 2020: fig. 10d)
- (4) as a tubular process, dorsally curved
- (5) swollen (full diameter) in relation to the stem (Fig. 18B)
- (6) swollen (only in dorsal portion) in relation to the stem

9. Penis, glans, stylus, apical winglets
- (0) absent (Fig. 8D)
- (1) present (Kury & Carvalho 2016: fig. 9e–g)

10. Penis, glans, stylus, apical winglets, spines
- (0) absent (Bragagnolo & Pinto-da-Rocha 2009: fig. 6a–c)
- (1) present (Kury & Carvalho 2016: fig. 9e–g)

11. Penis, glans, stylus, apical portion covered by spines
- (0) absent (Carvalho & Kury 2018: fig. 6g)
- (1) present (Kury & Carvalho 2016: fig. 9e–g)

12. Penis, glans, ventral process
- (0) conspicuously reduced or absent (Bragagnolo & Pinto-da-Rocha 2009: fig. 5b)
- (1) present (Fig. 8B)

Table 2 (continued).

13. Penis, glans, ventral process, composition
(0) not forming a stem
(1) stem plus flabellum (Fig. 8B)
14. Penis, glans, ventral process, shape of the stem
(0) inverted subconical
(1) tubular (Fig. 8B)
15. Penis, glans, ventral process, shape of the stem, tubular, pattern of curvature
(0) straight or with one curve on proximal half (Fig. 11D)
(1) sigmoid, with two conspicuous curves (Carvalho & Kury 2020: fig. 15d)
16. Penis, glans, ventral process, flabellum, frame
(0) middle axis (Fig. 8D)
(1) double V-shaped axis
17. Penis, glans, ventral process, flabellum, middle axis, type
(0) scallop-shaped (Fig. 8D)
(1) hand-shaped (Carvalho & Kury 2020: fig. 10d)
(2) inconspicuous, undifferentiated apex
(3) fan-shaped
18. Penis, glans, ventral process, flabellum, mono-frame, scallop-shaped, type
(0) bent to the basal portion (Fig. 8B)
(1) straight, sub-parallel to the stylus (Fig. 18D)
19. Penis, glans, ventral process, flabellum, mono-frame, type of ornamentation
(0) continuous serrulation (Fig. 8D)
(1) discrete spines (Carvalho & Kury 2020: fig. 18e)
20. Penis, glans, ventral process, diameter
(0) wider than the stylus
(1) a third or less than the stylus (Carvalho & Kury 2020: fig. 15a)
(2) same diameter of the stylus diameter (Fig. 8B)
21. Penis, glans, ventral process, length compared to the stylus
(0) lower than the stylus
(1) equal or higher than the stylus (Fig. 11D)
22. Penis, ventral plate, lateral outlines of the basal half
(0) straight
(1) elliptical (Fig. 8A)
(2) diagonal, narrowing basally (Kury & Carvalho 2016: fig. 8a)
23. Penis, ventral plate, outline of the basal half elliptical, laterally expanded than distal part
(0) absent (Fig. 8A)
(1) present (Carvalho & Kury 2018: fig. 6a–b)
24. Penis, ventral plate, basal convex format (in lateral view)
(0) absent
(1) present (Fig. 8B)
25. Penis, ventral plate, distal portion without a groove, type
(0) trapezoidal (widest apically) (Fig. 8A)
(1) trapezoidal (narrower apically) (Fig. 18A)
26. Penis, ventral plate, macrosetae A on the ventral plate's central part
(0) absent (Carvalho & Kury 2020: fig. 15c)
(1) present (Fig. 8A)

Table 2 (continued).

27. Penis, ventral plate, macrosetae B1
(0) absent
(1) present (Fig. 8C)
28. Penis, ventral plate, macrosetae B1, type
(0) only the apical portion exposed (Carvalho & Kury 2020: fig. 15c)
(1) more than the apical portion exposed (Fig. 8C)
29. Penis, ventral plate, macrosetae C1–C3, insertion
(0) all placed distally, united (Fig. 11A)
(1) C3 is set widely apart from the other C, forming a diastema (Carvalho & Kury 2018: fig. 6a–b)
(2) all placed distally with subequal intervals between them
30. Penis, ventral plate, macrosetae C, diameter
(0) same diameter between macrosetae A and C (Fig. 11A)
(1) macrosetae A 0.001 mm thicker than the C
(2) macrosetae A 0.002 mm thicker than the C
(3) macrosetae A 0.003+ mm thicker than the C (Kury & Carvalho 2016: fig. 8c)
(4) macrosetae C thicker than the A (Carvalho & Kury 2020: fig. 10b)
31. Penis, ventral plate, macrosetae C, length
(0) 0,06 mm or more (Kury & Carvalho 2016: fig. 8C)
(1) between 0,04 and 0,05 mm (Fig. 11A) (2) less than 0,035 mm
32. Penis, ventral plate, macrosetae E, longitudinal distribution pattern
(0) macrosetae E2 ventrally posterior the range of distribution of macrosetae C (Fig. 8C)
(1) macrosetae E ventrally among the range of distribution of macrosetae C (Carvalho & Kury 2018: fig. 6d)
(2) macrosetae E1 ventrally anterior of the range of distribution of macrosetae C (Carvalho & Kury 2020: fig. 15c)
33. Penis, ventral plate, shape of the field of type 1 microsetae
(0) field strongly reduced to a pair of latero-basal patches
(1) field entire, occupying most of VP (Fig. 8C)
(2) field restricted to the proximal third of VP (Bragagnolo & Pinto-da-Rocha 2009: fig. 8c)
34. Chelicera, basal article, relation with the DS anterior margin
(0) covered mainly by the DS anterior margin
(1) well-exposed (Fig. 17A)
35. Chelicerae, bulla, proximal margin, spines
(0) absent
(1) present (Fig. 19A)
36. Chelicerae, bulla, proximal margin, spines, mesal face, quantity
(0) one
(1) two (Kury & Carvalho 2016: fig. 5a)
37. Chelicerae, bulla, proximal margin, spines, ectal face, quantity
(0) one (Fig. 19A)
(1) two (Kury & Carvalho 2016: fig. 5a)
38. Pedipalpus, femur, quantity of the ventral spines
(0) a proximal spine (Kury & Orrico 2006: fig: 4)
(1) two spines
(2) three spines
(3) four spines

Table 2 (continued).

39. Ocularium, position on the carapace in relation to the insertion of legs
(0) at second pair of legs
(1) between the second and third pairs of legs (Fig. 19A)
(2) at third pair of legs
40. Ocularium, roof shape (in frontal view)
(0) convex, without depression (Fig. 19B)
(1) convex, with medial depression (Kury & Carvalho 2016: fig. 3d)
(2) straight, without depression
41. Ocularium, height (in lateral view)
(0) twice the diameter of the eyes (Kury & Carvalho 2016: fig. 3m)
(1) thrice or more the diameter of the eyes (Fig. 19B)
42. Ocularium, armature, quantity of spines or tubercles
(0) one (Carvalho & Kury 2018: fig. 10d)
1 two (Fig. 19B)
43. Ocularium, armature, pair, relation between the spines or tubercles
(0) independent (Kury & Orrico 2006: fig: 3)
(1) fused at the base (Fig. 19B)
44. Dorsal scutum of male, outline, shape
(0) gamma pyriform, *Eusarcus*-like (Kury & Medrano 2016: fig. 1t)
(1) gamma pyriform, *Acanthogonyleptes*-like (Kury & Medrano 2016: fig. 1v)
(2) gamma pyriform, *Gonyleptes*-like (Kury & Medrano 2016: fig. 1u)
(3) gamma pyriform, *Acanthogonyleptes*-like, with posterior curvature more convex than the original (Carvalho & Kury 2022: fig. 4f)
(4) gamma (Kury & Medrano 2016: fig. 1q)
(5) gamma triangular (Kury & Medrano 2016: fig. 1w)
(6) beta (Kury & Medrano 2016: fig. 1j)
(7) lambda (Kury & Medrano 2016: fig. 1x)
45. Dorsal scutum, dry marks
(0) absent (Fig. 3E)
(1) present (Carvalho & Kury 2020: fig. 1e–g)
46. Dorsal scutum, dry marks, distribution on mesotergum
(0) on the margins of areas I–III
(1) around the tubercles all over the mesotergum (Carvalho & Kury 2018: fig. 1a–f)
(2) restricted to the tip of tubercles all over the mesotergum (Kury & Carvalho 2016: fig. 1e)
(3) forming a Y-inverted pattern on the mesotergum (Carvalho & Kury 2020: fig. 1e–g)
47. Dorsal scutum, lateral margins, color
(0) matching with the mesotergum's (Fig. 3E)
(1) contrasting with the mesotergum's (Carvalho & Kury 2018: fig. 10e)
48. Dorsal scutum, mesotergum, 'wet' marks
(0) absent (Carvalho & Kury 2022: fig. 1a)
(1) present (Fig. 3E)
49. Dorsal scutum, mesotergum, 'wet' marks, type
(0) band-shaped (Fig. 4B–C)
(1) areolate pattern of spots (Fig. 4F–G)
50. Dorsal scutum, mesotergum, areolate pattern of spots, type
(0) cross-shaped
(1) on all areas of mesotergum, only absent on the lateral borders of the areas I–II (Fig. 4F–G)
(2) on all areas of mesotergum, full extension (Carvalho & Kury 2018: fig. 10b)

Table 2 (continued).

51. Dorsal scutum, mesotergum, tubercles' color contrasting with the background
(0) absent (Carvalho & Kury 2018: fig. 1b)
(1) present (Fig. 4D)
52. Dorsal scutum, mesotergum, width of the grooves between the areas
(0) very narrow, not clearly visible (Fig. 10D)
(1) ordinary, visible (Fig. 4A–G)
53. Dorsal scutum, mesotergum, area I, distribution pattern of tubercles
(0) transversal posterior row of 5–6 tubercles
(1) diffused ordinary tubercles on all area extension (Fig. 4E)
(2) pair of conspicuous tubercles (Fig. 4B)
(3) two pairs of conspicuous tubercles (Fig. 4G)
(4) three pairs of conspicuous tubercles (Carvalho & Kury 2020: fig. 9a)
54. Dorsal scutum, mesotergum, relation between the lateral margins of areas I (posterior) and II (anterior)
(0) anterior corners of area II not embracing area I (Fig. 4A)
(1) anterior corners of area II embracing area I (Fig. 4B–G)
55. Dorsal scutum, mesotergum, area II, tubercles
(0) absent (Fig. 4B–C)
(1) present (Fig. 4A, D–G)
56. Dorsal scutum, mesotergum, area II, distribution pattern of tubercles
(0) transversely row in all medial extension (Carvalho & Kury 2020: fig. 9a)
(1) two pairs of conspicuous tubercles (Fig. 4D)
(2) two anterior and six posterior tubercles (Carvalho & Kury 2018: fig. 7a)
(3) inconspicuous, without a clear pattern
(4) four anterior and six posterior tubercles
(5) a pair of conspicuous tubercles
(6) two anterior and eight posterior tubercles
57. Dorsal scutum, mesotergum, relation between the lateral margins of areas II (posterior) and III (anterior)
(0) posterior corners of area II not embracing area III (Fig. 4B–C)
(1) posterior corners of area II embracing area III (Fig. 4F–G)
58. Dorsal scutum, mesotergum, area III, prominent tubercles (in relation to ordinary ones) between the paramedian armature
(0) absent (Fig. 4B)
(1) present (Fig. 4D)
59. Dorsal scutum, mesotergum, area III, prominent tubercles (in relation to ordinary ones) between the paramedian large armature, quantity
(0) one pair (Fig. 4F–G)
(1) two pairs (Fig. 4A)
(2) three pairs
60. Dorsal scutum, mesotergum, area III, paramedian armature, type
(0) acuminated tubercles (Fig. 3H)
(1) spine(s) (Fig. 4F–G)
(2) domes (Carvalho & Kury 2020: fig. 9c)
61. Dorsal scutum, mesotergum, area III, paramedian armature, acuminated tubercles, shape
(0) without any inflection
(1) with inflection to the posterior portion

Table 2 (continued).

62. Dorsal scutum, mesotergum, area III, paramedian armature, domes, shape (in dorsal view) and height
(0) ellipses with little height (Carvalho & Kury 2018: fig. 10d)
(1) circular, slight compressed on the sides (Carvalho & Kury 2018: fig. 7a)
(2) circular, longitudinally elliptic
(3) almost forming a cylinder
(4) circular, almost forming a globe (Carvalho & Kury 2018: fig. 9a)
63. Dorsal scutum, mesotergum, area III, paramedian armature, spine(s), shape
(0) with medial constriction and rounded apex
(1) conical with rounded apex (Fig. 4A)
(2) with slight distal inflection to ventral portion, pointy apex (Fig. 17A, D)
(3) straight, pointy apex (Fig. 19A, D)
64. Dorsal scutum, mesotergum, area III, prominent pair of tubercles placed ectally to the paramedian large armature
(0) absent (Carvalho & Kury 2018: fig. 10d)
(1) present (Fig. 4B–D)
65. Dorsal scutum, mesotergum, area IV, longitudinal medial division
(0) absent (Fig. 4A)
(1) present (Fig. 4D)
66. Dorsal scutum, mesotergum, area IV posterior middle area
(0) invading area V (Fig. 4E)
(1) sub-straight (Fig. 4A)
(2) invaginating (area V antero-middle portion invading area IV) (Carvalho & Kury 2018: fig. 10c)
67. Free tergites IIII, conspicuous tubercles, type
(0) uniform row on all transversal extension (Fig. 4D)
(1) a prominent pair on the paramedian portion (Fig. 4F)
(2) a transversal row on all the extension, without armature on the medial portion
(3) increasing size towards the middle (Fig. 4A)
68. Ventral area, width proportion between the Cx I–III area and Cx IV (in situ)
(0) Cx IV twice larger than the sum of Cx I–III
(1) Cx IV thrice larger than the Cx I–III
(2) same proportion between them
69. Ventral area, coxa I, distance between the spines in the longitudinal row of spines
(0) transversely juxtaposed
(1) transversal row in regular intervals
70. Ventral area, coxa II, medial invasion by coxa I
(0) absent (Fig. 15C)
(1) present
71. Ventral area, coxa II, medial invasion by coxa III
(0) absent (Fig. 15C)
(1) present
72. Legs (most markedly III–IV), trichromatic striped pattern (yellow, black and red)
(0) absent (Fig. 3E–H)
(1) present (Carvalho & Kury 2020: fig. 1a)
73. Leg II, coxa, prodorsal proximal spine
(0) conical, geminated, anterior largest and swollen
(1) triad, central largest and swollen

Table 2 (continued).

(2) conical, not geminated
(3) conical, geminated, posterior largest and swollen

74. Leg II, femur, retro-dorsal distal spur
(0) absent (Carvalho & Kury 2020: fig. 11c)
(1) present (Fig. 3E)

75. Leg II, femur, retro-dorsal distal spur length, cx II apical width ratio
(0) approximately a third (Carvalho & Kury 2018: fig. 1b)
(1) approximately a half (Fig. 3E)

76. Leg III, femur, curvature
(0) straight (Carvalho & Kury 2020: fig. 10f)
(1) sinuous (Fig. 7D)

77. Leg III, femur, diameter
(0) 1.5× the diameter of femur II (Carvalho & Kury 2020: fig. 10f)
(1) 2.0× or more the diameter of femur II (Fig. 10A)

78. Leg III, femur, retro-dorsal distal spur
(0) absent (Carvalho & Kury 2020: fig. 8a)
(1) present (Fig. 7D)

79. Leg III, tibia, shape
(0) cylindrical (Carvalho & Kury 2022: fig. 1e)
(1) mace-shaped (Fig. 19E)

80. Leg III, tibia, proventral and retro-ventral rows of spines
(0) absent (Carvalho & Kury 2022: fig. 1e)
(1) present (Fig. 19E)

81. Leg IV, coxa, sides orientation in relation to the body main axis
(0) oblique (Fig. 19A)
(1) parallel (Carvalho & Kury 2022: fig. 4f)

82. Leg IV, coxa, prolateral margin, tubercles
(0) absent (Carvalho & Kury 2020: fig. 10d)
(1) present (Fig. 19A)

83. Leg IV, coxa, prolateral margin, tubercles, apex shape
(0) convex
(1) acuminated (Fig. 19A)

84. Leg IV, coxa, dorso-apical apophysis
(0) absent (Fig. 19A)
(1) present (Carvalho & Kury 2020: fig. 20a)

85. Leg IV, coxa, prodorsal apophysis, basal thickness compared to the central portion
(0) approximately the same (Fig. 12A)
(1) swollen (Carvalho & Kury 2022: fig. 4f)

86. Leg IV, coxa, prodorsal apophysis, posterior margin, shape
(0) flat, without any projection (Carvalho & Kury 2020: fig. 14a)
(1) with a central rectangular projection (Kury & Carvalho 2016: fig. 5a)
(2) crenated on the apical portion (Fig. 17A)

87. Leg IV, coxa, prodorsal apophysis, distal portion, angle in relation to the body axis
(0) obtuse, more than 90° (Carvalho & Kury 2018: fig. 5a)
(1) near to 90° (Fig. 17A)

88. Leg IV, coxa, retro-lateral apophysis
(0) absent (Carvalho & Kury 2018: fig. 7a)
(1) present (Fig. 17A)

Table 2 (continued).

89. Leg IV, coxa, retro-lateral apophysis, size compared to prodorsal distal apophysis
(0) shorter, with a tiny geminated branch (Fig. 17A)
(1) shorter, as a single branch (Carvalho & Kury 2018: fig. 5a)
(2) larger
90. Leg IV, trochanter, shape (in dorsal view)
(0) trapezoidal (distal side widest)
(1) trapezoidal (proximal side widest) (Carvalho & Kury 2018: fig. 10d)
(2) approximately quadrangular (Fig. 12G)
(3) rectangular (Carvalho & Kury 2020: fig. 20a)
91. Leg IV, trochanter, Tr IV:Tr III width ratio
(0) less than or equal to 1.5× (Fig. 12A)
(1) 2× or more (Carvalho & Kury 2020: fig. 20a)
92. Leg IV, trochanter, prolateral proximal apophysis
(0) absent (Carvalho & Kury 2018: fig. 10f)
(1) present (Fig. 12G)
93. Leg IV, trochanter, prolateral proximal apophysis, shape
(0) canine tooth
(1) isosceles triangle (Fig. 7A)
(2) hook-shaped (Fig. 15A)
(3) equilateral triangle
(4) isosceles triangle, with a central short sub-conical projection (Fig. 17A)
94. Leg IV, trochanter, prolateral proximal apophysis, isosceles triangle, distal curvature to the dorsal portion
(0) absent
(1) present (Fig. 7A)
95. Leg IV, trochanter, prolateral medial apophysis
(0) absent
(1) conspicuous
96. Leg IV, trochanter, retro-lateral proximal apophysis
(0) absent (Kury & Carvalho 2016: fig. 5a)
(1) conspicuous (Carvalho & Kury 2018: fig. 7a)
97. Leg IV, femur, Fe IV:Fe III average diameter ratio
(0) approsimately the same (Carvalho & Kury 2020: fig. 10f)
(1) larger (Carvalho & Kury 2020: fig. 10d)
98. Leg IV, femur, proximal: distal diameter ratio
(0) approximately the same (Fig. 17F)
(1) proximal larger than proximal
(2) distal larger than proximal (Fig. 19F)
99. Leg IV, femur, shape (in dorsal view)
(0) C-shaped, dorsal concavity (Carvalho & Kury 2018: fig. 5e–f)
(1) approximately straight (Fig. 17F–I)
(2) S-shaped, sinuous (Kury & Carvalho 2016: fig. 2d)
(3) C-shaped, prolateral concavity (Carvalho & Kury 2018: fig. 10c)
(4) entirely straight (Carvalho & Kury 2018: fig. 10f)
100. Leg IV, femur, dorsal face, armature between the proximal and medial portions
(0) absent (Carvalho & Kury 2018: fig. 5a)
(1) present (Fig. 19F)

Table 2 (continued).

101. Leg IV, femur, dorsal face, armature between the proximal and medial portions, type
(0) comb of spines (Kury & Carvalho 2016: fig. 2d)
(1) one or two spines (Carvalho & Kury 2018: fig. 10c)
(2) one to three spines, curved retro-laterad (Carvalho & Kury 2020: fig. 14d)
(3) three or four acuminated tubercles (Fig. 19F)
102. Leg IV, femur, dorsal portion, armature between the medial and distal portions
(0) absent (Carvalho & Kury 2018: fig. 5a)
(1) present (Fig. 19F)
103. Leg IV, femur, prodorsal distal spur
(0) absent (Kury & Carvalho 2016: fig. 2d)
(1) present (Fig. 12G)
104. Leg IV, femur, retro-lateral face, armature between the proximal-medial and distal portions
(0) absent (Fig. 15C)
(1) present (Fig. 12G)
105. Leg IV, femur, retro-lateral portion, armature between the proximal-medial and distal portions, type
(0) comb of spines, almost united (Carvalho & Kury 2018: fig. 7e–f)
(1) comb of spine, spaced in equal intervals (Fig. 12G)
106. Leg IV, femur, retro-lateral face, medial–distal spine
(0) absent
(1) present (Carvalho & Kury 2020: fig. 20d, f)
107. Leg IV, patella, dorsal face, prominent acuminated tubercles
(0) absent (Kury & Carvalho 2016: fig. 2c)
(1) present (Fig. 12G)
108. Leg IV, patella, proventral distal spur
(0) absent (Carvalho & Kury 2020: fig. 20f)
(1) present (Fig. 12H)
109. Leg IV, patella, proventral distal spur, length:width ratio
(0) approximately a fifth (Carvalho & Kury 2020: fig. 14f)
(1) approximately a third (Fig. 12H)
110. Leg IV, patella, retro-ventral row of tubercles
(0) absent
(1) present (Fig. 19H)
111. Leg IV, patella, retro-ventral portion, medial–distal armature
(0) absent
(1) present (Fig. 12I–J)
112. Leg IV, patella, retro-ventral portion, medial–distal armature, type
(0) two-three tiny similar sized spines
(1) two-three developed spines of different sizes (Fig. 12I–J)
113. Leg IV, tibia, dorsal portion, type of armature
(0) tubercles (Carvalho & Kury 2020: fig. 9d–e)
(1) spines (Fig. 19F–G, I)
114. Leg IV, tibia, dorsal portion, type of tubercles
(0) blunt (Carvalho & Kury 2020: fig. 20d–e)
(1) acuminated (Fig. 17F–G)
115. Leg IV, metatarsus, dorsal portion, dorsal row of spines
(0) absent (Carvalho & Kury 2020: fig. 14h)
(1) present (Fig. 17J)

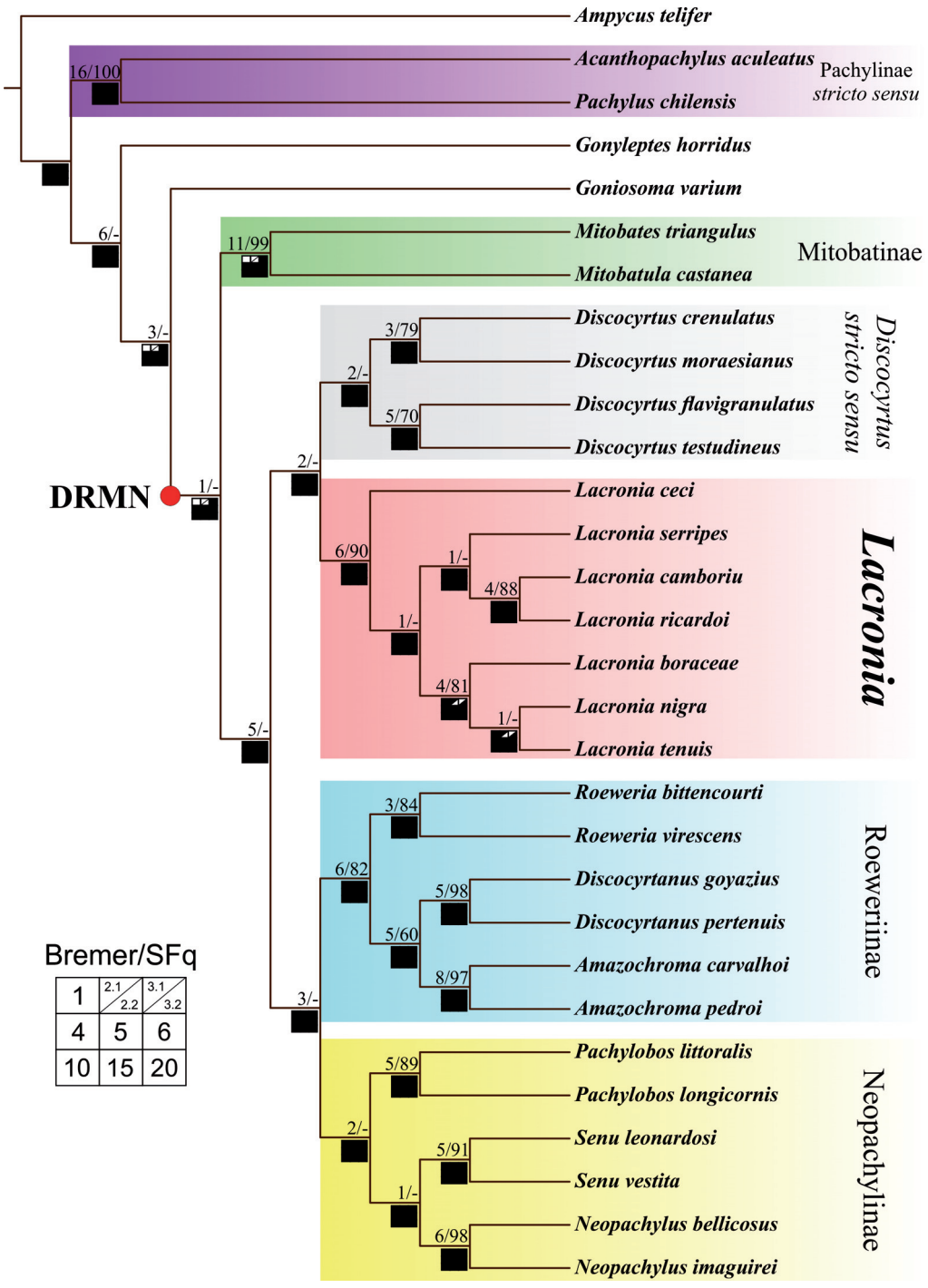

Fig. 1. The most frequent tree (k-values = 3, 4, 5, 6, 10, 15 and 20) retrieved using the Mendes (2011) protocol. Clade support values are indicated above the branches (Bremer index / SFq values). Clade stability is indicated below the branches by the sensitivity plots ('Navajo rugs'), which denotes the tested k-values (black squares indicate monophyly; white squares indicate non-monophyly). The k-values (= 2 and 3) retrieved two different trees, represented here as 2.1, 2.2, 3.1 and 3.2. in the Navajo rugs. Colored backgrounds indicate the following groups: *Discocyrtus* Holmberg, 1878 s. str. (grey), *Lacronia* Strand, 1942 (salmon), Mitobatinae Simon, 1879 (green), Neopachylinae Carvalho & Kury, 2020 (yellow), Pachylinae Sørensen, 1884 s. str. (purple) and Roeweriinae Carvalho & Kury, 2018 (blue). A red circle marks the DRMN-group. The unmarked groups are not members of either DRMN or Pachylinae s. str.

Table 3 (continued on next three pages). Matrix of characters used herein for the cladistic analysis presented here.

	01	02	03	04	05	06	07	08	09	10	11	12	13	14	15	16	17	18	19	20	21	22	23	24	25	26	27	28	29	30
Ampycus telifer	1	0	1	0	0	0	?	0	0	0	0	0	–	–	–	–	–	–	–	–	0	2	–	0	–	0	1	1	2	3
Acanthopachylus aculeatus	0	0	1	1	1	0	?	0	0	–	0	1	0	–	–	–	–	–	–	–	0	0	–	0	0	0	0	–	0	0
Pachylus chilensis	0	0	1	1	1	0	?	0	0	–	0	1	0	–	–	–	–	–	–	–	0	0	–	0	0	0	0	–	0	0
Gonyleptes horridus	0	1	1	0	3	0	?	3	0	–	0	1	1	1	?	0	3	–	?	0	1	1	0	1	–	0	1	1	0	0
Goniosoma varium	0	1	1	0	3	0	?	4	0	–	0	1	1	?	–	0	?	–	–	–	1	1	0	1	0	0	1	1	2	0
Discocyrtus crenulatus	0	1	1	2	5	1	0	2	0	–	0	1	1	1	0	0	0	0	0	2	1	1	0	1	0	0	1	1	0	0
Discocyrtus flavigranulatus	0	1	1	2	5	1	0	2	0	–	0	1	1	1	0	0	0	0	0	2	1	1	0	1	0	1	1	0	0	2
Discocyrtus moraesianus	0	1	1	2	5	1	0	2	0	–	0	1	1	1	0	0	0	0	0	2	1	1	0	1	0	0	1	0	0	0
Discocyrtus testudineus	0	1	1	2	5	1	0	2	0	–	0	1	1	1	0	0	0	0	0	2	1	1	0	1	0	1	1	0	0	2
Mitobates triangulus	0	1	1	0	2	1	1	6	0	–	0	1	1	0	–	1	–	–	–	0	1	1	0	1	–	0	1	0	0	1
Mitobatula castanea	0	1	1	0	2	1	1	6	0	–	0	1	1	0	–	1	–	–	–	0	1	1	0	1	–	0	1	0	0	1
Neopachylus bellicosus	0	1	1	2	6	0	?	3	0	–	1	1	1	1	0	0	2	–	1	1	1	1	0	1	0	0	1	0	2	1
Neopachylus imaguirei	0	1	1	2	6	0	?	3	0	–	1	1	1	1	0	0	1	–	1	1	1	1	0	1	0	0	1	0	2	1
Pachylobos littoralis	0	1	1	2	6	0	?	3	0	–	1	1	1	1	1	0	1	–	1	1	1	1	0	1	0	0	1	0	0	4
Pachylobos longicornis	0	1	1	2	6	0	?	3	0	–	1	1	1	1	1	0	1	–	1	1	1	1	0	1	0	0	1	0	0	4
Senu leonardosi	0	1	1	2	6	0	?	3	0	–	1	1	1	1	0	0	1	–	1	1	1	1	0	1	0	0	1	1	0	4
Senu vestita	0	1	1	2	6	0	?	3	0	–	1	1	1	1	0	0	1	–	1	1	1	1	0	1	0	0	1	0	0	4
Amazochroma carvalhoi	0	1	0	–	4	0	?	1	1	1	0	0	–	–	–	–	–	–	–	–	1	1	1	1	1	0	1	1	1	3
Amazochroma pedroi	0	1	0	–	4	0	?	1	1	1	0	1	1	1	?	0	?	–	1	1	1	2	–	1	1	0	1	1	1	1
Discocyrtanus goyazius	0	1	0	–	4	0	?	1	1	1	0	0	–	–	–	–	–	–	–	–	1	1	1	1	1	0	1	1	0	3
Discocyrtanus pertenuis	0	1	0	–	4	0	?	1	1	1	0	0	–	–	–	–	–	–	–	–	1	1	1	1	1	0	1	1	0	3
Roeweria bittencourti	1	1	0	–	7	0	?	1	1	0	0	0	–	–	–	–	–	–	–	–	1	1	1	1	1	0	1	1	1	3
Roeweria virescens	1	1	0	–	7	0	?	1	1	0	0	0	–	–	–	–	–	–	–	–	1	1	1	1	1	0	1	0	1	3
Lacronia boraceae comb. nov.	0	1	1	2	5	1	0	2	0	–	0	1	1	1	0	0	0	0	0	2	1	1	0	1	0	1	1	1	0	0
Lacronia camboriu	0	1	1	2	5	1	0	5	0	–	0	1	1	1	0	0	0	1	0	2	1	1	0	1	1	1	?	?	0	0
Lacronia ceci	0	1	1	2	5	1	0	2	0	–	0	1	1	1	0	0	0	0	0	2	1	1	0	1	1	0	1	1	0	0
Lacronia nigra comb. nov.	0	1	1	2	5	1	0	2	0	–	0	1	1	1	0	0	0	0	0	2	1	1	0	1	0	0	1	1	0	0
Lacronia ricardoi	0	1	1	2	5	1	0	5	0	–	0	1	1	1	0	0	0	0	0	2	1	1	0	1	1	0	1	1	0	0
Lacronia serripes	0	1	1	2	5	1	0	5	0	–	0	1	1	1	0	0	0	1	0	2	1	1	0	1	1	1	1	1	0	0
Lacronia tenuis comb. nov.	0	1	1	2	5	1	0	2	0	–	0	1	1	1	0	0	0	0	0	2	1	1	0	1	0	1	1	1	0	0

Table 3 (continued).

	31	*32*	*33*	*34*	*35*	*36*	*37*	*38*	*39*	*40*	*41*	*42*	*43*	*44*	*45*	*46*	*47*	*48*	*49*	*50*	*51*	*52*	*53*	*54*	*55*	*56*	*57*	*58*	*59*	*60*
Ampycus telifer	0	0	0	1	1	0	0	3	1	1	0	1	0	7	0	–	0	0	–	–	0	1	3	1	1	4	1	1	0	0
Acanthopachylus aculeatus	0	0	0	0	0	–	–	1	0	0	0	0	–	0	0	–	0	0	–	–	0	0	0	0	1	0	1	0	–	2
Pachylus chilensis	1	0	0	0	0	–	–	1	0	0	0	0	–	0	0	–	0	0	–	–	0	0	0	0	1	0	1	0	–	2
Gonyleptes horridus	1	0	1	1	0	–	–	?	1	2	0	1	0	2	0	–	0	0	–	–	1	1	3	0	1	1	1	0	–	0
Goniosoma varium	2	0	–	1	0	–	–	2	1	2	0	1	0	5	1	0	1	0	–	–	1	1	3	0	1	3	1	0	–	1
Discocyrtus crenulatus	1	0	1	1	1	–	0	0	2	0	1	1	1	3	0	–	0	1	1	1	0	1	1	0	1	3	1	0	–	2
Discocyrtus flavigranulatus	2	0	1	1	1	0	0	0	1	0	1	1	1	3	0	–	0	0	–	–	1	1	2	1	1	3	1	1	2	2
Discocyrtus moraesianus	1	0	1	1	1	–	0	0	2	0	1	1	1	3	0	–	0	1	1	1	0	1	1	0	1	3	1	0	–	2
Discocyrtus testudineus	2	1	1	1	1	0	–	0	1	0	1	1	1	3	0	–	0	0	–	–	0	1	2	0	1	3	1	0	–	2
Mitobates triangulus	1	0	1	1	0	–	–	0	1	2	0	1	0	6	0	–	1	1	1	0	?	1	1	0	1	3	0	1	2	1
Mitobatula castanea	1	0	1	1	0	–	–	0	1	2	0	1	0	6	1	2	1	1	1	0	?	1	2	0	1	6	0	0	–	1
Neopachylus bellicosus	1	0	1	1	?	?	?	?	1	0	0	0	–	4	0	–	0	0	–	–	0	1	2	1	1	5	1	?	?	2
Neopachylus imaguirei	1	0	1	1	0	–	–	?	1	0	0	0	–	4	0	–	0	0	–	–	0	1	1	1	1	3	1	0	–	2
Pachylobos littoralis	1	2	1	1	1	0	1	0	1	0	0	1	0	7	0	–	0	1	1	1	0	1	4	1	1	0	1	0	–	2
Pachylobos longicornis	1	2	1	1	1	0	1	0	1	0	0	1	1	7	0	–	0	1	1	1	0	1	4	1	1	0	1	0	–	1
Senu leonardosi	1	1	1	1	1	0	1	0	1	0	0	1	1	1	1	3	0	1	1	1	0	1	4	1	1	3	1	0	–	1
Senu vestita	1	1	1	1	1	0	1	0	1	0	0	1	1	4	1	3	0	1	1	1	0	1	4	1	1	3	1	0	–	1
Amazochroma carvalhoi	0	1	1	1	1	0	1	0	1	1	0	1	1	0	1	1	0	0	–	–	0	1	2	1	1	2	1	1	1	1
Amazochroma pedroi	1	1	1	1	1	0	1	0	1	1	0	1	1	0	1	1	0	0	–	–	0	1	2	1	1	2	1	1	1	2
Discocyrtanus goyazius	0	1	1	1	1	1	1	0	1	1	0	1	1	2	1	2	0	0	–	–	0	1	2	1	1	3	1	1	1	0
Discocyrtanus pertenuis	0	1	1	1	1	1	1	0	1	1	0	1	1	2	1	2	0	0	–	–	0	1	2	1	1	3	1	1	1	0
Roeweria bittencourti	0	1	2	1	1	0	1	0	1	1	0	1	1	1	0	–	0	1	1	2	0	1	2	1	1	3	1	0	–	1
Roeweria virescens	0	1	2	1	1	0	1	0	1	1	0	1	1	1	0	–	0	1	1	2	0	1	2	1	1	3	1	0	–	1
Lacronia boraceae comb. nov.	1	0	1	1	1	–	0	0	1	0	1	1	1	0	?	–	0	1	1	1	0	1	1	1	1	3	1	0	–	1
Lacronia camboriu	1	?	1	1	0	–	–	0	1	0	1	1	1	1	0	–	0	1	0	–	1	1	2	1	0	–	0	0	–	1
Lacronia ceci	1	0	1	1	1	–	0	0	1	1	0	1	0	1	0	–	0	0	–	–	1	1	3	0	1	6	1	1	1	1
Lacronia nigra comb. nov.	1	0	1	1	1	–	0	0	1	0	1	1	1	1	0	–	0	1	1	1	1	1	2	1	1	0	1	1	0	1
Lacronia ricardoi	1	?	1	1	0	–	–	0	1	0	1	1	1	0	0	–	0	1	0	–	–	1	–	1	0	–	0	0	–	1
Lacronia serripes	1	?	1	1	1	–	0	0	1	0	?	1	1	0	0	–	0	0	–	–	1	1	2	1	1	1	1	1	0	1
Lacronia tenuis comb. nov.	1	0	1	1	1	–	0	0	1	0	1	1	1	1	0	–	0	1	1	1	0	1	3	1	1	0	1	1	0	1

Table 3 (continued).

	61	*62*	*63*	*64*	*65*	*66*	*67*	*68*	*69*	*70*	*71*	*72*	*73*	*74*	*75*	*76*	*77*	*78*	*79*	*80*	*81*	*82*	*83*	*84*	*85*	*86*	*87*	*88*	*89*	*90*
Ampycus telifer	1	–	–	0	1	0	0	0	0	0	0	0	0	1	1	1	0	1	0	0	1	1	0	0	0	0	0	0	–	0
Acanthopachylus aculeatus	–	0	–	1	0	1	0	1	0	1	1	0	2	0	–	1	0	0	0	0	1	0	–	0	0	0	0	0	–	1
Pachylus chilensis	–	0	–	1	0	1	0	1	0	1	1	0	2	0	–	1	0	0	0	0	1	0	–	0	0	0	0	0	–	1
Gonyleptes horridus	1	–	–	0	–	–	2	0	0	0	0	0	?	0	–	1	0	0	0	0	0	1	0	0	0	0	0	0	–	2
Goniosoma varium	–	–	?	0	–	–	2	0	1	0	0	0	0	0	–	1	0	1	0	0	0	1	0	0	0	0	0	1	2	3
Discocyrtus crenulatus	–	2	–	0	1	2	1	0	1	0	0	0	0	1	1	1	0	1	0	0	0	1	0	0	0	0	0	1	0	3
Discocyrtus flavigranulatus	–	2	–	0	0	2	0	0	1	0	0	0	0	1	0	1	0	1	0	0	1	1	0	0	1	0	0	1	0	2
Discocyrtus moraesianus	–	2	–	0	1	2	1	0	1	0	0	0	0	1	1	1	0	1	0	0	0	1	0	0	0	0	0	1	0	3
Discocyrtus testudineus	–	2	–	0	1	2	1	0	1	0	0	0	0	1	0	1	0	1	0	1	1	1	0	0	1	0	0	1	0	3
Mitobates triangulus	–	–	0	0	1	2	2	2	1	0	0	0	3	0	–	0	0	0	0	0	0	1	0	0	–	–	–	–	–	3
Mitobatula castanea	–	–	0	0	1	2	2	2	1	0	0	0	3	0	–	0	0	0	0	0	0	1	0	0	–	–	–	–	–	3
Neopachylus bellicosus	–	4	–	0	1	2	0	0	1	?	?	0	0	0	–	1	0	0	0	1	0	1	0	1	0	0	1	1	0	3
Neopachylus imaguirei	–	3	–	0	1	2	0	0	1	0	1	0	0	0	–	1	0	0	0	1	0	1	0	1	0	0	1	1	0	3
Pachylobos littoralis	–	4	–	0	0	1	1	0	1	0	0	0	0	0	–	1	0	0	0	0	0	1	0	0	0	0	1	1	0	3
Pachylobos longicornis	–	–	1	0	0	1	1	0	1	0	0	0	0	1	0	1	0	0	0	0	0	1	0	0	0	0	1	1	0	3
Senu leonardosi	–	–	2	0	0	0	0	0	1	0	0	0	0	1	1	1	0	1	0	0	0	1	0	1	0	0	1	1	0	3
Senu vestita	–	–	2	0	0	1	0	0	1	0	0	0	0	1	1	1	0	1	?	0	0	1	0	1	0	0	1	1	0	3
Amazochroma carvalhoi	–	–	2	0	1	1	0	0	0	0	0	1	1	1	0	1	0	1	0	0	0	1	1	0	0	0	0	1	1	2
Amazochroma pedroi	–	1	–	0	1	1	0	0	0	0	0	1	1	1	0	1	0	1	0	0	0	1	1	0	0	0	0	0	–	2
Discocyrtanus goyazius	0	–	–	0	1	1	0	0	0	0	0	0	1	0	–	1	0	1	0	0	0	1	0	0	0	1	0	1	1	3
Discocyrtanus pertenuis	0	–	–	0	1	1	0	0	0	0	0	0	1	0	–	1	0	1	0	0	0	1	0	?	0	1	0	1	1	3
Roeweria bittencourti	–	–	0	0	1	1	1	0	0	0	0	0	0	0	–	1	0	0	0	0	0	1	0	0	0	0	0	1	1	3
Roeweria virescens	–	–	0	0	1	1	1	0	0	0	0	0	0	0	–	1	0	0	0	0	0	1	0	0	0	0	0	1	1	3
Lacronia boraceae comb. nov.	–	–	3	0	1	0	1	0	1	0	0	0	0	1	1	1	1	1	1	1	0	1	1	0	0	2	1	1	0	2
Lacronia camboriu	–	–	2	0	0	1	0	0	?	0	0	0	0	1	1	1	1	1	1	1	0	1	1	0	0	2	1	1	0	2
Lacronia ceci	–	–	1	0	0	1	3	0	?	0	0	0	0	1	1	1	0	1	1	1	0	1	1	0	0	2	1	1	0	2
Lacronia nigra comb. nov.	–	–	3	0	1	1	1	0	1	0	0	0	0	1	1	1	1	1	1	1	0	1	1	0	0	2	1	1	0	2
Lacronia ricardoi	–	–	2	0	0	1	0	0	1	0	0	0	0	1	1	1	0	1	1	1	0	1	1	0	0	2	1	1	0	2
Lacronia serripes	–	–	2	0	1	1	0	0	1	0	0	0	0	1	1	1	1	1	1	1	0	1	1	0	0	2	1	1	0	2
Lacronia tenuis comb. nov.	–	–	3	0	1	1	1	0	1	0	0	0	0	1	1	1	1	1	1	1	0	1	1	0	0	2	1	1	0	2

Table 3 (continued).

	91	*92*	*93*	*94*	*95*	*96*	*97*	*98*	*99*	*100*	*101*	*102*	*103*	*104*	*105*	*106*	*107*	*108*	*109*	*110*	*111*	*112*	*113*	*114*	*115*
Ampycus telifer	0	0	–	–	0	0	1	0	0	0	–	0	1	0	–	0	?	0	–	1	0	–	0	1	0
Acanthopachylus aculeatus	0	1	3	–	0	0	1	0	0	0	–	0	0	0	–	0	0	1	1	1	1	1	0	0	0
Pachylus chilensis	0	1	3	–	0	0	1	0	0	0	–	0	0	0	–	0	0	1	1	1	1	1	0	0	0
Gonyleptes horridus	0	0	–	–	1	0	1	1	1	1	–	0	?	0	–	0	0	0	–	1	?	?	0	0	0
Goniosoma varium	1	1	1	0	0	0	1	0	0	0	–	0	1	0	–	0	0	0	–	1	0	–	0	0	0
Discocyrtus crenulatus	1	1	1	0	0	1	1	0	3	1	1	1	1	0	–	0	1	1	0	1	1	1	0	1	0
Discocyrtus flavigranulatus	0	1	1	0	0	1	1	0	0	0	–	0	1	0	–	0	0	1	1	1	1	1	0	0	0
Discocyrtus moraesianus	1	1	1	0	0	1	1	0	3	1	1	1	1	0	–	0	1	1	0	1	1	1	0	1	0
Discocyrtus testudineus	1	1	1	0	0	1	1	0	3	0	–	0	1	0	–	0	0	1	1	1	1	1	0	0	0
Mitobates triangulus	1	0	–	–	0	0	0	0	4	–	–	–	–	–	–	–	0	0	–	1	0	–	0	0	0
Mitobatula castanea	0	0	–	–	0	0	0	0	4	–	–	–	–	–	–	–	0	0	?	1	0	–	0	0	0
Neopachylus bellicosus	1	0	–	–	0	1	1	0	0	1	2	0	0	0	–	0	0	?	?	1	1	0	0	0	0
Neopachylus imaguirei	1	0	–	–	0	1	1	0	0	1	2	0	0	1	1	0	0	1	0	1	0	–	0	0	0
Pachylobos littoralis	0	1	0	–	0	1	1	0	1	1	2	0	0	1	1	0	0	1	0	1	1	0	0	1	0
Pachylobos longicornis	0	1	0	–	0	1	1	0	1	1	2	0	1	1	1	0	0	1	0	1	1	0	0	1	0
Senu leonardosi	1	0	–	–	0	1	1	0	1	1	2	1	0	0	–	1	0	0	–	1	1	0	0	1	0
Senu vestita	1	0	–	–	0	1	1	0	1	1	2	1	1	0	–	1	0	0	–	1	1	0	0	0	0
Amazochroma carvalhoi	0	1	0	–	1	0	1	0	0	0	–	0	1	0	–	0	0	1	0	0	0	–	0	0	0
Amazochroma pedroi	0	1	0	–	1	0	1	0	0	0	–	0	0	1	0	0	0	1	0	0	0	–	0	1	0
Discocyrtanus goyazius	1	1	0	–	0	1	1	0	2	1	0	0	0	1	0	0	0	1	0	1	0	–	0	0	0
Discocyrtanus pertenuis	1	1	0	–	0	1	1	0	2	1	0	0	0	1	0	0	0	1	0	1	0	–	0	0	0
Roeweria bittencourti	1	0	–	–	0	0	1	0	1	0	–	0	0	0	–	0	0	0	–	0	0	–	0	1	0
Roeweria virescens	1	1	0	–	0	0	1	0	1	0	–	0	0	0	–	0	0	1	0	1	0	–	0	0	0
Lacronia boraceae comb. nov.	0	1	1	1	0	1	1	2	1	?	3	1	1	1	1	0	1	1	1	1	1	1	1	–	1
Lacronia camboriu	0	1	2	–	0	1	1	0	1	?	3	1	1	0	–	0	1	0	–	0	?	?	0	1	1
Lacronia ceci	0	1	4	–	0	1	1	0	1	?	3	0	1	0	–	0	1	1	0	1	1	1	0	?	0
Lacronia nigra comb. nov.	0	1	1	1	0	1	1	2	1	?	3	1	1	1	1	0	1	1	1	1	1	1	1	–	1
Lacronia ricardoi	0	1	2	–	0	1	1	0	1	?	3	1	1	0	–	0	1	0	–	1	?	?	0	1	1
Lacronia serripes	0	1	4	–	0	1	1	0	1	?	?	1	1	0	–	0	1	1	1	1	1	1	0	1	1
Lacronia tenuis comb. nov.	0	1	1	1	0	1	1	2	1	?	3	1	1	1	1	0	1	1	1	1	1	1	1	–	1

As the primary analysis results, the current species of *Lacronia* (Fig. 1, salmon clade) were retrieved (in all k-values tested) as a monophyletic taxon with the inclusion of *D. boraceae*, *D. niger* and *D. tenuis*. Therefore, these three spp. are transferred to *Lacronia*, and we propose the following three new combinations – *Lacronia boraceae* comb. nov., *Lacronia nigra* comb. nov. (Fig. 3A–D) and *Lacronia tenuis* comb. nov. (Fig. 3E–H). The new status of *Lacronia* presented here, composed of seven species, is supported by five non-homoplastic and nine homoplastic synapomorphies (Fig. 2). The most remarkable non-homoplastic synapomorphies occur on the legs, such as 'Ti III mace-shaped [79 (1)]' and 'Cx IV

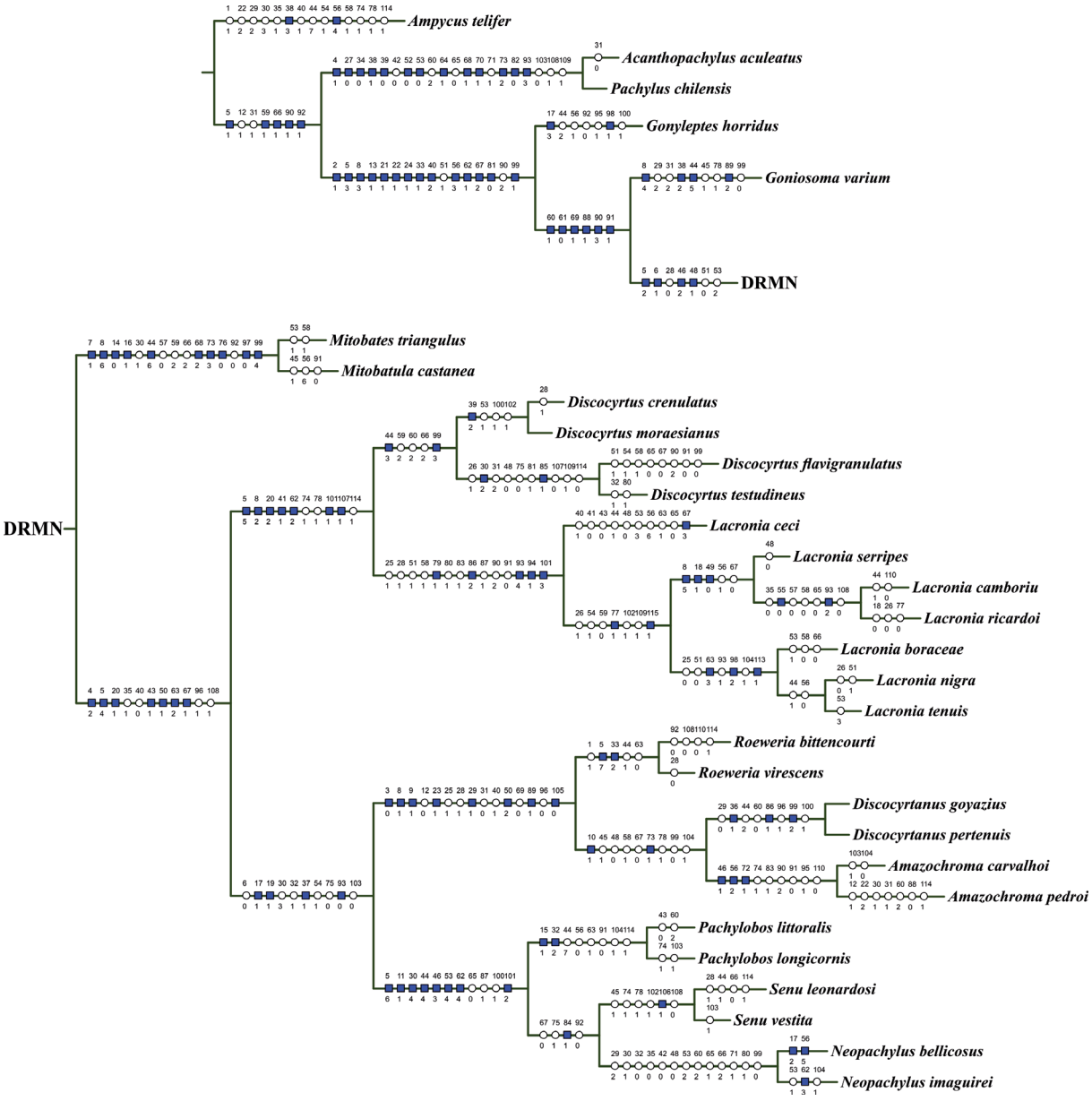

Fig. 2. Cladogram depicting phylogenetic relationships of *Lacronia* Strand, 1942 and the outgroups, with synapomorphies supporting each clade mapped using ACCTRAN optimization. The tree represents the topology with shortest number of steps (k-values = 3.2, 4, 5, 6, 10, 15 and 20) recovered by TNT. Blue squares = nonhomoplastic synapomorphies; white circles = homoplastic synapomorphies. Numbers above symbols are the characters numbers. Numbers under symbols are the states numbers.

Fig. 3. *Lacronia* spp., specimens in vivo. **A–D**. *L. nigra* (B. Soares, 1942) comb. nov., ♂, from Brazil, São Paulo, Santo André, Alto da Serra. **E–H**. *L. tenuis* (Roewer, 1917) comb. nov., ♂, from Brazil, Rio de Janeiro, Mangaratiba. Source: Adriano Kury.

Table 4. Values of consistency index (CI), retention index (RI) and number of steps of the trees retrieved in analyzed here. The k-values (= 2 and 3) retrieved two different trees, represented here as 2.1, 2.2, 3.1 and 3.2.

k-values	CI	RI	Steps
1, 2.1	51	73	350
2.2	51	73	350
3.1	51	73	349
3.2, 4, 5, 6, 10, 15, 20	52	73	347

prodorsal apophysis with crenated posterior border [86 (2)]'. *Lacronia* shows SFq support (= 90) and a relevant Bremer index (= 6) (Fig. 1).

In *Lacronia*, we retrieved three main clades (Fig. 1). The first is formed only by *Lacronia ceci* (Fig. 4A), recovered as the sister group of the remaining six species. It is supported by two unique synapomorphies: 'free tergites IIII with conspicuous tubercles increasing size towards the central portion [67 (3)]' and 'Mt IV dorsally unarmed [115 (0)]' (Fig. 2). The 'not areolated *Lacronia*' (*L. serripes* + (*L. camboriu* + *L. ricardoi*)) (Fig. 4B–D) forms a second clade, with very low branch support (SFq < 50; Bremer = 1) (Fig. 1). This clade is supported by synapomorphies as 'apical portion of the stylus swollen [8 (5)]' and the 'scallop-shaped flabellum straight, sub-parallel to the stylus [18 (1)]' (Fig. 2). In the 'not areolated

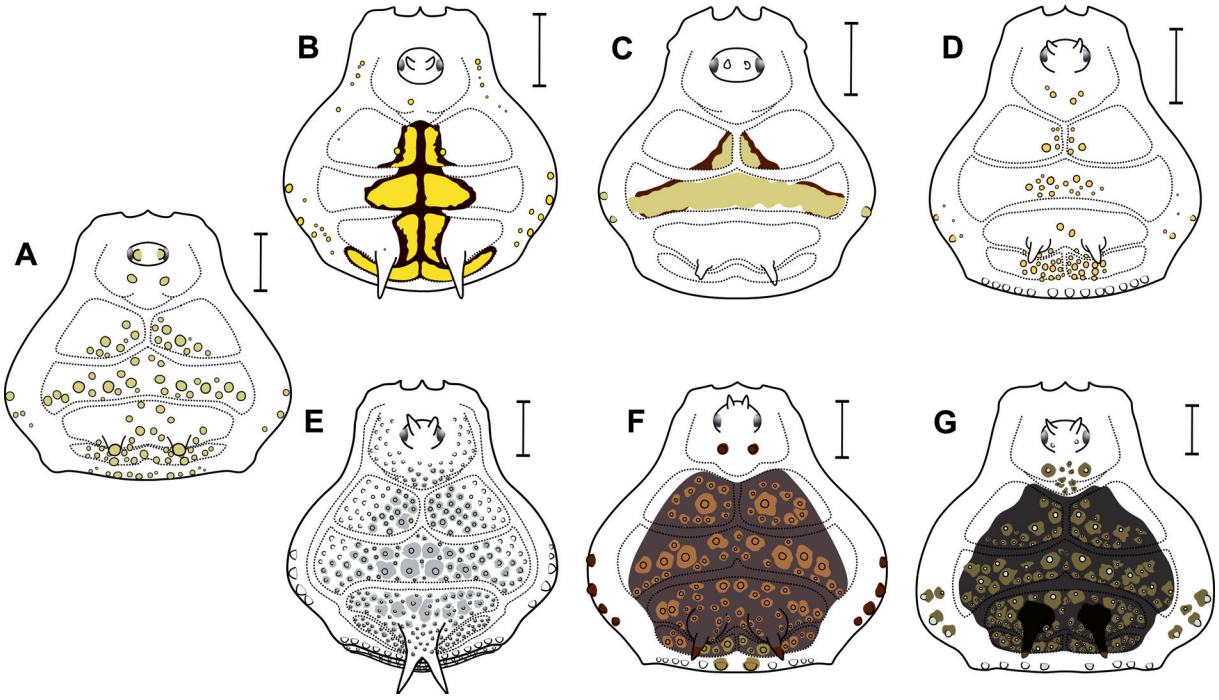

Fig. 4. *Lacronia* spp., schematic illustrations of the ♂ DS, showing the background variation and tubercles patterns of the specimens in vivo (except for *L. boraceae* (B. Soares, 1942) comb. nov., which information was only available in alcohol). **A**. *L. ceci* Kury & Orrico, 2006. **B**. *L. camboriu* Kury, 2003. **C**. *L. ricardoi* Kury, 2003. **D**. *L. serripes* (Mello-Leitão, 1923). **E**. *L. boraceae* comb. nov. **F**. *L. nigra* (B. Soares, 1942) comb. nov. **G**. *L. tenuis* (Roewer, 1917) comb. nov. Scale bars = 1 mm.

Lacronia' clade, the close relationship of *L. camboriu* and *L. ricardoi* (Fig. 4B–C) has interesting SFq support (88) and Bremer index (4) (Fig. 1) and it is supported by conspicuous non-homoplastic synapomorphies: 'DS marks band-shaped [49 (0)]', the 'absence of tubercles DS area II [55 (0)]' and 'Tr IV prolateral proximal apophysis hook-shaped [93 (2)]' (Fig. 2). The third clade is the 'areolated *Lacronia*' (Fig. 4E–G), formed by the three species transferred from *Discocyrtus* (*L. boraceae* comb. nov. + (*L. nigra* comb. nov. + *L. tenuis* comb. nov.)) (Fig. 1). The branch of the 'areolated *Lacronia*' does not show statistical relevance (Sfq = 81), but its Bremer index is consistent (= 4) (Fig. 1). Three exclusive synapomorphies supports 'areolated *Lacronia*': 'DS area III with a paramedian pair of straight spines with pointed apex [63 (3)]', 'Fe IV thickest at the distal portion [98 (2)]' and 'Ti IV dorsally armed with spines [113 (1)]' (Fig. 2). The areolated spots on the DS [49 (1)] of the 'areolated *Lacronia*' species are not detected in the other two clades inside *Lacronia* (as considered here). However, this character is homoplastic inside DRMN once that pattern is recovered in other members (e.g., *Pachylobos longicornis*).

Lacronia is recovered as the sister-group of *Discocyrtus* s. str., which could justify their synonymy (Fig. 1). Herein, we choose to preserve *Discocyrtus* and *Lacronia* as separated genera due to 1) the morphological difference between them (mainly in the legs III–IV of males), with *Lacronia* presenting e.g., Ti III mace-shaped, Cx IV prodorsal apophysis crenated and Fe IV approximately straight, and 2) the poor branch support values of *Discocyrtus* s. str. + *Lacronia* (SFq < 50; Bremer = 2) (Fig. 1).

The DRMN-clade, including *Lacronia*, was retrieved by almost all the analyses using different concavity values (except for k = 1 and 2) (Fig. 1). As occurred in previous works (e.g., Carvalho & Kury 2018, 2020, 2022), this clade presents low branch support (SFq < 50; Bremer = 1) (Fig. 1). The four non-homoplastic synapomorphies of DRMN shown in Fig. 2 are a result of the ACCTRAN optimization, and not detected in all of its representatives. However, even including *Lacronia*, the presence of 'stylus covered by medial or distal spines [6 (1)]' and at least 'a pair of conspicuous tubercles on mesotergum area I [53 (2)]' remains relevant diagnostic characters of DRMN-group.

The topological distance between DRMN and Pachylinae s. str. in Gonyleptidae is corroborated again (Fig. 1). Since its proposition, DRMN has been retrieved in many analyses, and it can be recognized as an essential clade to understanding the evolution of Gonyleptidae. Based on careful morphological observations and analyses (e.g., Carvalho & Kury 2018, 2020, 2022) it appears that this group is distinct from other Pachylinae (such as Pachylinae s. str. or Gonyassamiinae Soares & Soares, 1988). The concept of DRMN has been expanded as more genera are revised, becoming a key group for the process of redefinition of the Pachylinae.

Systematic accounts

Class Arachnida Lamarck, 1801
Order Opiliones Sundevall, 1833
Suborder Laniatores Thorell, 1876
Infraorder Grassatores Kury, 2002
Superfamily Gonyleptoidea Sundevall, 1833
Family Gonyleptidae Sundevall, 1833

Genus ***Lacronia*** Strand, 1942

Luederwaldtia Mello-Leitão, 1923a: 518 [junior homonym of *Luederwaldtia* Schmidt, 1922 (Hemiptera)] [type species: *Luederwaldtia serripes* Mello-Leitão, 1923, by original designation]. *Luederwaldtia* originally in Pachylinae.
Lacronia Strand, 1942: 397 [available replacement name for *Luederwaldtia* Mello-Leitão, 1923].

Luederwaldtia – Mello-Leitão 1926: 337; 1932: 166; 1935a: 99. — Roewer 1929: 218. — Kästner 1937: 389. — Soares & Soares 1954: 269. — H. Soares 1966: 286. — Muñoz-Cuevas 1973: 226.
Lacronia – Kury 2003a: 174; 2003b: 29. — Kury & Orrico 2006: 148.

Diagnosis

Lacronia resembles *Discocyrtus* s. str. due to: 1) stylus straight on the glans (Fig. 11A–B); 2) apical portion of the stylus only as an undifferentiated extension of its stem (Fig. 3A–D); 3) ventral process of the glans with the same diameter of the stylus (Fig. 20A, D); 4) ocularium height (in lateral view) with thrice or more the eyes diameter length (Fig. 7B, E); 5) Fe II–III with a retro-dorsal distal spur (Fig. 3A); 6) Pa IV covered by acuminated tubercles on the dorsal view (Fig. 12G–H, J).

Lacronia can be differentiated from *Discocyrtus* s. str. by: 1) mesotergum area III (on males) with a pair of paramedian spines (a pair of subconical structures in *L. ceci*) (Fig. 4B–G); 2) mesotergum area IV of the mesotergum not invading the posterior border of the dorsal scutum (area IV invading the posterior border of the dorsal scutum in *L. boraceae* comb. nov.) (Fig. 4A–D, F–G); 3) Ti III mace-shaped (Fig. 12D); 4) Cx IV with acuminated tubercles on the prolateral border (Fig. 12A); 5) Cx IV with a prodorsal apophysis crenated on the posterior portion (Fig. 12A); 6) Cx IV with a prodorsal apophysis transversally inserted in relation to the main body axis (Fig. 7A); 7) Tr IV approximately quadrangular-shaped (Fig. 12G, I); 8) Fe IV approximately straight (in dorsal view) (Fig. 17F).

Etymology

Luederwaldtia in honor of German born Brazilian zoologist Herman Luederwaldt (1858–1938). Gender feminine. *Lacronia* of obscure origin, possibly from a proper name 'Lacrona'. Gender feminine.

Included species

Lacronia boraceae (B. Soares, 1942) comb. nov., *Lacronia camboriu* Kury, 2003, *Lacronia ceci* Kury & Orrico, 2006, *Lacronia nigra* (Mello-Leitão, 1923) comb. nov., *Lacronia ricardoi* Kury, 2003, *Lacronia serripes* (Mello-Leitão, 1923) (type species) and *Lacronia tenuis* (Roewer, 1917) comb. nov.

Geographic distribution

BRAZIL: states of Rio de Janeiro, Santa Catarina and São Paulo (Fig. 5).

Key for males of species of *Lacronia*

1. Ocularium convex (in frontal view) without medial depression, with a pair of tubercles/spines fused at the base; mesotergum area II invading laterally the posterior portion of the area I; mesotergum area III with a pair of spines with acuminated apex; Fe and Mt IV dorsally armed with spines 2
– Ocularium convex (in frontal view) with medial depression, with an independent pair of tubercles; mesotergum area II not invading laterally the posterior portion of the area I; mesotergum area III with a pair of spines with rounded apex; Fe and Mt IV dorsally unarmed ....***L. ceci*** Kury & Orrico, 2006

2. Glans' stylus with apical portion swollen in relation is stem; mesotergum without areolate pattern of spots surrounding the tubercles; mesotergum area III with a pair of spines with slight distal inflection to ventral portion; free tergites I–III with a transversal row of ordinary tubercles; Fe IV with proximal and distal portions with approximately the same diameter; Ti IV dorsally covered by regular tubercles 3
– Glans' stylus with apical portion without an undifferentiated apex; mesotergum without areolate pattern of spots surrounding the tubercles; mesotergum area III with a pair of straight spines; free tergites I–III with a pair of highlighted tubercles on the paramedian portion; Fe IV with distal portion larger (in diameter) than the proximal; Ti IV dorsally covered by acuminated tubercles and/or spines 5

3. Mesotergum with band-shaped marks contrasting the background color; mesotergum areas II–IV without ordinary tubercles; mesotergum area II not invading laterally the anterior portion of the area III; Tr IV prolateral proximal apophysis hook-shaped 4
– Mesotergum with uniform background color; mesotergum areas II–IV with ordinary tubercles (contrasting with the background color) on the paramedian portion; mesotergum area II invading laterally the anterior portion of the area III; Tr IV prolateral proximal apophysis isosceles-triangle-shaped with a medial anterior bud ..... ***L. serripes*** (Mello-Leitão, 1923)

4. Scutal areas III–IV with band-shaped marks contrasting the background color; mesotergum area I with a pair of conspicuous tubercles; leg III with twice or more the diameter of the leg II; Pa IV retro-ventral portion unarmed ..... ***L. camboriu*** Kury, 2003
– Scutal areas III–IV with uniform background color; mesotergum area I without tubercles; leg III with 1.5 × the diameter of the leg II; Pa IV retro-ventral portion with a row of tubercles ..... ***L. ricardoi*** Kury, 2003

5. Mesotergum area I with one or two pair(s) of highlighted tubercles; mesotergum area III without any dorsal expansion; Mt IV dorsal row of spines composed only by regular spines or tubercles 6
– Mesotergum area I covered by ordinary tubercles; mesotergum area III posteriorly expanded with a paramedian dorsal monticule; Mt IV dorsal row of spines with the third spine bifid ..... ***L. boraceae*** (B. Soares, 1942) comb. nov.

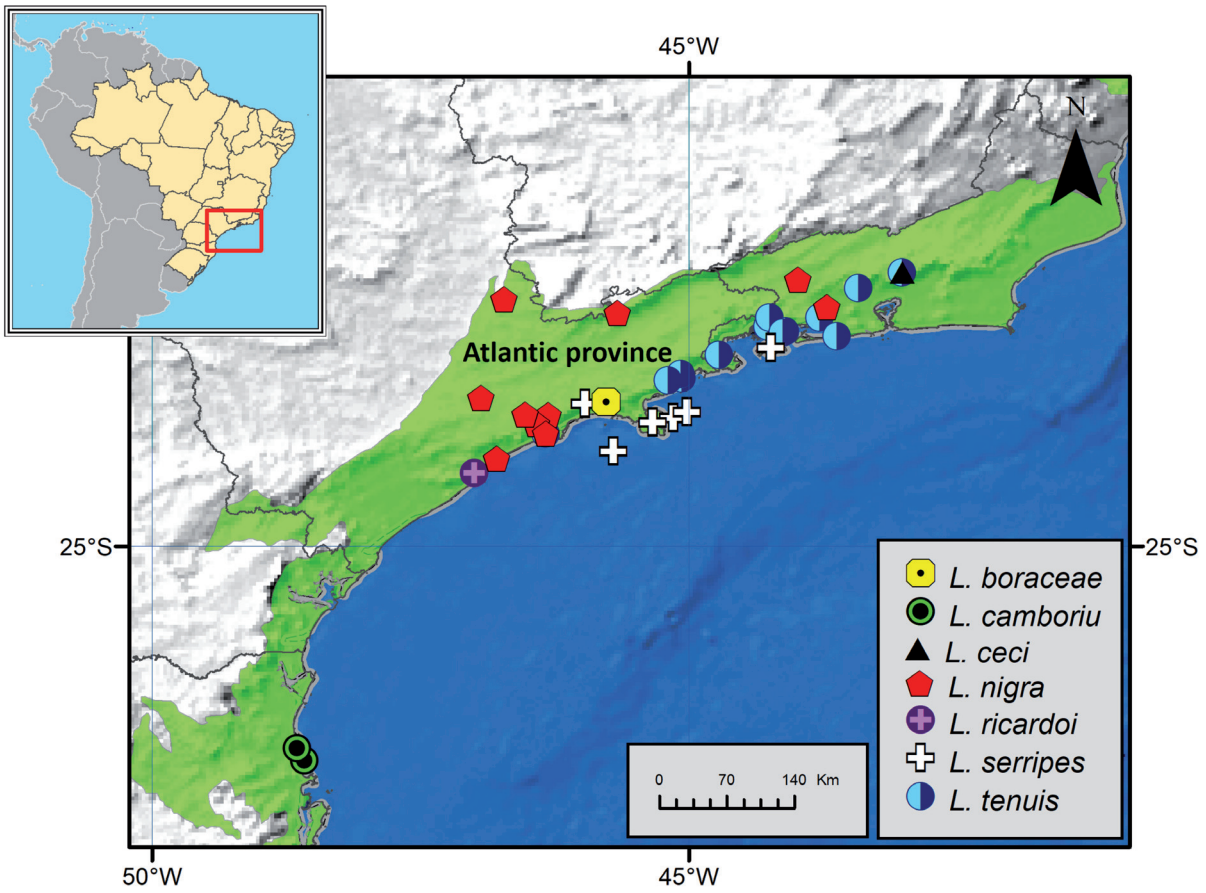

Fig. 5. Southeasten and Southern regions of Brazil, showing the distribution of the *Lacronia* spp. The area shaded in green represents the Atlantic province, as proposed by Morrone *et al.* (2022).

6. VP without macrosetae A on the medial portion; mesotergum tubercles and areolate spots with same color; mesotergum area I with a pair of conspicuous tubercles; Cx IV prolateral apophysis with a tiny spine on the apex; Tr IV prolateral distal portion with a hook-shaped apophysis ....***L. nigra*** (Mello-Leitão, 1923) comb. nov.
– VP with macrosetae A1 on the medial portion; mesotergum with tubercles' color contrasting with the areolate spots; mesotergum area I with two pairs of conspicuous tubercles; Cx IV prolateral apophysis regular, without a tiny spine on the apex; Tr IV prodorsal distal portion with transversal apophysis (covered by four prominent tubercles) ..... ***L. tenuis*** (Roewer, 1917) comb. nov.

Lacronia boraceae (B. Soares, 1942) comb. nov.
Figs 4E, 6–8, 9A

Discocyrtus boraceae B. Soares, 1942: 12.

Discocyrtus boraceae – B. Soares 1944a: 178, fig. 1; 1946: 514. — Soares & Soares 1954: 246. — Kury 2003a: 160.

Diagnosis

Lacronia boraceae comb. nov. can be differentiated from the other species of the genus by the following combination of characters: 1) mesotergum areas I–IV with areolate spots around the ordinary tubercles (Figs 6A, 7A); 2) mesotergum area I with ordinary tubercles diffusely distributed on all its extension (Fig. 7A); 3) mesotergum area II with ordinary tubercles diffusely distributed on all its extension (Fig. 7A); 4) mesotergum area III posteriorly expanded with a paramedian dorsal monticule (Figs 6A, C–D, 7A, C, E); 5) mesotergum area IV invading the posterior border of the dorsal scutum (Figs 6A, 7A); 6) Tr IV with a prominent sub-conical tubercle on the prodorsal distal face (Figs 6A, C, 7A); 7) Mt IV with a dorsal row of conical spines on its entire length, the third spine bifurcated (Fig. 6E).

Type material

Holotype
BRAZIL • ♀; State of São Paulo, Salesópolis; MZSP 114[!] (examined).

Additional material examined

BRAZIL – **State of São Paulo** • 1 ♂; Salesópolis, Boracéia; Jan. 1954; MZSP 1730[!] • 1 ♂; Estação Biológica de Boracéia; Jan. 1948; L. Travassos-Filho leg.; MNRJ-HS 122[!] • 1 ♂; same collection data as for preceding; 5 Sep. 1942; A. Zoppei leg.; MZSP 290[!] • 1 ♂, 1 ♀; same collection data as for preceding; 3–8 Mar. 1962; MZUSP leg.; MZSP 18185.

Redescription

Male (MNRJ-HS 122[!])
For the external body illustrations and description (Figs 4E, 6A–E, 7A–I) and genitalic illustrations (Fig. 8A–D).

Measurements. DS: CW 2.6, CL 2.0, AW 5.0, AL 3.2; Fe I–IV: I = 2.39, II = x, III = 3.78, IV = 4.41; right / left tarsal (distitarsal) counts: 6(3) / 6(3) - x / 12(3) - 7 / 7 - 7 / 7.

Dorsum. DS gamma-pyriform, longer than wide, with lateral borders of the AS convex, widest at mesotergum area II and thickest at mesotergum area III, with convex posterior border (Figs 6A, 7A). DS anterior border with two sets of five acuminated tubercles, divided by a small central projection and a pair of shallow cheliceral sockets (Fig. 7A, E). Carapace with tubercles on lateral and posterior portions (Fig. 7A). Ocularium elliptical (in dorsal view), high (ca 3 × the eye diameter), forming a 90º angle in

relation to the DS, placed in the anterior portion of the carapace (Figs 6A, C, 7A–B, E). Ocularium with a pair of divergent spines (ca 2.5 × the eye diameter), slightly inclined frontward (Figs 6A, C, 7A–B, E). Mesotergum divided in four clearly defined areas (Fig. 7A). Mesotergum areas I and IV divided into left and right halves by a longitudinal median groove (Fig. 7A). AS lateral borders with two rows of tubercles: one external, composed of four or five prominent tubercles at areas II–III (Fig. 7A); another internal one with ordinary tubercles from the carapace to mesotergum area III. All areas tuberculate, with almost all tubercles individually covered/surrounded by light colored spots (Figs 6A, 7A). Mesotergum areas III and IV with ordinary tubercles diffusely distributed on all of their extension (Fig. 7A, E). Mesotergum area III posteriorly expanded with a paramedian dorsal monticule bearing a pair of paramedian large spines (ca 2 × the ocularium's spines) (Figs 6A, C–D, 7A–C, E). DS posterior border and free tergites I–III each with a transversal row of prominent tubercles (Fig. 7A, E). Anal operculum covered by two rows of ordinary tubercles (Fig. 6D).

Venter. Cx I–III sub-parallel to each other (Fig. 6B), each with ventral longitudinal rows of 8–11 setiferous tubercles (Cx I rows with higher and sharper tubercles than the others). Cx II with a retro-ventral distal row of seven acuminated tubercles. Cx III with a retro-ventral distal row of 10 acuminated tubercles. Cx IV much larger than the others, directed obliquely (Fig. 6B). Intercoxal bridges well-marked (Fig. 6B). Stigmatic area Y-inverted-shaped, clearly sunken in relation to the Cx IV distal part (Fig. 6B). Cx IV covered by ordinary tubercles (Fig. 6B). Cx IV posterior border and stigmatic area each with a transversal row of ordinary tubercles. Stigmata visible (Fig. 6B, D). Free sternites with a transverse row of ordinary tubercles.

Chelicerae. Basichelicerite elongate (Fig. 7A), bulla well-marked, with marginal setiferous tubercles – one ectal, two central posteriors; hand not swollen.

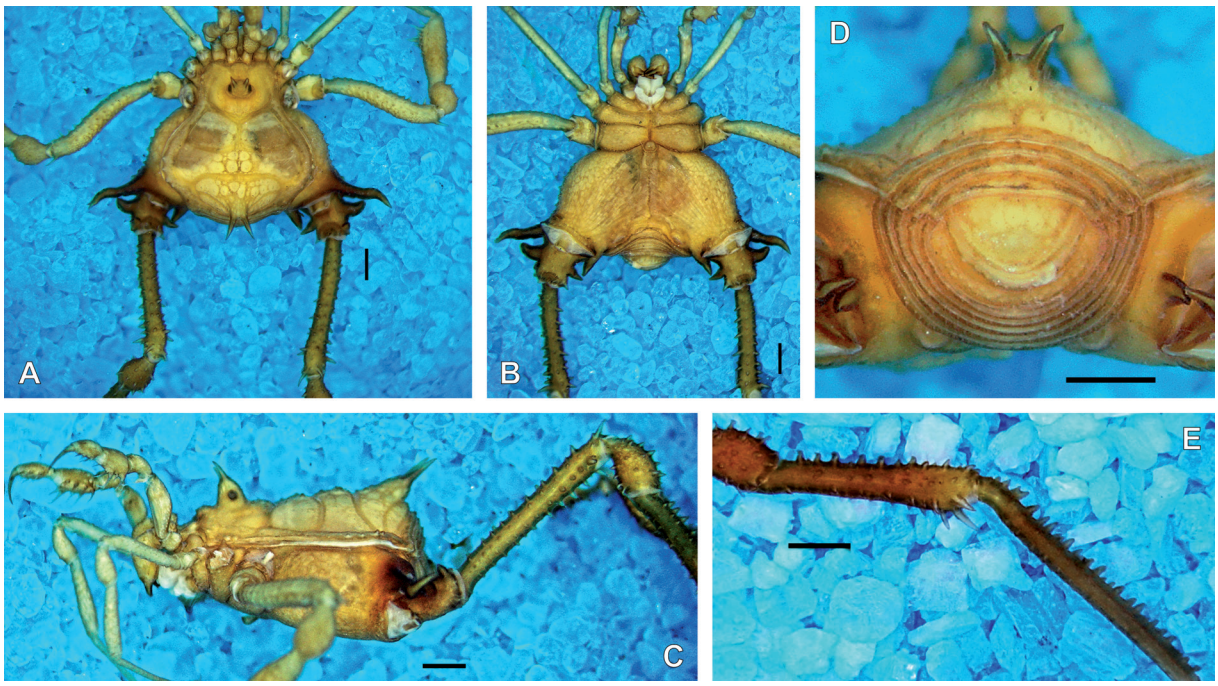

Fig. 6. *Lacronia boraceae* (B. Soares, 1942) comb. nov., ♂ (MNRJ-HS 122[I]), specimen in alcohol. **A**. Habitus, dorsal view. **B**. Same, ventral view. **C**. Same, lateral view. **D**. Armature of mesotergum area III, free tergites I–III and anal operculum, posterior view. **E**. Right Pa–Ti IV, retro-lateral view. Scale bars = 1 mm.

Pedipalps. Tr with two geminate ventral setiferous tubercles. Fe with a ventral basal and a mesal apical setiferous tubercle. Pa unarmed. Ti with two rows (ventro-mesal and ventro-ectal) of four spines (IiIi). Ta with two rows of spines: three (III) ventro-mesal and three (IIi) ventro-ectal.

Legs. Regarding the armature, all the unmentioned podomeres are unarmed or without relevant armature. Tr I–III each with several ventral tubercles. Fe I sub-straight; Fe II straight; Fe III sinuous (Fig. 6A, D). Fe and Ti I–III with all faces covered by lonigtudinal rows of small tubercles; Fe II–III with an apical retro-dorsal spur (Fig. 7D). Fe III (Fig. 7D) and Ti III with two rows (proventral and retro-ventral) of small acuminated tubercles, distally presenting spines (outstanding spines on Ti III). Pa I–III covered dorsally by prominent tubercles. Ti III mace-shaped (Fig. 6A). Cx IV reaching the posterior border of DS (Figs 6A, 7A). Cx IV tuberculate between prodorsal and ventral faces (Figs 6B, 7A). Cx IV with a thick prolateral distal conical apophysis, posteriorly crenated, with apical portion slightly curved backward (Figs 6A–B, 7A). Cx IV with a retro-lateral distal spiniform apophysis, fused with a small secondary branch (Figs 6A–B, 7A). Tr IV square-shaped in dorsal view (Figs 6A–B, 7A). Tr IV proximal portion with a conical apophysis on prolateral and retro-lateral faces (prolateral largest and curved dorsad) (Figs 6A–B, 7A). Tr IV prodorsal with a pair of highlighted sub-conical tubercles (proximal one largest) on distal portion, longitudinally arranged (Figs 6C, 7A, F). Tr IV retro-lateral distal face with a conical apophysis (Figs 6B, 7A, G). Tr IV ventral face tuberculate. Fe IV almost straight (using the right femur as a reference,in dorsal view), slightly arched on the distal portion towards prodorsal face (Figs 6A–C, 7A, F–G). Fe IV dorsal face with a row of sub-conical tubercles on the proximal half and four

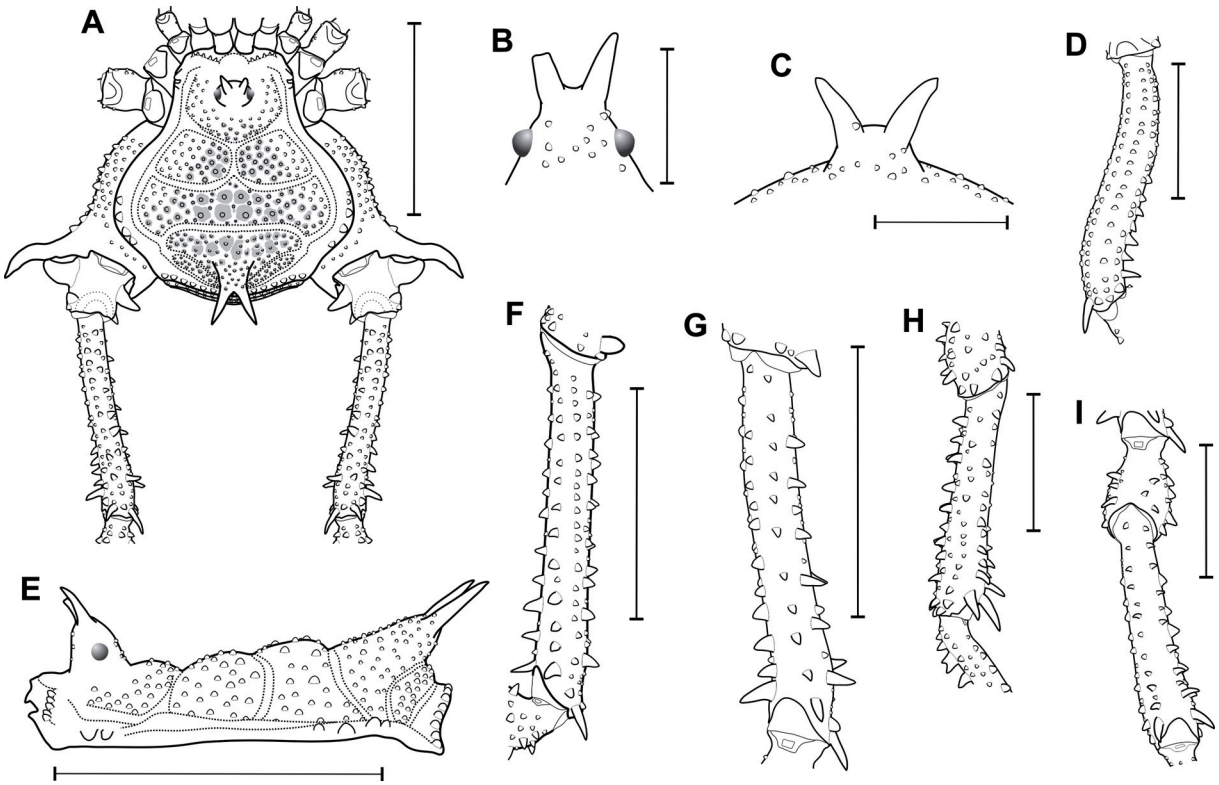

Fig. 7. *Lacronia boraceae* (B. Soares, 1942) comb. nov., ♂ (MNRJ-HS 122[!]). **A**. Habitus, dorsal view. **B**. Ocularium, frontal view. **C**. Armature of mesotergum area III, posterior view. **D**. Right Fe III, prodorsal view. **E**. Habitus, lateral view. **F**. Left Fe IV, proventral view. **G**. Right Fe IV, retro-ventral view. **H**. Right Pa–Ti IV, proventral view. **I**. Right Pa–Ti IV, ventral view. Scale bars: A, E = 4 mm; B–C = 1 mm; D, H–I = 2 mm; F–G = 3 mm.

spines (iIiI) on the distal half (Figs 6A–B, 7A). Fe IV prodorsal face with a row of sub-conical tubercles on the proximal and central thirds and two prominent conical tubercles on the distal third (Fig. 7A, F). Fe IV prolateral face with a row of sub-conical tubercles, the three distal more prominent than the others (Fig. 7A, F). Fe IV proventral face with a row of subconical tubercles (increasing in size distad) on the proximal and central thirds and five spines (iiiiI) on the distal third (Fig. 7F–G). Fe IV retro-ventral face with a row composed of subconical tubercles (increasing in size distad) on the proximal half and five spines (iiIII) on the distal half (Fig. 7F–G). Fe IV retro-lateral face with a row of seven conical spines (IIiIIiI) on its entire length (Fig. 7G). Fe IV retro-dorsal face with a row of subconical tubercles on its entire length, with an outstanding spine on the distal quarter (Fig. 7A). Fe IV distal apex with one prodorsal and a retro-dorsal outstanding spurs (Fig. 7A, F–G). Pa IV dorsally covered by acuminated prominent tubercles (Figs 6C, E, 7H). Pa IV proventral and retro-ventral faces with a row of three spines (proventral = iii; retro–ventral = IiI) (Fig. 7H–I). Ti IV dorsal face with ten subconical outstanding spines on its entire length (Figs 6E, 7H). Ti IV prodorsal, prolateral and retro-dorsal faces with a longitudinal row of ordinary tubercles (Figs 6E, 7H). Ti IV proventral face with a row of sub-conical tubercles, with two or three spines (ii or iii) on the proximal half and four spines (iiII) on the distal half (Fig. 7H–I). Ti IV retro-ventral face with a row of ten spines (iiiiiIIiII) on its entire length (Fig. 7I). Ti IV retro-lateral face with six prominent subconical tubercles. Mt IV with a dorsal row of conical spines on its entire length, the third spine bifurcated.

Color (in alcohol) (Fig. 6A, C). Ocularium, Cx I–IV and Tr IV *Strong Greenish Yellow* (99). DS background *Vivid Greenish Yellow* (97), with areolate spots *Light Yellow Green* (119) around the tubercles. Ch and Pp background Brilliant Yellow Green (116), with honeycombed *Moderate Olive Brown* (95) reticle. Tr–Ta I–III background *Light Yellow Green* (119), with honeycombed *Moderate Olive* (107) reticle. Cx IV distal portion and Tr IV *Light Olive Brown* (94). Fe–Ta IV background *Strong Greenish Yellow* (99).

Male genitalia. VP slightly divided into a distal half forming a rectangle with latero-apical flaps, and a proximal half elliptical (Fig. 8A, C). VP ventral surface entirely covered with microsetae of type 1 (Fig. 8B–C). All macrosetae inserted on ventro-lateral face of VP. MS A1–A3 cylindrical, thick, and acuminate, forming a triangle in lateral view (A1 on the basal portion of the distal half, A2–A3 on

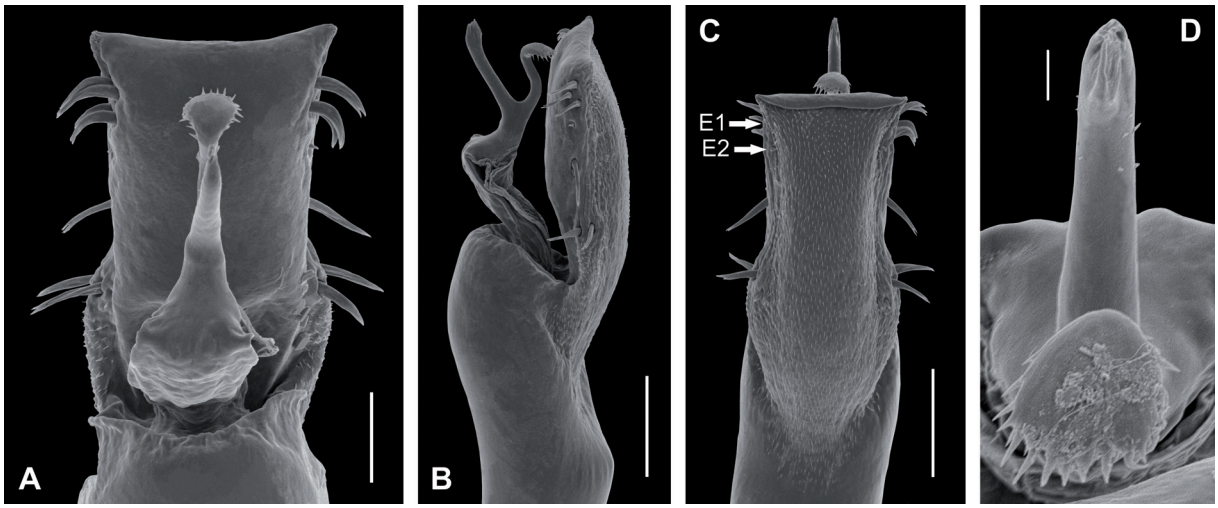

Fig. 8. *Lacronia boraceae* (B. Soares, 1942) comb. nov., ♂ (MNRJ-HS 122[!]), penis, distal part. **A**. Dorsal view. **B**. Lateral view. **C**. Ventral view. **D**. Detail of stylus and ventral process apex, dorsal view. Scale bars: A = 50 μm; B–C = 100 μm; D = 10 μm.

the proximal half, A2 placed ventralmost) (Fig. 8A–C). MS B1 small, inserted ventrally, posterior to A3 (Fig. 8B–C). MS C1–C3 (or C1–C4) similar to the MS A (slightly smaller than MS A), forming a triangle (with C2 more dorsal than others) or a square (C1–C2 and C3–C4 transversely matched) on the distal third of VP in lateral view (Fig. 8A–C). MS D1 small, -close to C3 (Fig. 8A–B). MS E1–E2 small, on the laterodistal flange of VP – E1 between MS C1–C2, E2 posterior to C3 (Fig. 8B–C). Glans sac arising from the middle bulge on the podium, not extended as a dorsal process (Fig. 8A–B). Stylus and its ventral process axis fused basally, forming a prominent pedestal (Fig. 8B). Stylus cylindrical, almost straight (apex slightly bent ventrally), inserted on pedestal forming a 45º angle, without conspicuous head, with a few small sub-distal tiny spines (Fig. 8A–D). Ventral process is ¾ of the stylus' length, almost sigmoid, with an apical flabellum curved ventrad (Fig. 8A–D). Flabellum scallop-shaped with serrulations, with approximately 40% of the ventral process stem length (Fig. 8A–D).

Female (MZSP 114[!]) (Fig. 9A)

DS, measurements: CW 3.0, CL 2.1, AW 5.2, AL 3.4; Fe I–IV measurements: I = 2.26, II = 4.58, III = 3.61, IV = 4.88; right / left tarsal (distitarsal) counts: 6(3) / 6(3) - 11(3) / 10(3) - 7 / 7 - 7 / 7.

DS gamma type. Mesotergal area III same as in male, but the pair of outstanding spines less curved posteriorly. Cx IV narrower than in males, with the prodorsal distal apophysis reduced to a single spine and without the retro-lateral apophysis. Tr IV prolateral proximal portion unarmed. Tr IV retro-lateral face with a proximal apophysis slightly smaller than the distal one. Fe IV thinner than in male. Pa–Ti dorsally covered by acuminated tubercles. Mt IV dorsally covered by ordinary tubercles.

Intraspecific variation

The material studied does not present *minor morph males*. It was also not found intraspecific variation among the *major morph males* or among females.

Records

Without further data.

Geographic distribution

BRAZIL: state of São Paulo: Salesópolis (Fig. 5).

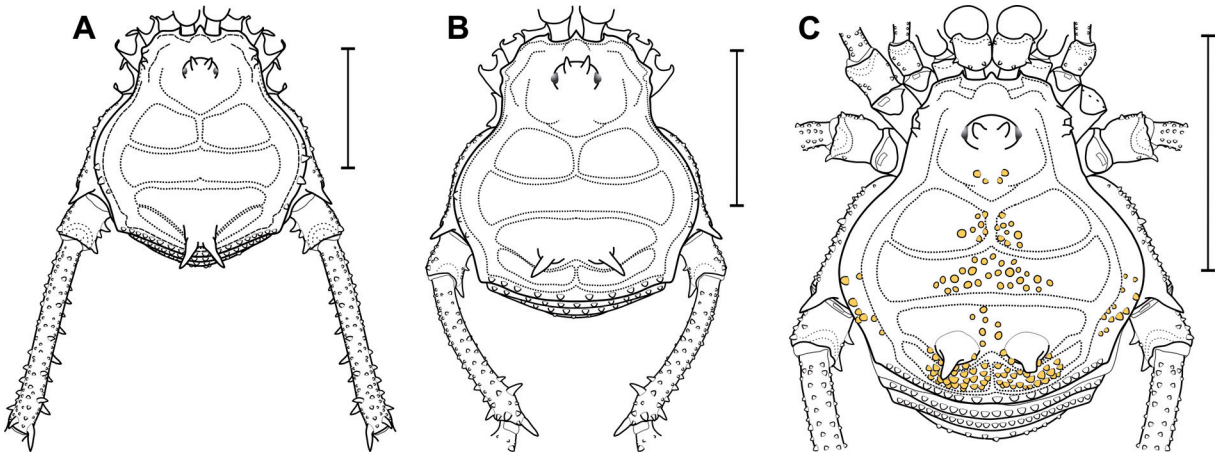

Fig. 9. *Lacronia* spp., female specimens, dorsal habitus. **A**. *L. boraceae* (B. Soares, 1942) comb. nov., holotype (MZSP 114[!]), schematic illustration. **B**. *L. nigra* (Mello-Leitão, 1923) comb. nov., holotype of *Discocyrtus fazi* Piza, 1942 (MZSP 1549[!]), schematic illustration. **C**. *L. serripes* Mello-Leitão, 1923 (MZSP 9973). Scale bars = 3 mm.

Lacronia camboriu Kury, 2003
Figs 4B, 10A

Lacronia camboriu Kury, 2003b: 33, figs 15–28

Lacronia camboriu – Kury & Orrico 2006: 148.

Diagnosis

Lacronia camboriu can be differentiated from the other species of the genus by the following combination of characters: 1) mesotergum areas I–IV without conspicuous tubercles, except for the paramedian pair on area I (Figs 4B, 10A); 2) mesotergum areas I–IV with yellow-colored stripes contrasting the background, with central longitudinal narrow stripes on areas I and III, an ellipse on central area II and a pair of large patches covering all the area IV (Figs 4B, 10A); 3) cheliceral bulla unarmed on its proximal border (Kury 2003b: fig. 15); 4) Ti III retro-ventral face with a row of three spines (III) on the distal third (Kury 2003b: fig. 25); 5) Tr IV prolateral proximal portion with a hook-shaped apophysis (Kury 2003b: fig. 15); 6) Mt IV with a dorsal row of outstanding conical spines (larger than the Mt IV diameter) (Kury 2003b: fig. 24); 7) subapical portion of the stylus covered by tiny spines on the dorsal face (Kury 2003b: fig. 28); 8) subapical portion of the stylus swollen (Kury 2003b: fig. 28); 9) flabellum of the ventral process scallop-shaped, not bent ventrad (Kury 2003b: fig. 28)

Type material

Holotype

BRAZIL • ♂; State of Santa Catarina, Balneário Camboriú, Praia da Laranjeira; MNRJ 4956! (examined)

Paratypes

BRAZIL – **State of Santa Catarina** • 1 ♂; same collection data as for holotype; MNRJ 4956! (examined) • 2 ♂♂, 6 ♀♀; Itajaí; MNRJ 5990! (examined).

Description

See Kury (2003b) for the extensive description and illustrations. We included a picture of the ♂ holotype dorsal view in the Fig. 10A.

Records

Without further data.

Geographic distribution

BRAZIL: state of Santa Catarina: Balneário Camboriú, Itajaí (Fig. 5).

Lacronia ceci Kury & Orrico, 2006
Figs 4A, 10B, 11

Lacronia ceci Kury & Orrico, 2006: 149, figs 1–12.

Diagnosis

Lacronia ceci can be differentiated from the other species of the genus by the following combination of characters: 1) ocularium convex with medial depression (in frontal view) (Kury & Orrico 2006: fig. 3); 2) ocularium height (in lateral view) twice more prominent than the eyes diameter (Kury & Orrico 2006: fig. 2); 3) ocularium with a pair of domed tubercles (Kury & Orrico 2006: fig. 3); 4) mesotergum areas I–IV with pale-colored tubercles contrasting with its background (Figs 4A, 10B); 5) mesotergum

area I with two pairs of conspicuous tubercles (Fig. 4A); 6) mesotergum area II of th with prominent tubercles organized in an anterior pair and four posterior pairs (Fig. 4A); 7) mesotergum area III with a paramedian pair of subconical apophyses (Figs 4A, 10B); 8) Fe IV dorsal face unarmed (Kury & Orrico 2006: fig. 9); 9) Mt IV unarmed on the dorsal face (Kury & Orrico 2006: fig. 10).

Type material

Holotype

BRAZIL • ♂; State of Rio de Janeiro, Teresópolis, Parque Nacional da Serra dos Órgãos, Trilha Rancho Frio, próximo ao Rio Paquequer (close to Paquequer River); 22.456548° S, 42.999458° W; 1177 m a.s.l.; A.B. Kury *et al*. leg.; MNRJ 16189! (examined).

Paratypes

BRAZIL – 3 ♂♂, 3 ♀♀; same collection data as for holotype; MNRJ 16189! (examined) • 1 ♂; same collection data as for holotype; MNRJ 17794! (examined).

Additional material examined

BRAZIL – **State of Rio de Janeiro** • 1 ♂; Teresópolis, Parque Nacional da Serra dos Órgãos; Aug. 2001; Equipe Biota leg.; IBSP 2158! • 1 ♂; same collection data as for preceding; 4–5 May 1996; M.S. Baptista *et al.* leg.; MNRJ 6945! • 1 ♂; same collection data as for preceding; 21 Apr. 2005; MNRJ 18764!.

Description

See Kury & Orrico (2006) for the extensive description and illustrations. We included a picture of a ♂ in vivo (Fig. 10B). Herein, we provide a redescription of the ♂ (MNRJ 6945!) genitalia based on its SEM picture.

Male genitalia (Fig. 11A–D). VP slightly divided in a distal part rectangle-shaped with latero-apical flaps, and a proximal part elliptical (Fig. 11A, C). VP ventral surface entirely covered with microsetae of type 1 (Fig. 11C). All macrosetae inserted on the ventro-lateral face of VP (Fig. 11A–C). MS A1–A3 cylindrical, thick, and acuminate, forming a triangle (A1 on the basal portion of the distal part, A2–A3 on the proximal part, A2 placed ventralmost) (Fig. 11A–C). MS B1 small, inserted ventrally, close to A2

Fig. 10. *Lacronia* spp. **A**. *L. camboriu* Kury, 2003, ♂, holotype (MNRJ 4956!), specimen in alcohol, from Brazil, Santa Catarina, Balneário Camboriú. **B**. *L. ceci* Kury & Orrico, 2006, ♂, specimen in vivo, from Brazil, Rio de Janeiro, Teresópolis. Photographs by Adriano Kury (A) and Glauco Machado (B).

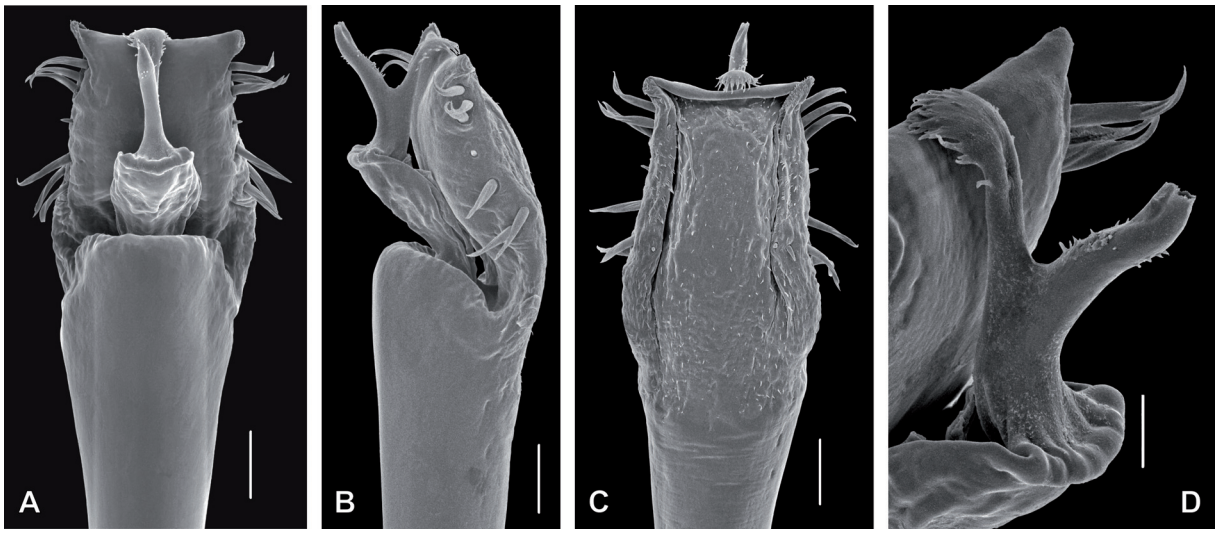

Fig. 11. *Lacronia ceci* Kury & Orrico, 2006, ♂ (MNRJ 6945[1]), penis, distal part. **A**. Dorsal view. **B**. Lateral view. **C**. Ventral view. **D**. Detail of stylus and ventral process, latero-dorsal view. Scale bars: A–C = 50 μm; D = 20 μm.

(Fig. 11C). MS C1–C3 similar to the MS A, forming a triangle (C2 ventralmost) on the distal third of VP (Fig. 11A–C). MS D1 small, placed in mid distance between A1 and C3 (Fig. 11A–B). MS E1–E2 small, on the distal flange of VP – E1 between C1–C2, E2 close to C3 (Fig. 11C). Glans sac arising from the middle bulge on the podium, not extended as a dorsal process (Fig. 11–B). Stylus and its ventral process axis fused basally, forming a prominent pedestal (Fig. 11B, D). Stylus cylindrical, sub-straight (apex slightly bent ventrad), inserted on pedestal forming a 45º angle (Fig. 11B, D), without conspicuous head, with a few small sub-distal tiny spines on dorsal and ventral faces (Fig. 11A–D). Ventral process of similar length as stylus, almost straight, with an apical flabellum curved ventrad (Fig. 11A–D). Flabellum scallop-shaped with serrulations, measuring about 40% length of the ventral process stem (Fig. 11A–D).

Records

Without further data.

Geographic distribution

BRAZIL: state of Rio de Janeiro: Teresópolis (Fig. 5).

Lacronia nigra (Mello-Leitão, 1923) comb. nov.
Figs 3A–D, 4F, 9B, 12–13; Table 5

Discocyrtus niger Mello-Leitão, 1923b: 125, fig. 8.
Discocyrtus fazi Piza, 1942: 388, fig. 2. **Syn. nov.**
Discocyrtus rarus B. Soares, 1944b: 297, figs 7–8. **Syn. nov.**

Discocyrtus niger – Roewer 1929: 208, fig. 10. — Mello-Leitão 1932: 180, fig. 102; 1937: 289. — B. Soares 1946: 518. — Soares & Soares 1945: 340, fig. 2; 1954: 253. — Kury 2003a: 164.
Discocyrtus fazi – B. Soares 1946: 515. — Soares & Soares 1954: 249. — Cekalovic 1985: 17. — Kury 2003a: 163.
Discocyrtus rarus – B. Soares 1946: 518. — Soares & Soares 1954: 254. — Kury 2003a: 165.

Diagnosis

Lacronia nigra comb. nov. can be differentiated from the other species of the genus by the following combination of characters: 1) mesotergum areas I–IV with areolate spots around the ordinary tubercles (Figs 3A–D, 4F, 12A); 2) free tergites I–III with areolate spots around the paramedian pair of prominent tubercles (Figs 3A–C, 4F, 12A); 3) Ti III retro-ventral face with a comb of three spines (iIi) on the distal third (Fig. 12D); 4) Cx IV prodorsal apical apophysis with a spine on its distal apex (Fig. 12A, E–F); 5) Tr IV prolateral distal portion with a hook-shaped apophysis (Fig. 12G–H); 6) Fe IV short, approximately the same length as mesotergum (Fig. 3A); 7) Mt IV dorsal face with a row of prominent tubercles on proximal ⅔ (Fig. 12K).

Type material

CHILE • 1 ♀, holotype of *Discocyrtus fazi* Piza, 1942; MZSP 1549! (examined) (doubtful record, see remarks section below).

BRAZIL • 1 ♀, holotype of *Discocyrtus niger* Mello-Leitão, 1923; state of Rio de Janeiro, "Pinheiro" [Piraí, Pinheiral]; MZSP 502! (not examined) • 1 ♂, holotype of *Discocyrtus rarus* B. Soares, 1944; State of São Paulo, Alto da Serra; MZSP 706! (examined).

Additional material examined

BRAZIL – **State of São Paulo** • 1 ♂; Cotia, Reserva Florestal Morro Grande–Torres; 15 Jul. 2006; R. Pinto-da-Rocha *et al.* leg.; MZSP 27935! • 1 ♂, 2 ♀♀; Cubatão, COPEBRAS; 22 Oct. 2004; C. Bragagnolo *et al.* leg.; MZSP 31869! • 6 ♂♂, 10 ♀♀; Cubatão, Trilha Cachoeira; 2 Dec. 2004; C. Bragagnolo *et al.* leg.; MZSP 31871! • 1 ♂, 2 ♀♀; Itanhaém, Cidade Santa Júlia; 30 Dec. 1978; L.R. Fontes and P.S. Terra leg.; MZSP 25146! • 5 ♂♂, 4 ♀♀; Santo André, Estação Biológica Paranapiacaba; 2 May 1999; G. Machado leg.; MZSP 28540! • 1 ♂; Santo André, Paranapiacaba; 18 Oct. 1952; Werner leg.; MNRJ 36! • 1 ♂; Santo André, Reserva Biológica do Alto da Serra [de Paranapiacaba]; 9 Sep. 1982; A. Cardoso, O.L. Peixoto and C.A.G. Cruz leg.; MNRJ 9207! • 1 ♂; same collection data as for preceding; 15 Oct. 1952; W. Bocherman leg.; MNRJ-HS 567! • 2 ♂♂; Santo André, Alto da Serra; 12–16 Apr. 2019; L.N. Ázara *et al.* leg.; MNRJ 60385 • 1 ♂; Santo Antônio do Pinhal, Eugênio Lefévre; 30 May 2009; R. Pinto-da-Rocha *et al.* leg.; MZSP 31070 • 2 ♂♂, 2 ♀♀; Santos, Vale do Rio Jurubatuba, margem direita, Trilha 1; 4 Oct. 2007; C. Bragagnolo *et al*. leg.; MZSP 31887! • 2 ♂♂, 1 ♀; same collection data as for preceding; MZSP 31889! • 5 ♂♂, 1 ♀; same collection data as for preceding; 21 Mar. 2007; A. Nogueira leg.; MZSP 31883 • 1 ♂, 1 ♀; São Bernardo do Campo, Parque Estoril; 5–10 Apr. 2006; B. Tavora *et al.* leg.; IBSP 8853.

Redescription

Male

MNRJ 60385 for the external body illustrations and description; MNRJ 9207! for genitalic illustrations.

Measurements. DS: CW 2.7, CL 1.9, AW 5.1, AL 3.0; legs I–IV measurements in the Table 5; right / left tarsal (distitarsal) counts: 6(3) / 6(3) – 10(3) / 9(3) – 7 / x - 7 / 7.

Dorsum. DS gamma-pyriform, longer than wide, with lateral borders of the AS convex, widest at area II and thickest at area III, with a slightly convex posterior border (Fig. 12A, E). DS anterior border with a set of five acuminated tubercles, divided by a small central projection and a pair of shallow cheliceral sockets (Fig. 12A). Carapace with a paramedian pair of prominent tubercles posterior to the ocularium, surrounded by many ordinary tubercles lateral- and posteriorly (Fig. 12A, E). Ocularium elliptic (in dorsal view), high (ca 3 × the eye diameter), almost forming a 90º angle in relation to the DS, placed in the anterior portion of the carapace (Fig. 12A–B, E). Ocularium with a pair of divergent spines (ca 2.5 ×

Table 5. Leg measurements of *Lacronia nigra* (B. Soares, 1942) comb. nov., ♂ (MNRJ 60385).

	Tr	Fe	Pa	Ti	Mt	Ta	Cl	Total
Pp	0.55	1.35	0.60	0.92	–	0.71	0.66	4.81
Leg I	0.57	2.11	0.81	1.45	2.14	1.43	–	8.53
Leg II	0.78	3.94	1.28	2.98	3.73	3.24	–	15.98
Leg III	0.83	3.17	1.24	1.95	3.20	1.79	–	12.19
Leg IV	1.01	3.44	1.46	2.56	4.61	2.25	–	15.34

the eye diameter), slightly inclined frontwards (Fig. 12A–B, E). Mesotergum divided in four clearly defined areas (Fig. 12A, E). Mesotergum areas I and IV divided into left and right halves by a longitudinal median groove (Figs 4F, 12A). AS lateral borders with a row of three prominent tubercles (Fig. 12A). All areas tuberculate, with almost all tubercles individually covered and surrounded by light colored spots (Figs 3A–B, 4F, 12A). Mesotergum area I with a pair of prominent tubercles (Fig. 12A). Mesotergum area II with a transversal row of prominent tubercles on the central portion (Fig. 12A). Mesotergum area III with a pair of paramedian outstanding spines (ca 3 × the ocularium spines) (Fig. 12A, C, E). Mesotergum area IV with with a transversal row of tubercles bearing six to seven prominent tubercles (Fig. 12A, E). DS posterior border with a transversal row of prominent tubercles, the central pair largest and covered/surrounded by light colored spots (Figs 3A–C, 4F, 12A). Free tergites I–III each with a transversal row of prominent tubercles, central pair covered/surrounded by light colored spots (Figs 3A–C, 4F, 12A). Anal operculum tuberculate.

Venter. Cx I–III sub-parallel to each other, each with ventral longitudinal rows of 8–12 setiferous tubercles (Cx I rows with higher and sharper tubercles than the others). Cx II–III with a retro-ventral distal row of acuminate tubercles. Cx IV much larger than the others, directed obliquely. Intercoxal bridges well-marked. Stigmatic area Y-inverted-shaped, clearly sunken in relation to the Cx IV distal part. Cx IV covered by ordinary tubercles. Cx IV posterior border and stigmatic area each with a transversal row of ordinary tubercles. Stigmata visible. Free sternites with a transverse row of ordinary tubercles.

Chelicera. Basichelicerite elongate, bulla well-marked, with marginal setiferous tubercles – one mesal, one ectal, one posterior (Fig. 12A); hand not swollen.

Pedipalps. Tr with two geminate ventral setiferous tubercles. Fe with a ventral basal and a mesal apical setiferous tubercle. Pa unarmed. Ti with two rows (ventro-mesal and ventro-ectal) of four spines (IiIi). Ta with two rows of spines: three (iII) ventro-mesal and four (iIII) ventro-ectal.

Legs. All the unmentioned podomeres are unarmed or without relevant armature. Tr I–III each with several ventral tubercles. Fe I sub-straight; Fe II straight; Fe III sinuous (Fig. 12D). Fe and Ti I–III with all faces containing longitudinal rows of small tubercles (Fig. 12D); Fe II–III with an apical retro-dorsal spur (Fig. 3A–B). Fe III with an apical prodorsal spur (reduced when compared to the retro-dorsal spur) (Fig. 12D). Fe III and Ti III with two rows (proventral and retro-ventral) of small acuminate tubercles, distally presenting spines (outstanding spines on Ti III) (Fig. 12D). Pa I–III covered dorsally by tubercles (Fig. 12D). Ti III mace-shaped (Fig. 12D). Cx IV reaching as far as the mesotergum area IV (Fig. 12A). Cx IV tuberculate between prodorsal and ventral faces (Figs 3D, 12A). Cx IV with a prolateral distal, thick cylindrical apophysis (distally curved backwards, bearing a conical spine on the apex), posteriorly crenated (Fig. 12A, E–F). Cx IV with a retro-lateral spiniform apophysis, fused with a small secondary

branch (Fig. 12A). Tr IV square-shaped in dorsal view (Fig. 12A, G, I). Tr IV proximal portion with a conical apophyses on prolateral and retro-lateral faces (prolateral largest, retro-lateral slightly curved to dorsal on the distal portion) (Fig. 12A, G–J). Tr IV with a hook-shaped prolateral distal apophysis (Fig. 12A, G–H). Tr IV with a retro-lateral subconical distal apophysis (Fig. 12G, I–J). Tr IV ventral face

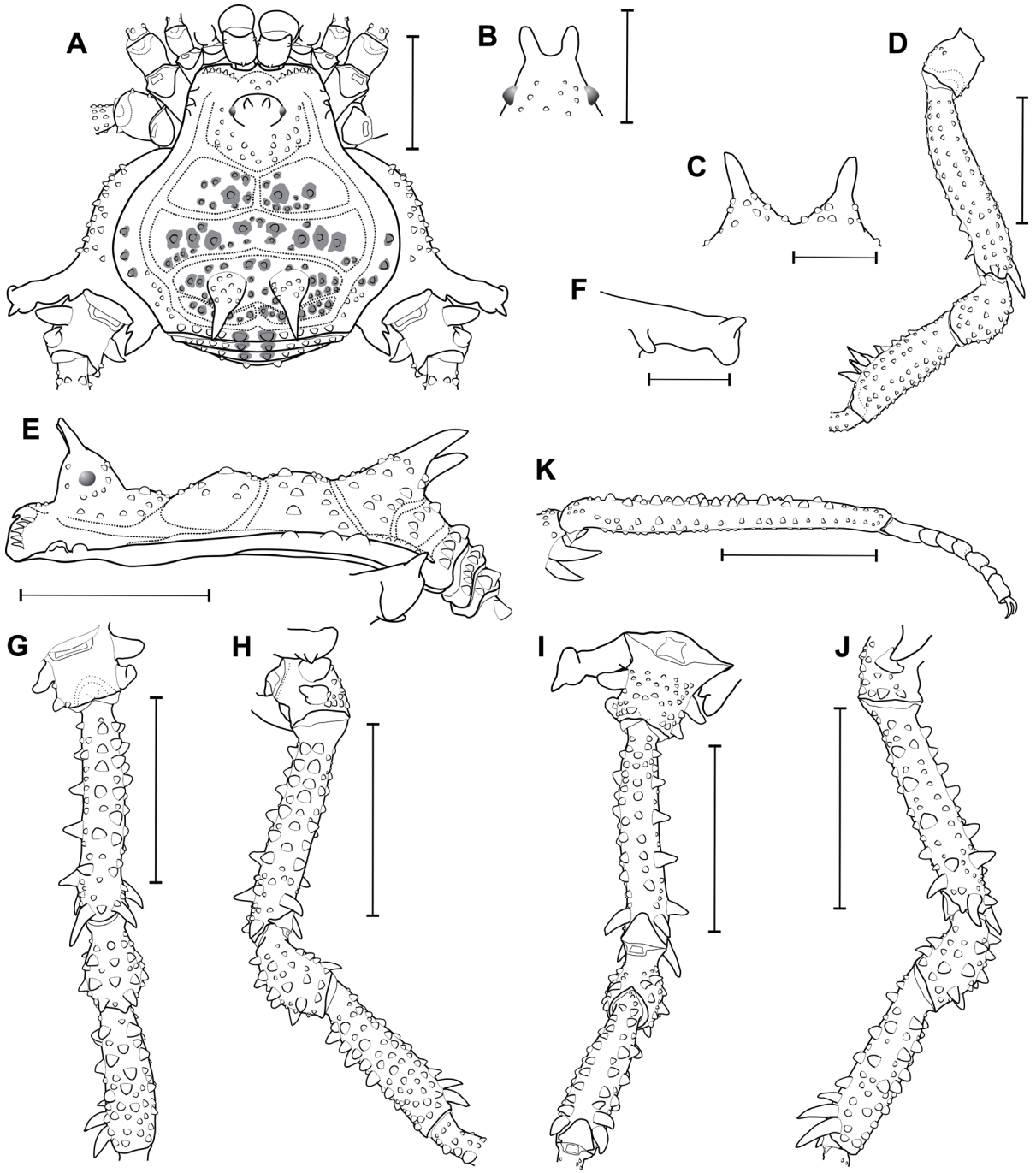

Fig. 12. *Lacronia nigra* (B. Soares, 1942) comb. nov., ♂ (MNRJ 60385). **A**. Habitus, dorsal view. **B**. Ocularium, frontal view. **C**. Armature of mesotergum area III, posterior view. **D**. Fe–Ti III, prodorsal view. **E**. Habitus, lateral view. **F**. Detail of the Cx IV prodorsal distal apophysis, posterior view. **G**. Right Fe–Ti IV, dorsal view. **H**. Same, prolateral view. **I**. Same, ventral view. **J**. Same, retro-lateral view. **K**. Right Mt–Ta IV, retro-lateral view. Scale bars: A, D–E, K = 2 mm; B–C, F = 1 mm; G–J = 3 mm.

tuberculate (Fig. 12H–J). Fe IV almost straight (in dorsal view), slightly arched on the central portion towards retro-dorsal face (Fig. 12G–J). Fe IV dorsal face with a row of five subconical outstanding tubercles on basal ⅔, with a conical tubercle on the distal apex (Fig. 12G–H, J). Fe IV prodorsal face with a row of seven outstanding subconical tubercles and a sizeable distal spur (Fig. 12G–H). Fe IV prolateral face with a row of four subconical tubercles on the proximal third and two prominent tubercles on the central third (Fig. 12G–I). Fe IV proventral face with a row of three subconical tubercles on the central-distal portion and a sizeable distal spine (Fig. 12H–I). Fe IV ventral with a row of five prominent tubercles, which turns to the retro-ventral face with three prominent tubercles, a subconical outstanding tubercle and a sizeable distal spine (Fig. 12I). Fe IV retro-lateral face with a row of two prominent subconical tubercles, one spine on the proximal half, and two outstanding spines on the distal half (Fig. 12G, I–J). Fe IV retro-dorsal face with a row of ordinary tubercles on basal ⅔ and a spine and a sizeable spur on the distal third (Fig. 12G, J). Pa IV dorsally covered by sub-conical or acuminated prominent tubercles (Fig. 12G–H, J). Pa IV proventral face with a row of four spines (iiiI) (Fig. 12H–I). Pa IV retro-ventral face with two spines (II) (Fig. 12I–J). Ti IV dorsally covered by tubercles, with subconical outstanding tubercles and spines on the proximal half (Fig. 12G–H, J). Ti IV proventral face with a row of 11 spines, the two distalmost much larger than others (Fig. 12H–I). Ti IV retro-ventral face with a row of five prominent subconical tubercles and three distal outstanding spines (two distalmost largest) (Fig. 12I–J). Mt IV dorsal face with a row of prominent tubercles on the basal ⅔ (Fig. 12K).

Color (in vivo) (Fig. 3A–D). Ocularium, carapace, external portions of mesotergum areas I–II, AS lateral borders and Cx IV *Dark Red* (16). Mesotergum *Reddish Black* (24) with areolate spots *Brilliant Orange Yellow* (97) on mesotergum areas I–III and *Dark Greenish Yellow* (103) on mesotergum area IV. Proximal portion of the spines on mesotergum area III's and AS posterior border *Dark Olive Brown* (96). Free tergites I–III background *Deep Brown* (56). Paramedian pair of prominent tubercles on AS posterior border and free tergites I–III and Fe II–III retro-dorsal spur *Moderate Greenish Yellow* (102). Ch and Pp background *Grayish Olive Green* (127), with honeycombed *Dark Grayish Olive Green* (128) reticle. Tr I background *Moderate Greenish Yellow* (102) and *Moderate Olive* (107). Tr II–III background *Deep Yellowish Brown* (75). FeMt I–III background *Dark Grayish Olive* (111). Fe–Mt IV background *Dark Reddish Brown* (44). The apex of the spines on DS area III and apex of the apophyses on Cx and Tr IV *Dark Reddish Orange* (39). Tips of tubercles and spines on Fe–Mt IV *Deep Orange* (51).

Male genitalia. VP slightly divided into a distal half forming a rectangle with latero-apical flaps and a proximal half elliptical (Fig. 13A, C). VP ventral surface entirely covered with microsetae of type 1. All macrosetae inserted on the laterals of VP. MS A1–A3 cylindrical, thick, and acuminate, forming a triangle (A1 on the basal portion of the distal part, A2–A3 on the proximal part, A2 placed dorsalmost) (Fig. 13A–C). MS B1 small, inserted ventrally, close to A2 (Fig. 13B–C). MS C1–C3 similar to MS A, forming a row inserted on the ventral border (C3 dorsalmost) on the distal third of VP (Fig. 13A–C). MS D1 small, inserted on VP's ventral border, close to C3 (Fig. 13A–B). MS E1–E2 small, inserted on the distal flange of VP – E1 between MS C1–C2, E2 below C3 (Fig. 13A–B). Glans sac arising from the middle bulge on the podium, not extended as a dorsal process (Fig. 13A–B). Stylus and its ventral process axis fused basally, forming a prominent pedestal (Fig. 13A–B). Stylus cylindrical, almost straight (apex slightly bent ventrally), inserted on a pedestal forming a 45º angle, without a conspicuous head and armed with a few small sub-distal tiny spines (Fig. 13A–B). Ventral process is ¾ of the stylus length, slightly bent dorsally, with an apical flabellum curved ventrad (Fig. 13A–B). Flabellum scallop-shaped with serrulations, with approximately 35% of the ventral process stem length (Fig. 13A–B).

Female (MZSP 1549[I]) (Fig. 9B)

DS, measurements: CW 2.3, CL 1.6, AW 4.0, AL 2.7; Fe I–IV measurements: I = 1.73, II = 3.13, III = 2.36, IV = 2.87; right / left tarsal (distitarsal) counts: 6(3) / 6(3) - x / x - x / 7 - x / 7.

DS gamma type. Cx IV narrower than in males, with the prodorsal apophysis reduced to a single spine and retro-lateral distal portion unarmed. Tr IV prolateral face unarmed. Tr IV retro-lateral proximal apophysis as a tiny spine. Tr IV retro-lateral distal apophysis as a prominent conical spine, slightly curved dorsally. Fe IV thinner than in male, with armature reduced to a prominent spine on the distal third and a pair of dorso-distal spurs (retro-dorsal largest). Mt IV dorsally covered by ordinary tubercles.

Intraspecific variation

In the *minor morph males* (compared to *major morph*): DS narrower; Cx IV with reduced prolateral and retro-lateral apophyses; Fe IV is thinner, with reduced armature size. It was not found intraspecific variation among the *major morph males* or among females.

Historical taxonomic remarks

The female holotype of *Discocyrtus niger* (recognized here as *Lacronia nigra* comb. nov.), recorded as specimen MZSP 502, was not found during this study. However, its morphology (after reviewing the original description and illustration, especially referring to the large retro-lateral distal apophysis on Tr IV) is identical to the females of *Discocyrtus rarus*. The type locality of *L. nigra* comb. nov. (Pinheiral, Piraí, Rio de Janeiro) is congruent with the current geographical occurrences of *D. rarus* (Fig. 14), especially because there is a record by Soares & Soares from Seropédica, which is quite close to Piraí (40 km in a straight line). Therefore, *D. rarus* is considered here a subjective junior synonym of *L. nigra* comb. nov.

Discocyrtus fazi was described by Piza (1942) based on the female holotype (MZUSP 1549[!]), in a paper focused on Chile's diversity of Opiliones. The type locality of *D. fazi* was reported as Chile (Fig. 14), without any additional data. There are no other recorded specimens of *D. fazi*, either nominal or of something that could be interpreted as this species, since its description, in spite of several authors

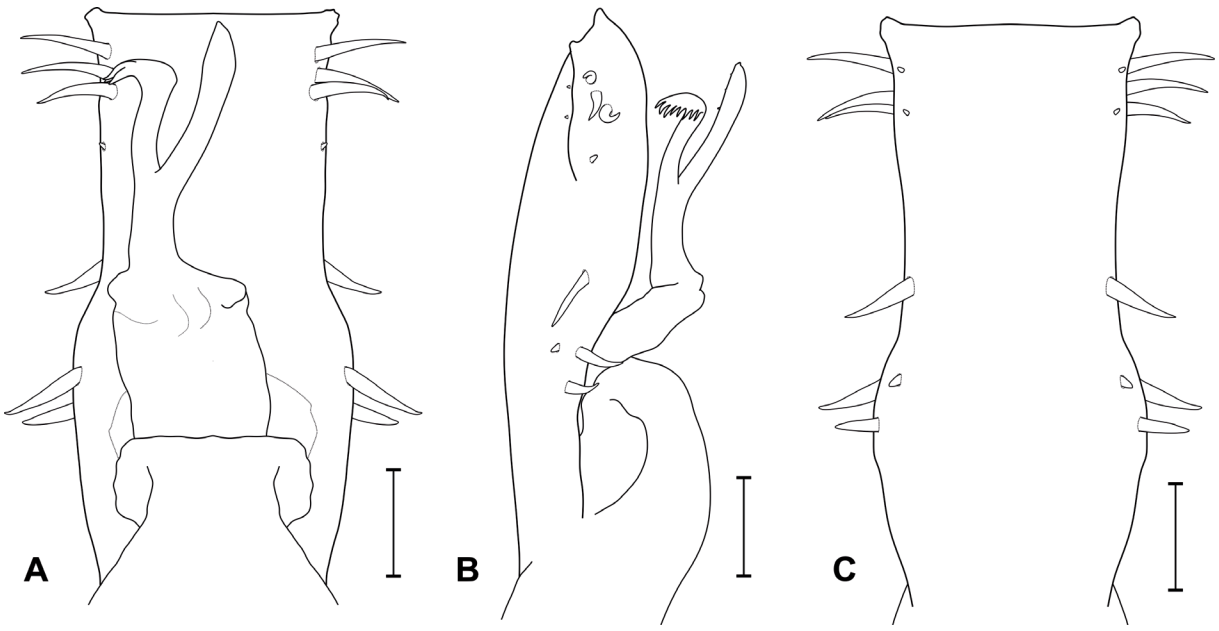

Fig. 13. *Lacronia nigra* (B. Soares, 1942) comb. nov., ♂ (MNRJ 9207[!]), penis, distal part. **A**. Dorsal view. **B**. Lateral view. **C**. Ventral view. Scale bars = 20 μm.

reviewing the Chilean opilionofauna (e.g., Pérez-Schultheiss 2021). The holotype of *D. fazi* is a perfect match to all the females assigned here as *L. nigra* comb. nov. This unlikely record could be a result of a mislabeling by Piza, who mostly worked with the material of Opiliones from São Paulo throughout his career. According to this scenario, 1) *D. fazi* is herein considered a junior subjective synonym of *L. nigra* comb. nov., and 2) its record from Chile is considered incorrect. Therefore, this revision of *Lacronia* unveils a previously undetected monophyletic group in one hand, helping to depurate the polyphyletic Pachylinae, while on the other hand allowing for a gradually clearer concept of *Discocyrtus*, both morpho- and geographically.

Records

BRAZIL, state of Rio de Janeiro: Seropédica (Soares & Soares 1945). State of São Paulo: [Monte Alegre], Três Pontes (Mello-Leitão 1937).

Geographic distribution (new records with an asterisk)

BRAZIL: state of Rio de Janeiro: Piraí, Seropédica. State of São Paulo: Alto da Serra, Cotia*, Cubatão*, Itanhaém*, Monte Alegre, Santo André*, Santo Antônio do Pinhal*, Santos*, São Bernardo do Campo* (Fig. 5).

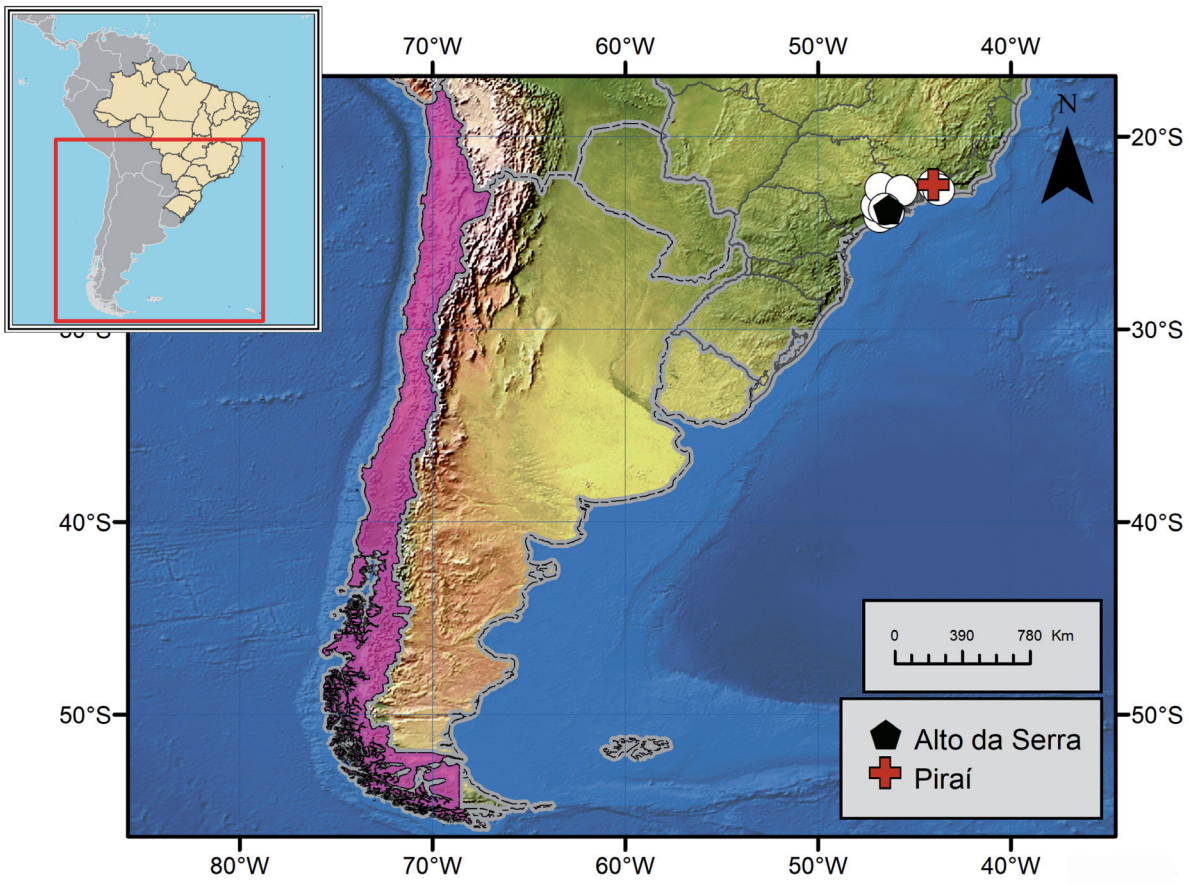

Fig. 14. South America, showing the distribution of the *Lacronia nigra* (B. Soares, 1942) comb. nov. non-type specimens (as white circles). The legend refers to the type localities of *Discocyrtus niger* B. Soares, 1942 (Piraí) and *Discocyrtus rarus* B. Soares, 1944 (Alto da Serra). The area shaded in magenta represents Chile, the type locality of *Discocyrtus fazi* Piza, 1942.

Lacronia ricardoi Kury, 2003
Figs 4C, 15

Lacronia ricardoi Kury 2003b: 31, figs 1–14.

Lacronia ricardoi – Kury & Orrico 2006: 148.

Diagnosis

Lacronia ricardoi can be differentiated from the other species of the genus by the following combination of characters: 1) mesotergum areas I–II with pale-colored stripes contrasting the background, forming a divided triangular spot (Figs 4C, 15A); 2) mesotergum areas I–IV without conspicuous tubercles (Figs 4C, 15A); 3) cheliceral bulla proximal border unarmed (Fig. 15A); 4) Tr IV with a prolateral proximal hook-shaped apophysis (Fig. 15A–B); 5) Mt IV dorsal face with a row of subconical tubercles on the proximal half and subconical spines on the distal half (Kury 2003b: fig. 10); 6) stem of the stylus covered by tiny spines on the ventral face (Kury 2003b: fig. 14); 7) subapical portion of the stylus swollen (Kury 2003b: fig. 14); 8) ventral process of the glans with lateral rows of spines (Kury 2003b: figs 13–14).

Type material

Holotype

BRAZIL – ♂; State of São Paulo, Peruíbe; MZSP 21373 (examined).

Paratypes

BRAZIL – • 1 ♀, 1 juv.; same collection data as for holotype; MZSP 21373 (examined) • 1 ♀; same collection data as for holotype; MZSP 10589 (not examined).

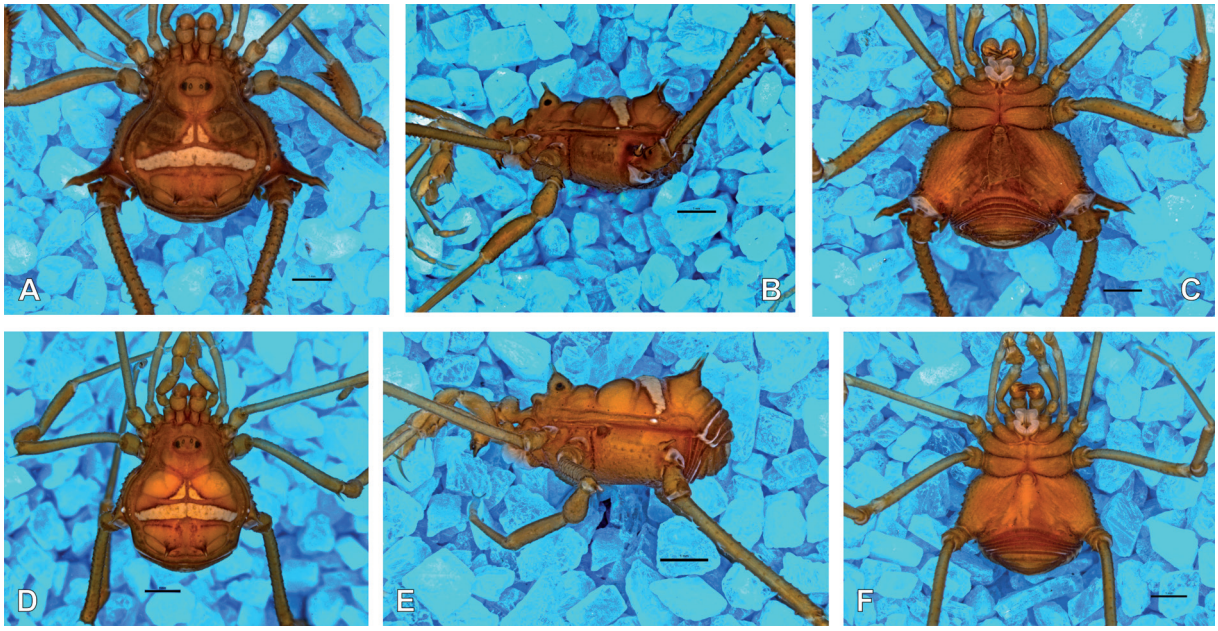

Fig. 15. *Lacronia ricardoi* Kury, 2003 (MZSP 21373), specimens in alcohol. **A–C**. Holotype, ♂ (MZSP 21373). **A**. Habitus, dorsal view. **B**. Same, lateral view. **C**. Same, ventral view. **D–F**. Paratype, ♀ (MZSP 10589). **D**. Habitus, dorsal view. **E**. Same, lateral view. **F**. Same, ventral view. Scale bars = 1 mm.

Description

See Kury (2003b) for the extensive description and illustrations. We included pictures of the male holotype and female paratype for comparative purposes (Fig. 15A–F).

Records

Without further data.

Geographic distribution

BRAZIL: state of São Paulo: Peruíbe.

Lacronia serripes (Mello-Leitão, 1923)
Figs 4D, 9C, 16–18; Tables 6–7

Luederwaldtia serripes Mello-Leitão, 1923a: 519, fig. 5.

Luederwaldtia serripes – Roewer 1929: 218. — Mello-Leitão 1932: 166. — B. Soares 1946: 520. — Soares & Soares 1954: 270. — H. Soares 1966: 284, figs 7–10. — Muñoz-Cuevas 1973: 226.
Lacronia serripes – Strand 1942: 397. — Kury 2003a: 174; 2003b: 30. — Kury & Orrico 2006: 148.

Diagnosis

Lacronia serripes can be differentiated from the other species of the genus by the following combination of characters: 1) mesotergum areas I–IV with light-colored tubercles contrasting with its background (without areolated spots surrounding the tubercles) (Figs 16A, C, 17A, D); 2) mesotergum area II with two paramedian pairs of conspicuous tubercles (Fig. 17A); 3) Ti III proventral face with a comb of three spines (iII) on the distal third, the larger ones touching each others' tip (Fig. 17E); 4) Tr IV prolateral proximal/central portion with an isosceles triangle-shaped apophysis with a prodorsal protuberance (Fig. 17A, G); 5) Tr IV prodorsal and prolateral distal portions only with ordinary tubercles (Fig. 16F–G); 6) Mt IV with a dorsal row of conical spines (absent only on the proximal a fifth) (Fig. 17J); 7) sub-apical portion of the stylus covered by tiny spines on lateral faces (Fig. 18B, D); 8) sub-apical portion of the stylus swollen (Fig. 18B, D); 9) ventral process flabellum scallop-shaped, straight (not bent ventrad) (Fig. 18A–D);

Type material

Holotype

BRAZIL • ♂; State of São Paulo, Ilha dos Alcatrazes; MZSP 550 (examined).

Additional material examined

BRAZIL – **State of Rio de Janeiro** • 7 ♂♂, 2 ♀♀, 1 juv; Angra dos Reis, Ilha Grande; 14 Dec. 1985; R.L.C. Baptista leg.; MNRJ 6100!. – **State of São Paulo** • 1 ♂; Ilhabela, Ilha São Sebastião; 8–10 Feb. 1948; H. Urban leg.; MNRJ 9286! • 3 ♂♂, 1 ♀; Salesópolis; MZSP 9973 • 10 ♂♂, 8 ♀♀; Estação Biológica de Boracéia; 26 Nov. 1968; E.X. Rabello leg.; MZSP 14343 • 3 ♂♂, 3 ♀♀; same collection data as for preceding; 6 Nov. 1968; MZSP 18308! • 1 ♀; São Sebastião, Ilha dos Alcatrazes; Oct. 1921; MZSP 13590.

Redescription

Male

MZSP 14343 for the external body illustrations and description; MZSP 9973 for genitalic illustrations.

Measurements. DS: CW 2.0, CL 1.5, AW 3.7, AL 2.4; legs I–IV measurements in the Table 6; right / left tarsal (distitarsal) counts: 5(3) / 4(2) - 11(3) / 11(3) - 7 / 7 - 7 / 7.

Dorsum. DS gamma-pyriform, longer than wide, with lateral borders of the AS convex, widest and thickest at mesotergum area II, with a slightly convex posterior border (Figs 16A, 17A). DS anterior border with a pair of shallow cheliceral sockets divided by a small central projection (Fig. 17A). Carapace with one or two pair(s) of prominent tubercles posterior ro ocularium (Figs 16A, 17A). Ocularium elliptical (in dorsal view), high (ca 3 × the eye diameter), almost forming a 90º angle to the DS, placed in the anterior portion of the carapace (Figs 16A–B, 17A–B, D). Ocularium with a pair of divergent spines (ca 3 × the eye diameter), slightly inclined frontwards (Figs 16A–B, 17A–B, D). Mesotergum divided in four clearly defined areas (Fig. 17A, D). AS lateral borders with two yellowish prominent tubercles contrasting with the background (Figs 16A–B, 17A). Mesotergum areas I and IV divided into left and right halves by a longitudinal median groove (Fig. 17A). All areas tuberculate on the center, with all yellowish tubercles contrasting with the background (Figs 16A–B, 17A, D). Mesotergum area I with a pair of prominent tubercles (Figs 16A, 17A). Mesotergum area II with two pairs of prominent tubercles (Figs 16A, 17A). Mesotergum area III with a pair of paramedian outstanding spines (ca 1.5 × the ocularium spines) (Fig. 17A, C–D). Mesotergum area IV with transversal rows of four to five prominent tubercles (Fig. 17A). DS posterior border with a transversal row of prominent tubercles (same color as the background) (Figs 16A–B, 17A, D). Free tergites III with a transversal row of prominent tubercles (Fig. 17A). Free tergite III with a transversal row of ordinary tubercles (Fig. 17A). Anal operculum covered by ordinary tubercles.

Venter. Cx I–III sub-parallel to each other (Fig. 16C), each with ventral longitudinal rows of setiferous tubercles (Cx I rows with higher and sharper tubercles than the others). Cx II and III with a retro-ventral distal row of acuminate tubercles. Cx IV much larger than the others, directed obliquely (Figs 16C, 17A). Intercoxal bridges well-marked (Fig. 16C). Stigmatic area Y-inverted-shaped, clearly sunken in relation to the Cx IV distal part (Fig. 16C). Cx IV covered by ordinary tubercles. Cx IV posterior border and stigmatic area each with a transversal row of ordinary tubercles. Stigmata visible (Fig. 16C). Free sternites each with a transverse row of ordinary tubercles.

Chelicera. Basichelicerite elongate, bulla well-marked, with one setiferous tubercle on the ectal margin; hand not swollen.

Pedipalps. Tr with two geminate ventral setiferous tubercles. Fe with a ventral basal and a mesal apical setiferous tubercle. Pa unarmed. Ti with two rows (ventro-mesal and ventro-ectal) of four spines (IiIi). Ta with two rows of spies: three (iII) ventro-mesal and three (III) ventro-ectal.

Legs. All the unmentioned podomeres are unarmed or without relevant armature. Tr I–III each with several ventral tubercles. Fe I sub-straight; Fe II straight; Fe III sinuous (Fig. 17E). Fe and Ti I–III all

Fig. 16. *Lacronia serripes* (Mello-Leitão, 1923), ♂ (MZSP 14343), specimen in alcohol. **A**. Habitus, dorsal view. **B**. Same, lateral view. **C**. Same, ventral view. Scale bars = 1 mm.

Table 6. Leg measurements of *Lacronia serripes* (Mello-Leitão, 1923), ♂ (MZSP 14343).

	Tr	Fe	Pa	Ti	Mt	Ta	Cl	Total
Pp	0.59	1.85	0.82	1.35	–	0.94	0.91	6.48
Leg I	0.78	2.66	1.78	2.09	3.11	2.09	–	11.91
Leg II	1.01	5.57	1.75	4.73	5.82	5.30	–	24.19
Leg III	1.11	4.84	1.52	2.87	4.19	2.46	–	17.00
Leg IV	1.39	5.89	1.78	4.11	6.41	3.23	–	22.82

faces with rows of small tubercles (Fig. 17E). Fe II–III with an apical retro-dorsal spur. Fe III with an apical prodorsal spur (reduced when compared to the retro-dorsal spur). Fe III and Ti III with proventral and retro-ventral rows of small acuminate tubercles with spines on the distal third [four proventral (iiII); three retro-ventral (iII), the largest ones touching each other's tip] (Fig. 17E). Pa I–III covered dorsally by acuminated tubercles (Fig. 17E). Ti III mace-shaped (Fig. 17E). Cx IV reaching as far as mesotergum areas III–IV (Fig. 17A). Cx IV tuberculate between prodorsal and ventral faces (Fig. 17A). Cx IV with a thick prolateral distal conical apophysis, posteriorly crenated, with apical portion slightly curved backward (Fig. 17A, F–H). Cx IV with a retro-lateral distal spiniform apophysis, fused with a small secondary branch (Fig. 17A, H–I). Tr IV square-shaped in dorsal view (Fig. 17A, F, H). Tr IV with a prolateral proximal/central apophysis that is isosceles triangle-shaped, with a secondary prolateral medial protuberance (Fig. 17A, F–H). Tr IV with a prolateral distal sub-conical tubercle (Fig. 17A, F–G). Tr IV with a retro-lateral proximal conical apophysis (Fig. 17A, F, H–I). Tr IV with a retro-lateral distal spine (Fig. 17A, F, H–I). Tr IV ventral face tuberculate (Fig. 17G–I). Fe IV almost straight (in dorsal view), slightly arched on the central portion towards dorsal face (Fig. 17F–I). Fe IV with all the faces covered by longitudinal rows of acuminated tubercles (largest in size on the proventral and retro-ventral distal half) (Fig. 17G–I). Fe IV with three dorsal conical spines (two on central portion, one on apex) (Fig. 17F–G, I). Fe IV retro-lateral face with two to three central spines (iIi) (Fig. 17F, H–I). Fe IV retro-dorsal face with one conical spine (I) on the distal ¼ (Fig. 17F, I). Fe IV prodorsal and retro-dorsal faces with an outstanding spur on distal apex (Fig. 17F–G, I). Fe IV proventral and retro-ventral faces with an outstanding spine on distal portion (Fig. 17F–I). Pa IV dorsally covered by spines and acuminated prominent tubercles (Fig. 17F–G, I). Pa IV proventral face with a row of four spines (iiii) (Fig. 17G–H). Pa IV retro-ventral face with two spines (ii) (Fig. 17H–I). Ti IV with all the faces (except ventral) covered by longitudinal rows of acuminated tubercles (retro-lateral and retro-dorsal faces with largest ones) (Fig. 17F–I). Ti IV prolateral face with two spines (iI) on the distal ¼ (Fig. 17F–H). Ti IV retro-lateral face with two outstanding spines (II) on the distal ¼ (Fig. 17F, H–I). Mt IV with a dorsal row of spines (absent on the proximal a fifth) (Fig. 17J).

Color (in alcohol) (Fig. 16A–C). Ocularium, DS background and Cx IV *Strong Orange* (50). Spines on ocularium *Deep Brown* (56). Tubercles on DS *Brilliant Yellow* (83). Spines of the mesotergum area III and Cx IV prodorsal distal apophysis *Dark Violet* (212). Ch and Pp background *Strong Yellow* (84). Legs –III background *Moderate Greenish Yellow* (102). Tr IV background *Dark Orange Yellow* (72) with apophyses *Dark Grayish Red* (20). Fe–Mt IV background *Dark Yellow* (88). Tubercles and spines on legs IIV *Deep Brown* (56).

Male genitalia. VP slightly divided into a distal trapezoidal half (widest at base, with latero-apical flaps), and a proximal half elliptical (Fig. 18A, C). VP ventral surface entirely covered with microsetae of type 1. All macrosetae inserted on the ventro-laterals of VP. MS A1–A3 cylindrical, thick, and acuminate, forming a triangle in lateral view (A1 on the basal portion of the distal part, A2–A3 on the

proximal part, A2 dorsalmost) (Fig. 18A–B, D). MS B1 small, inserted ventrally, ventral and close to A3 (Fig. 18B–D). MS C1–C3 longer than the MS A, forming a row (C3 dorsalmost) on the distal ¼ of VP (Fig. 18A–D). MS D1 small, close to C3 (Fig. 18A–D). MS E1–E2 small, on the laterodistal flange of VP – E1 more ventrally placed between MS C1–C2, E2 same, below C3 (Fig. 18D). Glans sac arising

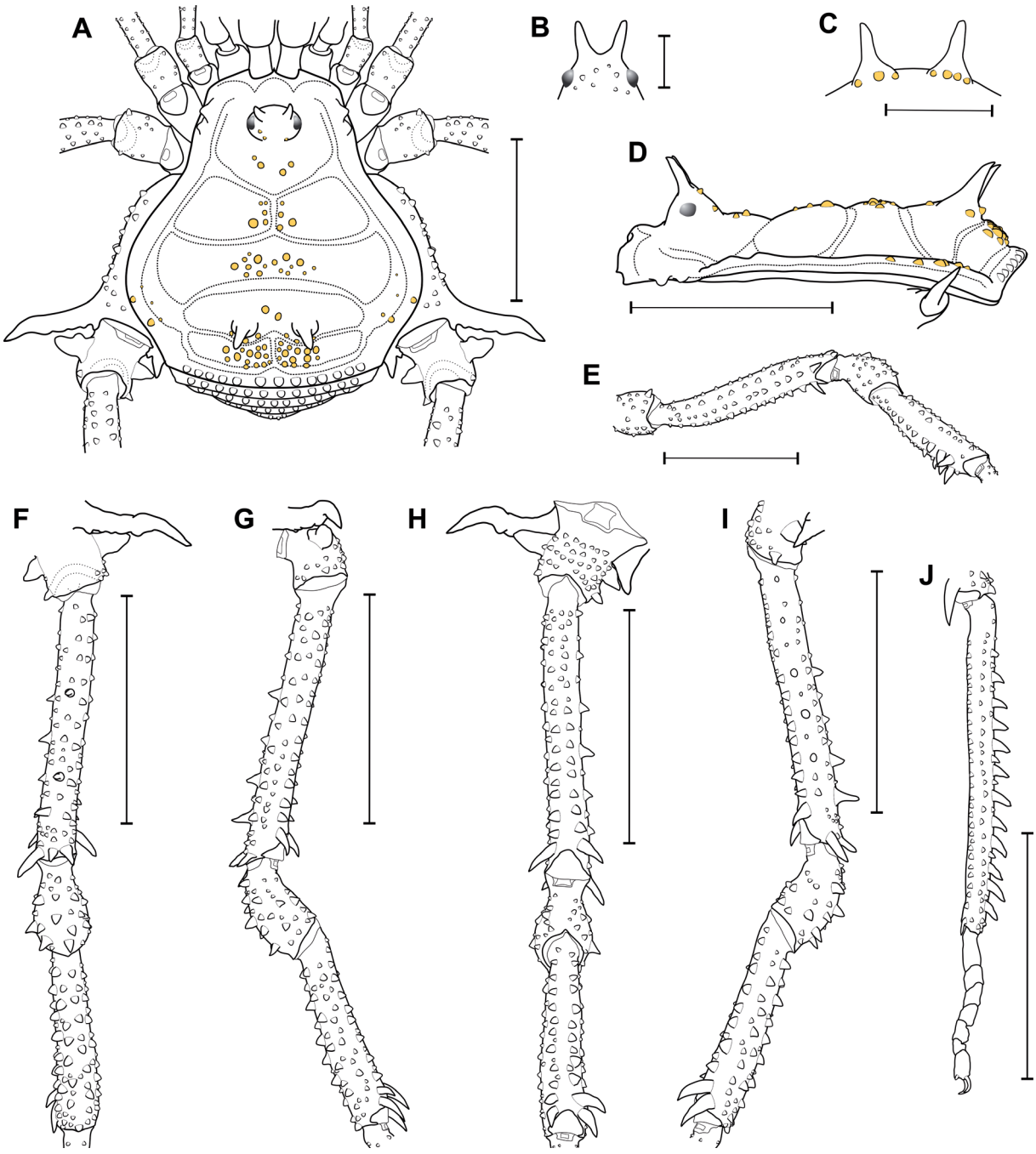

Fig. 17. *Lacronia serripes* (Mello-Leitão, 1923), ♂ (MZSP 14342). **A**. Habitus, dorsal view. **B**. Ocularium, frontal view. **C**. Armature of mesotergum area III, posterior view. **D**. Habitus, lateral view. **E**. Left Fe–Ti III, proventral view. **F**. Right Fe–Ti IV, dorsal view. **G**. Same, prolateral view. **H**. Same, ventral view. **I**. Same, retro-lateral view. **J**. Right Mt–Ta IV, retro-lateral view. Scale bars: A, D–E, J = 2 mm; B–C = 1 mm; F–I = 3 mm.

Table 7. Leg measurements of *Lacronia serripes* (Mello-Leitão, 1923), ♀ (MZSP 9973).

	Tr	Fe	Pa	Ti	Mt	Ta	Cl	Total
Pp	0.64	1.71	0.89	1.16	–	1.00	0.66	6.07
Leg I	0.71	2.55	1.03	1.75	2.85	1.93	–	10.84
Leg II	0.94	5.05	1.59	4.21	5.41	4.44	–	21.66
Leg III	1.03	3.94	1.60	2.50	4.16	2.30	–	15.55
Leg IV	1.34	5.39	1.76	3.55	6.23	2.75	–	21.03

from the middle bulge on the podium, not extended as a dorsal process (Fig. 18A–B, D). Stylus and its ventral process axis fused basally, forming a prominent trapezoidal-shaped pedestal (Fig. 18A–B, D). Stylus cylindrical, almost straight, inserted on the pedestal forming a 25º angle, without conspicuous head (slightly swollen at subapical portion), with subdistal tiny spines (Fig. 18A–B, D). Ventral process is ¾ of the stylus length, slightly bent dorsad, with an apical flabellum (Fig. 18B, D). Flabellum not curved ventrally, scallop-shaped with serrulations and, with approximately 50% of the ventral process stem length (Fig. 18B–D).

Female (MZSP 9973) (Fig. 9C)
DS, measurements: CW 2.2, CL 1.6, AW 3.9, AL 2.6; legs I–IV measurements in the Table 7; right / left tarsal (distitarsal) counts: 5(3) / 5(3) - 10(3) / 10(3) - 7 / 7 - 7 / 7.

DS gamma type. Cx IV narrower than in the males, with the prodorsal distal apophysis reduced to a single spine and without the retro-lateral distal apophysis. Tr IV prolateral face with a row of acuminated tubercles (without apophyses). Tr IV retro-lateral face with a prominent proximal spine and a distal one.

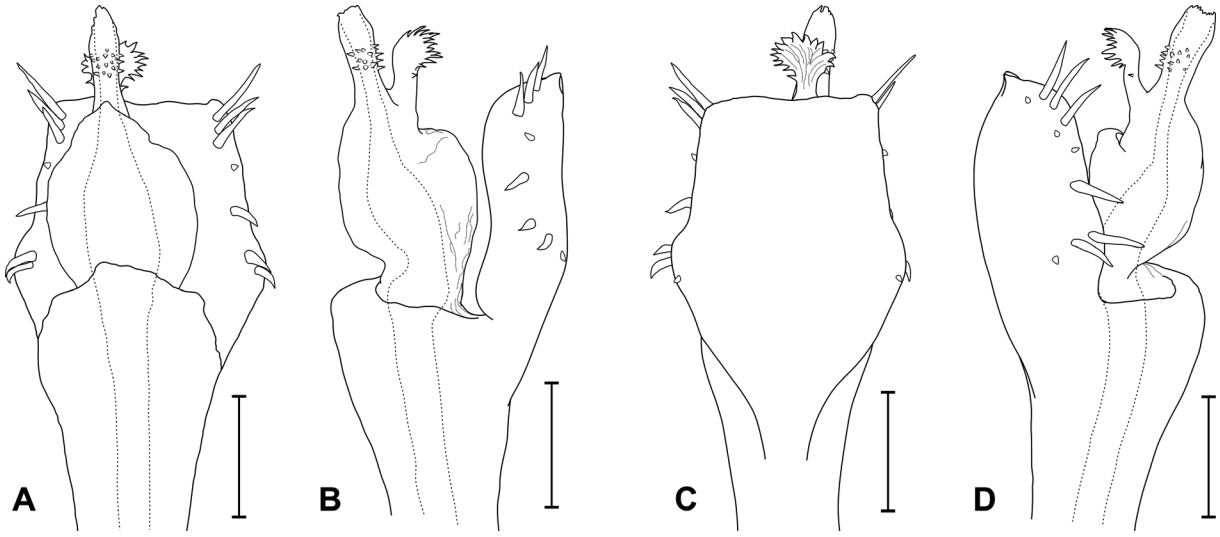

Fig. 18. *Lacronia serripes* (Mello-Leitão, 1923), ♂ (MNRJ 9973), penis, distal part. **A**. Dorsal view. **B**. Right lateral view. **C**. Ventral view. **D**. Left lateral view. Scale bars = 100 μm.

Fe IV thinner than in the male and unarmed on the distal portion. Mt IV dorsally covered by ordinary tubercles.

Intraspecific variation

In the *minor morph males* (compared to *major morph*): DS narrower; Cx IV with reduced prolateral and retro-lateral distal apophyses; Fe IV thinner, with reduced armature size. It was not found intraspecific variation among the *major morph males* or among females.

Records

BRAZIL, state of São Paulo: [Ilhabela]: Ilha dos Búzios; Ilha da Vitória (H. Soares 1966).

Geographic distribution (new records with an asterisk)

BRAZIL: state of Rio de Janeiro: Angra dos Reis*. State of São Paulo: Ilhabela, São Sebastião, Salesópolis*.

Lacronia tenuis (Roewer, 1917) comb. nov.
Figs 3E–H, 4G, 19–20; Table 8

Discocyrtus tenuis Roewer, 1917: 116, fig. 19
Discocyrtanus nigrolineatus Mello-Leitão, 1935b: 381, fig. 11. **Syn. nov.**
Discocyrtus infelix Mello-Leitão, 1940: 7, fig. 9. **Syn. nov.**
Discocyrtus textor Piza, 1943: 53, fig. 8. [Junior subjective synonym of *Discocyrtus infelix* Mello-Leitão, 1940 by B. Soares (1944d: 172)].

Discocyrtus tenuis – Roewer 1923: 440, fig. 553; 1929: 207. — Mello-Leitão 1932: 177, fig. 97. — B. Soares 1945: 374. — Soares & Soares 1954: 255. — Acosta 1996: 216. — Kury 2003a: 166.
Discocyrtanus nigrolineatus – Mello-Leitão 1935a: 102.
Discocyrtus nigrolineatus – B. Soares 1945: 374; 1946: 518. — Soares & Soares 1954: 253. — Kury 2003a: 164.
Discocyrtus infelix – B. Soares 1944c: 172; 1945: 373; 1946: 516. — Soares & Soares 1954: 250.

Diagnosis

Lacronia tenuis comb. nov. can be differentiated from the other species of the genus by the following combination of characters: 1) mesotergum areas I–IV with areolate spots around the ordinary tubercles (Figs 3E–H, 4G, 19A); 2) mesotergum area I with two pairs of conspicuous tubercles (Figs 4G, 19A); 3) mesotergum area II with a transversal central row of prominent tubercles on all of its width (Figs 4G, 19A); 4) Ti III proventral face with a comb of four spines (iiII) on the distal third (Fig. 19E); 5) Ti III retro-ventral face with a pair of spines (iI) on the distal third (Fig. 19E); 6) Tr IV with a transversal prodorsal distal apophysis covered by a row of four prominent tubercles (Fig. 19A, F–G); 7) Fe IV with a dorsal row of spines (Fig. 19F–G, I); 8) Mt IV dorsal face with a row of subconical spines decreasing in size distally, becoming rounded tubercles (Fig. 19J).

Type material

BRAZIL – 1 ♂, holotype of *Discocyrtus infelix* Mello-Leitão, 1940; State of Rio de Janeiro, Mangaratiba; MNRJ 181! (examined) • 1 ♀ (wrongly assigned as ♂ in the original description), holotype of *Discocyrtanus nigrolineatus* Mello-Leitão, 1935; State of Rio de Janeiro, Angra dos Reis, Jussaral; MNRJ 42428! (examined) • 1 ♀, holotype of *Discocyrtus tenuis* Roewer, 1917; State of São Paulo, Santos; SMF RI 1316 (examined by photographs) • 1 ♂, 1 ♀, syntypes of *Discocyrtus textor* Piza, 1943; State of São Paulo, Serra da Bocaina, Fazenda Águas de Santa Rosa; MZSP 810 (examined).

Additional material examined

BRAZIL – **State of Rio de Janeiro** • 1 ♂, 2 ♀♀; Angra dos Reis, Estrada Lídice-Angra; 22.865° S, 44.247° W; 500 m a.s.l.; 1 Feb. 1997; A.B. Kury, R. Pinto-da-Rocha and L. Mestre leg.; MNRJ 5533! • 1 ♂; RPPN Fazenda do Tanguá; Aug. 2009; C.A.S. Souza leg.; MZSP 36480 • 2 ♂♂; Itaguaí: 1948; Mattos and Maciel leg.; MNRJ 0037! • 1 ♂; Mangaratiba, Matutu, Caquizal da Márcia Khede; 22.87491° S, 43.99133° W; 500 m a.sl.; A.F. García, A.B. Kury and D.R. Pedroso leg.; MNRJ 260 • 3 ♂♂, 6 ♀♀; Reserva Ecológica do Rio das Pedras; 11–12 Nov. 2004; A.P.L. Giupponi leg.; MNRJ 17678! • 2 ♂♂, 1 ♀, 1 juv.; Parati, Trilha da Praia do Sono; Nov. 2005; M.B. da Silva and H.Y. Yamaguti leg.; MZSP 30100! • 2 ♂♂; Rio Claro; MNRJ 5545! • 1 ♂; Estação Repetidora da TV Globo; 22.865° S, 44.244° W; 800 m a.s.l.; 1 Mar. 1997; A.B. Kury, R. Pinto-da-Rocha and L. Mestre leg.; MNRJ 9275! • 2 ♂♂, 1 ♀; Rio de Janeiro, Restinga da Marambaia; 21 Oct. 1990; R.N. Costa leg.; MNRJ 6669! • 3 ♀♀; Teresópolis, Parque Nacional da Serra dos Órgãos; Aug. 2001; Equipe Biota leg.; IBSP 1935!. – **State of São Paulo** • 2 ♂♂; Ubatuba, Fazenda Capricórnio; 23 Feb. 1996; G. Machado leg.; MNRJ 5688! • 1 ♂; Picinguaba, Morro do Cuscuzeiro; 19–20 Jul. 1995; G.Machado; MNRJ 5689! • 1 ♀; same collection data as for preceding; MNRJ 5690! • 1 ♂; same collection data as for preceding; MNRJ 5691!.

Redescription

Male

MNRJ 260 for the external body illustrations and description; MNRJ 5533! for genitalic illustrations.

Measurements. DS: CW 3.1, CL 2.2, AW 6.1, AL 3.6; legs I–IV measurements in the Table 8; right / left tarsal (distitarsal) counts: 6(3) / 6(3) - 12(3) / 11(3) - 7 / 7 - 7 / 7.

Dorsum. DS gamma-pyriform, as long as wide, with lateral borders of the AS convex, widest and thickest at mesotergum area III, with a sub-straight posterior border (Fig. 19A, E). DS anterior border with a set of six acuminated tubercles on each side, divided by a small central projection and a pair of shallow cheliceral sockets (Fig. 19A). Carapace with a paramedian pair of prominent tubercles, surrounded by ordinary tubercles on lateral and posterior portions (those on the central portion covered and surrounded by lighter spots compared to the background) (Figs 3E–H, 4G, 19A). Ocularium elliptical (in dorsal view), high (ca 4 × the eye diameter), slightly inclined frontwards, placed in the anterior portion of the carapace (Fig. 19A–B, D). Ocularium with a pair of divergent spines (ca 3.5 × the eye diameter), slightly inclined frontwards (Fig. 19A–B, D). Mesotergum divided into four clearly defined areas (Figs 3E–H, 4G, 19A). Mesotergum areas I and IV divided into left and right halves by a longitudinal median groove (Figs 3E–H, 4G, 19A). AS lateral borders with a row of three prominent tubercles (Figs 4G, 19A). AS lateral borders with two rows of ordinary tubercles from the anterior corner of the carapace to the posterior border (Fig. 19A). All areas tuberculate, with all tubercles individually covered and surrounded by lighter spots (compared with their background) (Figs 4G, 19A). Mesotergum area I with two pairs of prominent tubercles (Figs 4G, 19A). Mesotergum area II with a transversal central row of prominent tubercles occupying all the width (Figs 4G, 19A). Mesotergum area III with a pair of paramedian outstanding spines (ca 2 × the ocularium spines) (Figs 4G, 19A, C–D). Mesotergum area IV with four to five prominent tubercles in a row surrounded by ordinary tubercles (Figs 4G, 19A). DS posterior border with a transversal row of prominent tubercles increasing in size to the center (Figs 4G, 19A). Free tergites I–III with a transversal row of prominent tubercles (Fig. 19A). Anal operculum tuberculate.

Venter. Cx I–III sub-parallel to each other, each with ventral longitudinal rows of setiferous tubercles (Cx I rows with higher and sharper tubercles than the others). Cx II–III with a retro-ventral distal transversal row of acuminate tubercles. Cx IV much larger than the others, directed obliquely. Intercoxal bridges well-marked. Stigmatic area Y-inverted-shaped, clearly sunken in relation to Cx IV distal part.

Table 8. Leg measurements of *Lacronia tenuis* (Roewer, 1917) comb. nov., ♂ (MNRJ 260).

	Tr	Fe	Pa	Ti	Mt	Ta	Cl	Total
Pp	0.46	1.64	0.74	1.09	–	1.00	0.83	5.78
Leg I	0.71	2.69	0.91	1.95	3.12	1.69	–	11.09
Leg II	0.86	5.88	1.39	4.33	6.28	3.85	–	22.59
Leg III	1.02	4.02	1.58	2.90	4.30	2.00	–	15.83
Leg IV	1.28	4.86	1.80	3.88	6.45	2.21	–	20.49

Cx IV covered by ordinary tubercles. Cx IV posterior border and stigmatic area each with a transversal row of ordinary tubercles. Stigmata visible. Free sternites with a transverse row of ordinary tubercles.

Chelicerae. Basichelicerite elongate, bulla well-marked, with marginal setiferous tubercles – two ectal, one posterior (Fig. 19A); hand not swollen.

Pedipalps. Tr with two geminate ventral setiferous tubercles. Fe with a ventral basal and a mesal apical setiferous tubercle. Pa unarmed. Ti with two rows (ventro-mesal and ventro-ectal) of four spines (IiIi). Ta with two rows of spines: three (iII) ventro-mesal and four (iIII) ventro-ectal.

Legs. All the unmentioned podomeres are unarmed or without relevant armature. Tr I–III each with several ventral tubercles. Fe I sub-straight (Fig. 3E); Fe II straight (Fig. 3E); Fe III sinuous (Figs 3E, 19E). Fe and Ti I–III with all faces covered by longitudinal rows of small tubercles (Fig. 19E). Fe II–III with an apical retro-dorsal spur (Fig. 3A–B). Fe III with an apical prodorsal spur (reduced when compared to the retro-dorsal spur). Fe III and Ti III with two rows (proventral and retro-ventral) of small acuminate tubercles, distally presenting spines (outstanding spines on Ti III) (Fig. 19E). Pa I–III covered dorsally by tubercles. Ti III mace-shaped (Fig. 19E); Cx IV reaching the posterior border of DS (Fig. 19A). Cx IV tuberculate between prodorsal and ventral faces (Fig. 19A). Cx IV with a prolateral distal thick cylindrical apophysis (distally curved backwards, bearing a spine on the apex), posteriorly crenated (Fig. 19A, F–H). Cx IV with a retro-lateral distal spiniform apophysis, fused with a small secondary branch (Fig. 19A, H–I). Tr IV square-shaped (in dorsal view) (Fig. 19A, F, H). Tr IV with a dorsal central prominent subconical tubercle (Fig. 19A, F). Tr IV with a prolateral proximal sub-conical apophysis (Fig. 19A, F–H). Tr IV prodorsal distal face with transversal apophysis covered by four prominent tubercles (Fig. 19A, F–G). Tr IV ventral face tuberculate (Figs 19G–I). Tr IV retro-lateral face with a proximal conical apophysis (slightly curved dorsad on the distal portion) (Fig. 19A, F, H–I). Tr IV retro-lateral face with a short distal spiniform apophysis (Fig. 19F, H–I). Fe IV straight (in dorsal view) and swollen at distal third (Fig. 19F–I). Fe IV with a dorsal row of eight conical spines (only the distalmost not curved to retro-lateral) (Fig. 19F–G, I). Fe IV prodorsal face with a row of nine prominent subconical tubercles (Fig. 19F–G). Fe IV prolateral face with a row of 1012 sub-conical tubercles (Fig. 19F–H). Fe IV proventral face with a row of sub-conical tubercles on proximal half and prominent conical tubercles on distal half (Fig. 19G–H). Fe IV with a central ventral row of sub-conical tubercles on the proximal third (Fig. 19G–I). Fe IV retro-ventral face with a row of subconical tubercles on basal two thirds and three conical spines on distal third (Fig. 19H–I). Fe IV with a retro-lateral row of seven spines, the three distalmost largest (Fig. 19F, H–I). Fe IV with a sizeable spur on prodorsal and retro-dorsal apical faces (Fig. 19F–I). Fe IV proventral and retro-dorsal faces with an outstanding spine on distal portion (Fig. 19G–I). Pa IV dorsally covered by sub-conical or acuminated prominent tubercles (Fig. 19F–G, I). Pa IV with a proventral row of four spines (III) (Fig. 19G–H). Pa IV with retro-ventral

three spines (iII) (Fig. 19H–I). Ti IV (in dorsal view) irregularly covered by conical tubercles, with nine or ten outstanding conical spines: three on dorsal face central third; three or four on prodorsal basal ⅔ thirds; and two basalmost and one distalmost on retro-dorsal face) (Fig. 19F–G, I). Ti IV with a prolateral and retro-lateral row of sub-conical tubercles (Fig. 19F–I). Ti IV with a proventral row of sub-conical tubercles and two outstanding spines on distal portion (Fig. 19G–H). Ti IV retro-ventral with a row of spines (four outstanding spines on the distal half, the two distalmost largest (Fig. 19H–I). Mt IV dorsal face with a row of subconical spines decreasing in size distally, becoming rounded tubercles (Fig. 19J).

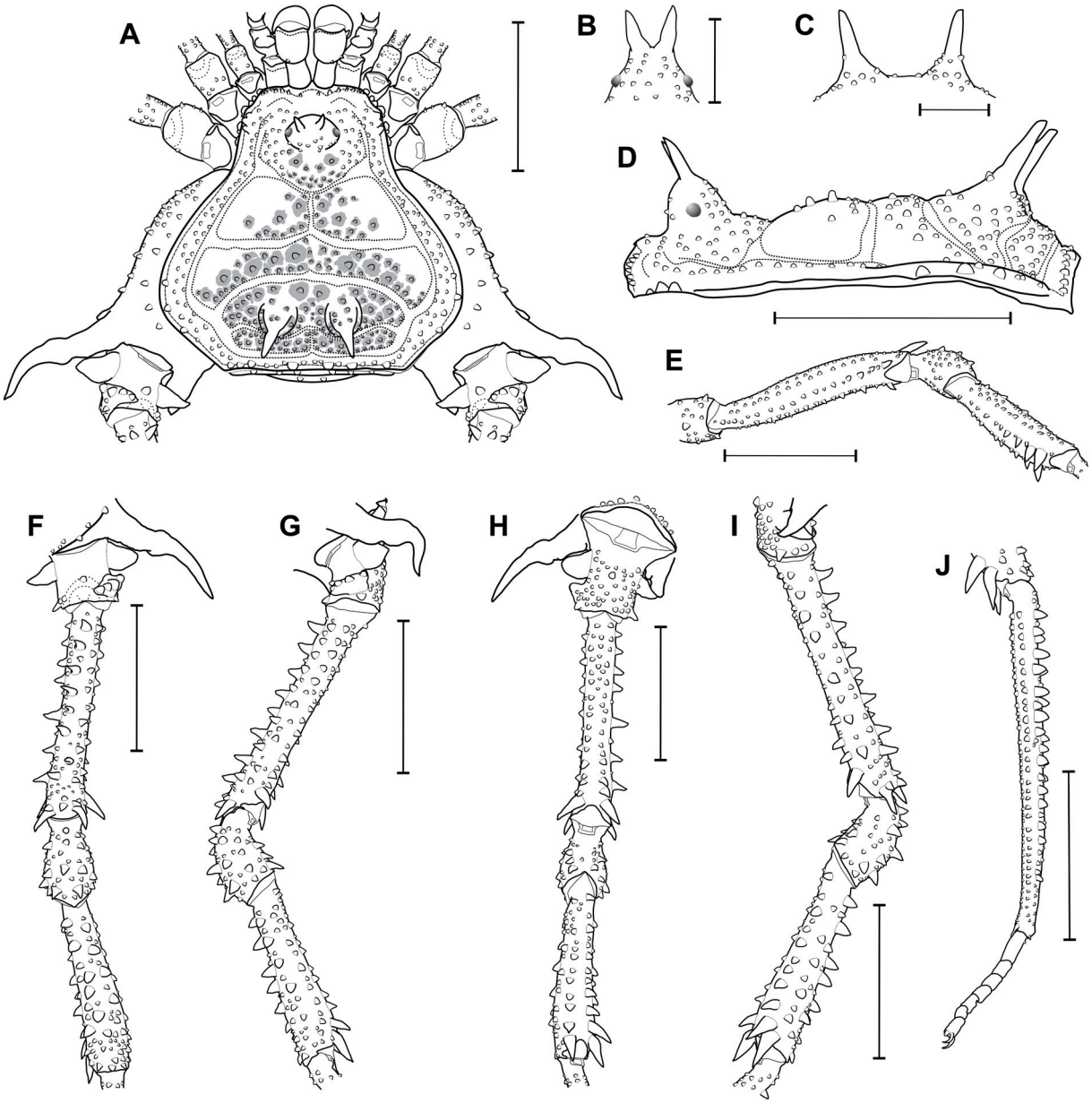

Fig. 19. *Lacronia tenuis* (Roewer, 1917) comb. nov., ♂ (MNRJ 260). **A**. Habitus, dorsal view. **B**. Ocularium, frontal view. **C**. Armature of mesotergum area III, posterior view. **D**. Habitus, lateral view. **E**. Left Fe–Ti III, proventral view. **F**. Right Fe–Ti IV, dorsal view. **G**. Same, prolateral view. **H**. Same, ventral view. **I**. Same, retro-lateral view. **J**. Right Mt–Ta IV, retro-lateral view. Scale bars: A, D–J = 3 mm; B–C = 1 mm.

Color (in vivo) (Fig. 3E–H). Ocularium background (including its pair of spines) *Strong Brown* (55). Carapace background, DS anterior portion and external portions of DS areas III *Dark Yellowish Brown* (78), with areolate spots *Strong Greenish Yellow* (99). AS lateral and posterior borders and free tergites I–III *Dark Olive Brown* (96). Mesotergum background and spines on the DS area III *Brownish Black* (65) with areolate spots *Strong Greenish Yellow* (99). AS lateral borders and the apex of the spines on the DS area III *Strong Yellowish Brown* (74). Tubercles on the DS, free tergites I–III and Cx IV dorsal face *Greenish White* (153). Ch and Pp background *Moderate Olive Green* (125), with honeycombed *Olive Black* (114) reticle. Tr I–III background in a mix of *Dark Orange Yellow* (72) and *Dark Yellowish Brown* (78). Fe–Mt I–III background *Deep Greenish Yellow* (100), with honeycombed *Dark Grayish Olive Green* (128) reticle. Tr III apophyses and Fe II–III retro-dorsal spurs *Vivid Orange Yellow* (66). Cx–Tr IV background *Dark Reddish Brown* (44) with *Strong Reddish Brown*'s apophyses (40). FeMt IV background *Dark Grayish Brown* (62), with its distal tubercles and spines *Deep Orange Yellow* (69).

Male genitalia. VP slightly divided into a distal half forming a rectangle with latero-apical flaps, and a proximal half elliptical (Fig. 20A, C). VP ventral surface entirely covered with microsetae of type 1 (Fig. 20B–C). All macrosetae inserted on the laterals of VP. MS A1–A3/A4 cylindrical, thick, and acuminate, forming a loose triangle in lateral view (A1 on the basal portion of the distal part, A2–A3/A4 on the proximal part, A3 ventralmost) (Fig. 20A–C). MS B1 small, inserted ventrally close to A3 (Fig. 20B–C). MS C1–C3 similar in shape and size to MS A, forming a triangle in lateral view (C2 ventralmost) on the distal third of VP (Fig. 20A–C). MS D1 small, close to C3 (Fig. 20B). MS E1–E2 small, located on the distal flange of VP – E1 between MS C1–C2, E2 below C3 (Fig. 20C). Glans sac arising from the middle bulge on the podium, not extended as a dorsal process (Fig. 20A–B). Stylus and its ventral process axis fused basally, forming a prominent pedestal (Fig. 20A–B). Stylus cylindrical, almost straight (apex slightly bent ventrad), inserted on pedestal forming a 45º angle, without conspicuous head and with a few small subdistal tiny spines (Fig. 20A–B, D). Ventral process is half of the stylus length, slightly bent dorsad, with an apical flabellum (Fig. 20A, D). Flabellum curved ventrally, scallop-shaped with serrulations, with approximately 35% of the ventral process stem length (Fig. 20A–D).

Female (MNRJ 5533[!])

Remark: measurements and tarsal counts not assessed before its loss.

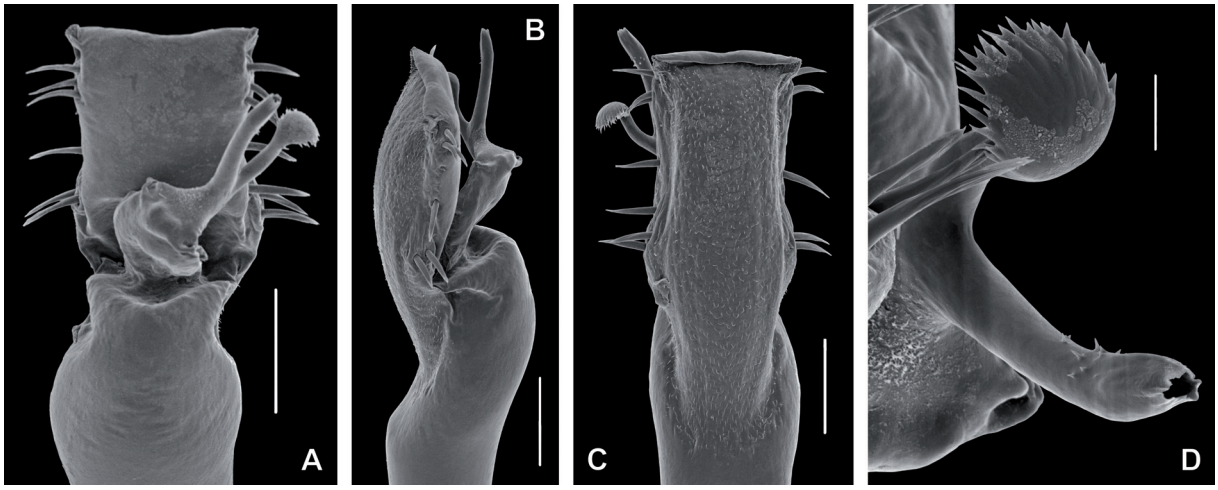

Fig. 20. *Lacronia tenuis* (Roewer, 1917) comb. nov., ♂ (MNRJ 5533[!]), penis, distal part. **A**. Dorsal view. **B**. Left lateral view. **C**. Ventral view. **D**. Detail of stylus and ventral process, dorso-lateral view. Scale bars: A–C = 100 μm; D = 20 μm.

DS gamma type. Cx IV narrower than in the males, with the prodorsal distal apophysis as a single outstanding spine and retro-ventral distal apophysis reduced to a tiny spine. Tr IV prolateral proximal portion unarmed. Tr IV retro-lateral face with a prominent proximal spine and distal one. Fe IV thinner than in the male, with five prominent spines on dorsal and retro-lateral faces. Mt IV dorsally covered by ordinary tubercles.

Intraspecific variation

In the *minor morph males* (compared to *major morph*): DS narrower; Cx IV with reduced prolateral and retro-lateral distal apophyses; Fe IV thinner, with reduced armature size. It was not found intraspecific variation among the *major morph males* or among females.

Historical taxonomic remarks

Discocyrtus tenuis (treated here as *Lacronia tenuis* comb. nov.) is known only from its female holotype (SMF RI 1316). *Discocyrtus nigrolineatus* was described based on the female holotype (MNRJ 42428[!]), which was incorrectly reported as a male by Mello-Leitão (1935b: 29). His mistake could have been caused by the well-developed armature of the specimen's leg IV, a common pattern in males of Pachylinae. Both holotypes (*Lacronia tenuis* comb. nov. and *D. nigrolineatus*) have been studied for this project and they were considered to be morphologically identical, especially based on the unique diagnostic leg IV armature. The type localities of *L. tenuis* comb. nov. (Santos, São Paulo) and *D. nigrolineatus* (Angra dos Reis, Rio de Janeiro) are congruent within the geographic range of the other records of that morphotype. Therefore, *D. nigrolineatus* is herein considered a junior subjective synonym of *L. tenuis* comb. nov.

Discocyrtus infelix was described based on the male holotype (MNRJ 181[!]) with an illustration of its dorsal habitus (Mello-Leitão 1940: 9). It matches all *major form* males of *L. tenuis* comb. nov. studied here (we only used males coupled with females in the same vial previously identified as "*D. nigrolineatus*"). The type locality of *D. infelix* (Mangaratiba, Rio de Janeiro) is situated in the center of the geographic distribution of *L. tenuis* comb. nov. Hence, *D. infelix* is considered here a junior subjective synonym of *L. tenuis* comb. nov.

Records

BRAZIL, state of São Paulo: Juquiá (H. Soares 1966).

Geographic distribution (new records with an asterisk)

BRAZIL: state of Rio de Janeiro: Angra dos Reis, Itaguaí*, Mangaratiba, Parati*, Rio Claro*, Rio de Janeiro*, Teresópolis*. State of São Paulo: Santos, Ubatuba*.

Discussion

In the context of a project aiming to disentangle decades of unsatisfactory taxonomic practice regarding the species of *Discocyrtus* and the more immediately related genera, one should aim to provide emended diagnoses which are not limited to meristic features. Such diagnoses encompassing diverse sets of features (e.g., several aspects of shape and armature of sexually dimorphic podomeres of legs III and IV, macrosetation, shape and proportions of penis ventral plate, structure of glans) are gradually being provided for several genera (e.g., for *Opisthoplatus* Holmberg, 1878 in Carvalho & Kury 2021a). The current diagnosis of *Lacronia* (proposed by Kury & Orrico 2006) belongs to this latter group, and it is here used with minimal change. In that project, little by little, the Roewerian diagnoses are being replaced with modern ones, thus allowing a comparison without distortions.

Herein, the decision to keep *Discocyrtus* and *Lacronia* as separated genera has two consequences that deserve attention. The first is the traditional placement of *Lacronia* in Pachylinae. As *Lacronia* was recovered in this study as the sister group of *Discocyrtus* s. str. as part of DRMN and consequently does not show any close phylogenetic relationship with Pachylinae s. str. (Fig. 1), it would be logical to propose a new subfamily to nest them. However, a previous work in progress (focused on the internal relationships of Gonyleptoidea, with the collaboration of many opilionologists) is already handling the subfamilial status of *Discocyrtus* and phylogenetically close genera. So, in deference to the results of that collective work, we refrain for now from proposing a new subfamilial status for *Discocyrtus* s. str. + *Lacronia*. However, the placement of *Lacronia* in Pachylinae does not make any sense in the light of our results. Therefore, we decided to remove *Lacronia* from Pachylinae without including it into any other subfamily, in the same way we did with *Propachylus* Roewer, 1913 in Carvalho *et al.* (2018).

Concerning the DRMN internal relationships, considering *Lacronia* as sister-group of *Discocyrtus* s. str., the analysis presented here agrees with the results given by Carvalho & Kury (2020, 2021b), with Mitobatinae as the sister group of (*Discocyrtus* s. str. + (Neopachylinae + Roeweriinae)). However, in other published results, this basal topology of DRMN does not resolve in the same manner (Carvalho & Kury 2018; Carvalho *et al.* 2021; Saraiva *et al.* 2021).

In spite of a monophyletic DRMN consistently being retrieved as the best phylogenetic hypothesis, nodal support for this clade is always low (as exemplified here, Fig. 1), and more investigation is needed to address this question.

Lacronia presents a distribution exclusively associated with the Atlantic province (Fig. 5). While *L. camboriu* is the only species from the coast of Santa Catarina, the other six species are in the mountain ranges of Rio de Janeiro and São Paulo. Most of the species of *Lacronia* have an allopatric distribution, except for *L. tenuis*, which is sympatric with *L. ceci* and *L. nigra* comb. nov. Considering the sympatry of *L. ceci* and *L. tenuis* comb. nov. (both recorded from Teresópolis, Rio de Janeiro), the phylogenetic distance between them (indicated by the cladistic analysis presented here, Figs 1–2) and their morphology are pieces of evidence of their co-existence as different species. The situation that needs more attention is the case of *L. nigra* comb. nov. and *L. tenuis* comb. nov., which are sympatrid in Santos, São Paulo. Both species are retrieved here as a clade (Figs 1–2) and belong to the 'areolated *Lacronia*' group. However, the armature pattern of the males' leg IV (mainly in the Cx IV prodorsal apophysis shape, the Tr IV prodorsal distal armature and the Mt IV dorsal row of spines and/or prominent tubercles) does not show any morphological intersection between these species (see the diagnosis' section of *L. nigra* comb. nov. and *L. tenuis* comb. nov. above). So, here we decide to preserve both species as separated entities.

Acknowledgments

This study has been supported by: (1) # E-26/200.085/2019 (Apoio Emergencial ao Museu Nacional) from Fundação de Amparo à Pesquisa do Estado do Rio de Janeiro (FAPERJ), (2) # E-26/210.148/2019 (249116) (APQ1 - Auxílio à Pesquisa básica - 2019) from Fundação de Amparo à Pesquisa do Estado do Rio de Janeiro (FAPERJ), (3) #311531/2019-9 (Produtividade em Pesquisa) from the Conselho Nacional de Desenvolvimento Científico e Tecnológico (CNPq) (4) #430748/2018-3 (Chamada MCTIC/CNPqNº 28/2018 - Universal) from the Conselho Nacional de Desenvolvimento Científico e Tecnológico (CNPq) to ABK, and 5) scholarship grant #145594/2018-1 from the Conselho Nacional de Desenvolvimento Científico e Tecnológico (CNPq) to RNC. The SEM micrographs were taken in the Center for Scanning Electron Microscopy of Museu Nacional/UFRJ (financed by PETROBRAS), with the kind assistance of Beatriz Cordeiro and Camila Messias. The photographs were taken with the stereo microscope (CNPq Universal 14/2013) with the kind assistance of Manoela Cardoso. We would like to thank Antônio Brescovit (IBSP) and Ricardo Pinto-da-Rocha (MZSP) for helping us to continue this project with loan

of material, Glauco Machado for providing a picture of *L. ceci* in vivo and Alexandra Rizzo and Amanda Mendes (UERJ) for assisting RNC in their laboratory after the loss of the Laboratório de Aracnologia/ MNRJ in the 2018's fire. The authors wish to thank Paula Cushing, Jürgen Gruber, Marcos R. Hara and Alan Martin for material support in dire times. The final manuscript benefited from useful criticism from Marcos R. Hara and an anonymous reviewer.

References

Acosta L.E. 1996. Die Typus-Exemplare der von Carl-Friedrich Roewer beschriebenen Pachylinae (Arachnida: Opiliones: Gonyleptidae). *Senckenbergiana biologica* 76 (1–2): 209–225.

Benavides L.R., Pinto-da-Rocha R. & Giribet G. 2021. The phylogeny and evolution of the flashiest of the armored harvestmen (Arachnida: Opiliones). *Systematic Biology* 70 (4): 648–659. https://doi.org/10.1093/sysbio/syaa080

Bremer K. 1994. Branch support and tree stability. *Cladistics* 10: 295–304. https://doi.org/10.1111/j.1096-0031.1994.tb00179.x

Bragagnolo C. & Pinto-da-Rocha R. 2009. Review of the Brazilian harvestman genus *Roeweria* Mello-Leitão, 1923 (Opiliones: Gonyleptidae). *Zootaxa* 2270: 39–52. https://doi.org/10.11646/zootaxa.2270.1.2

Carvalho R.N. & Kury A.B. 2018. Further dismemberment of *Discocyrtus* with description of a new Amazonian genus and a new subfamily of Gonyleptidae (Opiliones, Laniatores). *European Journal of Taxonomy* 393: 1–32. https://doi.org/10.5852/ejt.2018.393

Carvalho R.N. & Kury A.B. 2020 (2021). A new subfamily of Gonyleptidae formed by false *Discocyrtus* Holmberg, 1878 from Brazil, with revalidation of *Pachylobos* Piza, 1940 and description of a new genus. *Zoologischer Anzeiger* 290: 79–112. https://doi.org/10.1016/j.jcz.2020.11.004

Carvalho R.N. & Kury A.B. 2021a. Intraspecific spination pattern in *Discocyrtus prospicuus* (Holmberg, 1876) (Opiliones: Gonyleptidae) reviewed: revalidation of the harvestman genus *Opisthoplatus*, with two new synonymies and biogeographical notes on their morphs. *Austral Entomology* 60: 364–389. https://doi.org/10.1111/aen.12537

Carvalho R.N. & Kury A.B. 2021b. Wide distribution and wide bodies: a new genus of Neopachylinae (Opiliones, Gonyleptidae) formed by false *Discocyrtus*. *Zoologischer Anzeiger* 294: 137–164. https://doi.org/10.1016/j.jcz.2021.08.006

Carvalho R.N. & Kury A.B. 2022. Review of *Paradiscocyrtus* Mello-Leitão, 1927 (Gonyleptidae, Opiliones), with the transfer of *Paradiscocyrtus cerayanus* Mello-Leitão, 1927 to *Discocyrtus* Holmberg, 1878 and a new interpretation of its type locality. *Zoosystema* 44 (9): 209–225. https://doi.org/10.5252/zoosystema2022v44a9

Carvalho R.N., Kury A.B. & Santos M.S. 2018. Conspecificity of semaphoronts – the synonymy of *Metadiscocyrtus* with *Propachylus* (Opiliones: Laniatores: Gonyleptidae). *Journal of Arachnology* 46: 488–497. https://doi.org/10.1636/JoA-S-17-082.1

Carvalho R.N., Kury A.B. & Hara M.R. 2021. Reevaluation of the systematic position of some southern Brazilian *Discocyrtus* (Gonyleptidae: Roeweriinae), with the reinstatement of *Bunopachylus*. *Invertebrate Systematics* 35: 701–724. https://doi.org/10.1071/IS20083

Cekalovic K.T. 1985. Catálogo de los Opiliones de Chile (Arachnida). *Boletín de la Sociedad de Biología de Concepción* 56: 7–29.

Goloboff P.A. & Catalano S.A. 2016. TNT version 1.5, including a full implementation of phylogenetic morphometrics. *Cladistics* 32 (3): 221–238. https://doi.org/10.1111/cla.12160

Goloboff P.A., Carpenter J.M., Arias J.S. & Esquivel D.R.M. 2008. Weighting against homoplasy improves phylogenetic analysis of morphological datasets. *Cladistics* 24 (5): 758–773. https://doi.org/10.1111/j.1096-0031.2008.00209.x

Kästner A. 1937. Chelicerata. 7. Ordnung der Arachnida: Opiliones Sundeval = Weberknechte. *In*: Kukenthal W. & Krumbach T. (eds) *Handbuch der Zoologie* Vol. 3: 300–393. Walter de Gruyter & Co., Berlin & Leipzig.

Kury A.B. 2003a. Annotated catalogue of the Laniatores of the New World (Arachnida, Opiliones). *Revista Ibérica de Aracnología* volumen especial monográfico 1: 1–337.

Kury A.B. 2003b. Two new species of *Lacronia* Strand from southern Brazil (Opiliones, Gonyleptidae, Pachylinae). *Revista Ibérica de Aracnología* 7: 29–37.

Kury A.B & Carvalho R.N. 2016. Revalidation of the Brazilian genus *Discocyrtanus*, with description of two new species (Opiliones: Gonyleptidae: Pachylinae). *Zootaxa* 4111 (2): 126–144. https://doi.org/10.11646/zootaxa.4111.2.2

Kury A.B. & Orrico V.G.D. 2006. A new species of *Lacronia* Strand, 1942 from the highlands of Rio de Janeiro (Opiliones, Gonyleptidae, Pachylinae). *Revista Ibérica de Aracnología* 13: 147–153.

Kury A.B., Giupponi A.P.L. & Mendes A.C. 2018. Immolation of Museu Nacional, Rio de Janeiro — unforgettable fire and irreplaceable loss. *Journal of Arachnology* 46: 556–558. https://doi.org/10.1636/JoA-S-18-094.1

Kury A.B, Mendes A.C., Cardoso L., Kury M.S., Granado A. de A., Giribet G., Cruz-López J.A., Longhorn S.J., Medrano M., Kury I.S. & Souza-Kury M.A. 2022. World Catalogue of Opiliones. WCO-Lite Ver. 2.4.0. Available from https://wcolite.com/ [accessed 15 Apr. 2022].

Maddison W. & Maddison D.R. 2017. Mesquite: a modular system for evolutionary analysis. Available from http://mesquiteproject.org [accessed 15 Apr. 2022].

Mello-Leitão C.F. 1923a. Arachnideos da Ilha dos Alcatrazes. *Revista do Museu Paulista* 13: 515–520.

Mello-Leitão C.F. 1923b. Opiliões Laniatores do Brasil. *Archivos do Museu Nacional* 24: 107–197.

Mello-Leitão C.F. 1926. Notas sobre Opiliones Laniatores sul-americanos. *Revista do Museu Paulista* 14: 327–383.

Mello-Leitão C.F. 1932. Opiliões do Brasil. *Revista do Museu Paulista* 17: 1–505.

Mello-Leitão C.F. 1935a. Algumas notas sobre os Laniatores. *Archivos do Museu Nacional* 36: 87–116.

Mello-Leitão C.F. 1935b. A propósito de alguns opiliões novos. *Memórias do Instituto Butantan* 9: 369–411.

Mello-Leitão C.F. 1937. Notas sobre opiliões do Instituto Butantan. *Memórias do Instituto Butantan* 10: 289–295.

Mello-Leitão C.F. 1940. Sete gêneros e vinte e oito espécies de Gonyleptidae. *Arquivos de Zoologia do Estado de São Paulo* 1: 1–52.

Mendes A.C. 2011. Phylogeny and taxonomic revision of Heteropachylinae (Opiliones: Laniatores: Gonyleptidae). *Zoological Journal of the Linnean Society* 163: 437–483. https://doi.org/10.1111/j.1096-3642.2011.00706.x

Morrone J.J., Escalante T., Rodríguez-Tapia G., Carmona A., Arana M. & Mercado-Gómez J. 2022. Biogeographic regionalization of the Neotropical region: new map and shapefile. *Anais da Academia Brasileira de Ciências* 94 (1): e20211167. https://doi.org/10.1590/0001-3765202220211167

Muñoz-Cuevas A. 1973. Sur les caractères génériques de la familie des Gonyleptidae (Arachnida, Opilions, Laniatores). *Bulletin du Muséum national d'histoire naturelle* 87: 225–234.

Myers N., Mittermeier R.A., Mittermeier C.G., DaFonseca G. & Kent J. 2000. Biodiversity hotspots for conservation priorities. *Nature* 403: 853–858. https://doi.org/10.1038/35002501

Nixon K.C. 2002. WinClada, version 1.00.08. Published by the author, Ithaca, NY.

Pérez-Schultheiss J. 2021. Capítulo III. Opiliones de Chile: estado del conocimiento y checklist de las especies. *Parasitología Latinoamericana* 70 (2): 51–81.

Pinto-da-Rocha R., Da Silva M.B. & Bragagnolo C. 2005. Faunistic similarity and historical biogeography of the harvestmen of southern and southeastern Atlantic Rain Forest of Brazil. *Journal of Arachnology* 33: 290–299. https://doi.org/10.1636/04-114.1

Pinto-da-Rocha R., Bragagnolo C., Marques F.P.L. & Antunes-Jr M. 2014. Phylogeny of harvestmen family Gonyleptidae inferred from a multilocus approach (Arachnida: Opiliones). *Cladistics* 30: 519–539. https://doi.org/10.1111/cla.12065

Piza S.T. 1942. Novos opiliões do Chile. *Revista Brasileira de Biologia* 2: 387–390.

Piza S.T. 1943. Novos Gonyleptidas brasileiros. *Papéis avulsos do Departamento de Zoologia* 3: 39–60.

Roewer C.F. 1917. 52 neue Opilioniden. *Archiv für Naturgeschichte* 82a: 90–158.

Roewer C.F. 1923. *Die Weberknechte der Erde. Systematische Bearbeitung der bisher bekannten Opiliones*. Gustav Fischer, Jena.

Roewer C.F. 1929. Weitere Weberknechte III. (3. Ergänzung der Weberknechte der Erde, 1923). *Abhandlungen der Naturwissenschaftlichen Verein zu Bremen* 27: 179–284.

Saraiva N.E. de V., Hara M.R. & DaSilva M.B. 2021. Harvestmen in the semiarid: a new genus and three new species of Pachylinae (Opiliones: Gonyleptidae) from Caatinga dry vegetation, with a cladistic analysis. *Arthropod Systematics & Phylogeny* 79: 485–507. https://doi.org/10.3897/asp.79.e66321

Soares B.A.M. 1942. Contribuição ao estudo dos opiliões da Serra do Mar — Opiliões de Boracéa. *Papéis Avulsos do Departamento de Zoologia do Estado de São Paulo* 2: 1–13.

Soares B.A.M. 1944a. Mais alguns opiliões de Boracéa. *Papéis avulsos do Departamento de Zoologia do Estado de São Paulo* 4: 177–186.

Soares B.A.M. 1944b. Opiliões do Alto da Serra II. *Papéis avulsos do Departamento de Zoologia do Estado de São Paulo* 4: 277–302.

Soares B.A.M. 1944c. Notas sobre opiliões da coleção do Museu Nacional do Rio de Janeiro. *Papéis avulsos do Departamento de Zoologia do Estado de São Paulo* 6: 163–180.

Soares B.A.M. 1944d. Notas sobre opiliões XIV. *Papéis avulsos do Departamento de Zoologia do Estado de São Paulo* 6: 221–224.

Soares B.A.M. 1945. Opiliões da coleção do Museu Nacional do Rio de Janeiro. *Archivos de Zoologia do Estado de São Paulo* 4: 341–394.

Soares B.A.M. 1946. Opiliões do Departamento de Zoologia. *Arquivos de Zoologia do Estado de São Paulo* 4: 485–534.

Soares B.A.M. & Soares H.E.M. 1945. Um novo gênero e dois alótipos de "Gonyleptidae" (Opiliones). *Revista Brasileira de Biologia* 5: 339–343.

Soares B.A.M & Soares H.E.M. 1954. Monografia dos gêneros de opiliões neotrópicos III. *Arquivos de Zoologia do Estado de São Paulo* 8: 225–302.

Soares H.E.M. 1966. Opiliões das ilhas dos Búzios e Vitória (Opiliones: Gonyleptidae, Phalangodidae). *Papéis Avulsos do Departamento de Zoologia do Estado de São Paulo* 19: 279–293.

Strand E. 1942. Miscellanea nomenclatoria zoologica et paleontologica X. *Folia Zoologica et Hydrobiologica* 11: 386–402.

Manuscript received: 4 May 2022
Manuscript accepted: 20 October 2022
Published on: 13 February 2023
Topic editor: Tony Robillard
Section editor: Rudy Jocqué
Desk editor: Pepe Fernández